อุทกพลศาสตร์และการถ่ายเทมวลสารของกระบวนการดูดซึมเบนซีน
ในถังปฏิกรณ์แบบฟองอากาศ

นางสาวศิริกาญจน์ เหล่ารัดเดชา

วิทยานิพนธ์นี้เป็นส่วนหนึ่งของการศึกษาตามหลักสูตรปริญญาวิทยาศาสตรมหาบัณฑิต
สาขาวิชาการจัดการสิ่งแวดล้อม (สหสาขาวิชา)
บัณฑิตวิทยาลัย จุฬาลงกรณ์มหาวิทยาลัย
ปีการศึกษา 2551

HYDRODYNAMIC AND MASS TRANSFER OF BENZENE
ABSORPTION PROCESS IN BUBBLE COLUMN

Miss Sirikarn Laoraddecha

A Thesis Submitted in Partial Fulfillment of the Requirements

for the Degree of Master of Science Program in Environmental Management
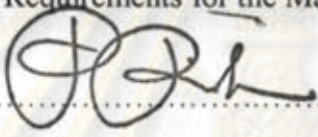
(Interdisciplinary Program)

Graduate School

Chulalongkorn University

Academic Year 2008
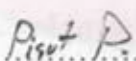
Thesis Title   HYDRODYNAMIC AND MASS TRANSFER OF BENZENE
                   ABSORPTION PROCESS IN BUBBLE COLUMN
By   Miss Sirikarn Laoraddecha
Field of Study   Environmental Management
Thesis Advisor   Pisut Painmanakul, Ph.D.

Accepted by the Graduate School, Chulalongkorn University in Partial Fulfillment of the Requirements for the Master's Degree

....Dean of the Graduate School
(Associate Professor Pornpote Piumsomboon, Ph.D.)

THESIS COMMITTEE

....Chairperson
(Chantra Tongcumpou, Ph.D.)

..........Pisut P...................Thesis Advisor
(Pisut Painmanakul, Ph.D.)

....Examiner
(Chaiyaporn Puprasert, Ph.D)

....Examiner
(Pichet Chaiwiwatworakul, Ph.D.)

....External Examiner
(Sarayut Rachu, Ph.D.)

ศิริกาญจน์ เหล่ารัตเดชา : อุทกพลศาสตร์และการถ่ายเทมวลสารของกระบวนการดูดซึมเบนซีนในถัง
ปฏิกรณ์แบบฟองอากาศ (Hydrodynamic and mass transfer of benzene absorption process in bubble
column) อ. ที่ปรึกษาวิทยานิพนธ์หลัก: อ.ดร.พิสุทธิ์ เพียรมนกุล, 142 หน้า

งานวิจัยนี้ได้ทำการศึกษากระบวนการดูดซึมสารอินทรีย์ระเหยง่ายชนิดไม่ชอบน้ำ (ชนิดเบนซีน) ในตัว
แปรด้านอุทกพลศาสตร์และการถ่ายเทมวลสารของฟองอากาศภายในคอลัมน์แบบฟองอากาศขนาดเล็ก (เส้นผ่าน
ศูนย์กลาง 4.4 เซนติเมตรและความสูง 30 เซนติเมตร) ทำการประยุกต์ใช้น้ำประปา สารละลายของสารลดแรงตึง
ผิวชนิดไม่มีประจุ (Tween80) และอิมัลชันของน้ำมันเครื่องร่วมกับสารลดแรงตึงผิวชนิดไม่มีประจุเป็นสารดูดซึม
โดยความเข้มข้นของสารลดแรงตึงผิวชนิดต่าง ๆ ในสารดูดซึมเท่ากับ 0.1, 0.5, 1, 3, และ 5 ซีเอ็มซี และความ
เข้มข้นของน้ำมันเท่ากับ 50 และ 300 มิลลิกรัมต่อลิตร ทำการเดินระบบภายใต้อุณหภูมิห้องที่อัตราการไหลของ
ก๊าซเท่ากับ 0.5, 1.3, 2.2, และ 3.0 มิลลิลิตรต่อวินาที ในงานนี้ ปัจจัยที่ศึกษา ได้แก่ ประสิทธิภาพในการดูดซึม ตัว
แปรด้านอุทกพลศาสตร์ของฟองก๊าซ และตัวแปรด้านการถ่ายเทมวลสารของฟองก๊าซภายในคอลัมน์แบบ
ฟองอากาศ

จากผลการทดลองพบว่าประสิทธิภาพในการดูดซึมฟองก๊าซเบนซีนในสารดูดซึมประเภทอิมัลชันน้ำมัน
ร่วมกับสารลดแรงตึงผิว (47.67%) มีค่าสูงกว่าที่ได้จากสารละลายร่วมกับสารลดแรงตึงผิว (27.56%) และ
น้ำประปา (8.97%) โดยความเข้มข้นของน้ำมันและสารลดแรงตึงผิวที่สูงขึ้นในเฟสของเหลวส่งผลต่อการเพิ่มขึ้น
ของความสามารถในการละลายของเบนซีนในสารดูดซึม นอกจากนี้ ประสิทธิภาพในการดูดซึมก๊าซเบนซีนมีค
วามสัมพันธ์กับค่าสัมประสิทธิ์การถ่ายเทมวลสารโดยรวม (K_La) ซึ่งรวมค่าพื้นที่ผิวสัมผัสจำเพาะ (a) และค่า
สัมประสิทธิ์การถ่ายเทมวลสารของฟิล์มของเหลว (K_L) เข้าด้วยกัน โดยพบว่าที่อัตราการไหลของก๊าซที่สูงขึ้น
ส่งผลให้ค่า K_La และ a เพิ่มสูงขึ้น แต่กลับให้ประสิทธิภาพการบำบัดที่ลดลงเป็นผลมาจากกลไกการไล่ก๊าซ
(Desorption or Stripping process) ที่สัมพันธ์กับการเพิ่มขึ้นของพลังงานกวนผสมภายในเฟสของเหลว โดยผลเสีย
ดังกล่าวเกิดกับสารดูดซึมประเภทอิมัลชันน้ำมันในสัดส่วนที่สูงกว่าสารดูดซึมประเภทอื่น นอกจากนี้ พบว่าค่า
สัมประสิทธิ์ K_L และค่าพื้นที่ผิวสัมผัสจำเพาะ (a) หักล้างซึ่งกันและกัน ทำให้ส่งผลเสียโดยรวมต่อการลดลงของ
ค่าสัมประสิทธิ์ K_La ในกรณีสารดูดซึมประเภทสารลดแรงตึงผิวที่ความเข้มข้นมากกว่า 1 ซีเอ็มซี และอิมัลชันของ
น้ำมัน ที่ความเข้มข้นของน้ำมันเครื่องเพิ่มสูงขึ้น พบว่าส่งผลกระทบค่อนข้างน้อยต่อค่าสัมประสิทธิ์การถ่ายเท
มวลสารของฟิล์มของเหลว (K_L) โดยสรุป การเลือกใช้อัตราการไหลของก๊าซซึ่งให้ลักษณะทางอุทกพลศาสตร์
ของฟองก๊าซที่เหมาะสม รวมไปถึงการประยุกต์ใช้สารลดแรงตึงผิว และอิมัลชันของน้ำมันเป็นสารดูดซึมนั้น
สามารถช่วยเพิ่มประสิทธิภาพในการดูดซึมเบนซีนในถังปฏิกิริยาฟองอากาศ โดยเมื่อพิจารณาในด้านการเตรียม
สารดูดซึม ด้านการบำบัดน้ำเสียจากสารดูดซึม และประสิทธิภาพบำบัด กล่าวได้ว่าการเติมสารลดแรงตึงผิวชนิดที่
ความเข้มข้นสูง (5 ซีเอ็มซี) มีความเหมาะสมในการประยุกต์ใช้งาน

สาขาวิชา........การจัดการสิ่งแวดล้อม.................... ลายมือชื่อนิสิต...ศิริกาญจน์ เหล่ารัตเดชา...........

ปีการศึกษา....2551.................... ลายมือชื่อ อ.ที่ปรึกษาวิทยานิพนธ์หลัก.................

5087545520 : MAJOR ENVIRONMENTAL MANAGEMANT
KEYWORDS: VOLATILE ORGANIC COMPOUNDS / SURFACTANT/ ABSORPTION / HYDRODYNAMIC / MASS TRANSFER.

SIRIKARN LAORADDECHA: HYDRODYNAMIC AND MASS TRANSFER OF BENZENE ABSORPTION PROCESS IN BUBBLE COLUMN. ADVISOR: PISUT PAINMANAKUL, Ph.D., 142 pp

The objective of this work is to study the hydrophobic VOCs absorption process in terms of bubble hydrodynamic and mass transfer parameters in bubble column (4.4 cm in diameter and 30 cm in height). The absorbate used in this work were benzene and the absorbent used in this work were the aqueous solution of non-ionic surfactant and oil-in-water emulsion with non-ionic surfactant, respectively. Moreover, the ranges of surfactant concentrations (0.1, 0.5, 1, 3, 5 CMC), oil-in-water concentrations (50 and 300 mg/L) were analyzed with the gas flow rates applied 0.5, 1.3, 2.2, 3.0 ml/s. The analytical parameters were the VOCs removal efficiency, bubble hydrodynamic parameters, and also the mass transfer parameters.

This result has shown that the VOCs removal efficiency obtained in liquid phase containing with oil-in-water emulsion absorbent (47.67%) were greater than those obtained with surfactant absorbent (27.56) and tap water (8.97%). These results relate with the augmentation of benzene solubility in liquid phase due to the lubricant oil and surfactants presence in liquid phase. Moreover, the VOCs removal efficiency obtained experimentally correspond with the overall mass transfer coefficient (K_La) that is the product between the interfacial area (a) and the liquid-film mass transfer coefficient (K_L). It can be stated that, not only the influence of high gas flow rates can caused the increasing of K_La and a, but also the decreasing of VOCs removal efficiency due to the desorption or stripping process that related to the power mixing in liquid phase. This desorption phenomena obtained with oil-in-water emulsion was more pronounces than those obtained with other liquid phases. Furthermore, it can be noted that the values of a and K_L are compensated to each other that can be effected to the K_La coefficient in case of liquid phase containing of oil-in-water emulsion and aqueous solution of surfactant. Moreover, small effect of surfactants and oil-in water emulsion on the K_L coefficients was observed at high concentrations injected in liquid phase. Therefore, the appropriate gas flow rates providing the suitable bubble hydrodynamic condition and also concentrations of surfactant and oil-in-water emulsion as absorbents were essential to provide the high removal efficiency of benzene absorption process. By considering the preparation of absorbent, wastewater treatment, and removal efficiency, it can be concluded that the additional of surfactant at 5 CMC was suggested for absorbent used in this study.

Field of Study: Environmental Management   Student's Signature: Sirikarn Laoraddecha

Academic Year: 2008   Advisor's Signature: Pisut P.

ACKNOWLEDGEMENTS

CONTENTS

LIST OF TABLES

LIST OF FIGURES

Figure   **Page**

LIST OF ABBREVIATIONS

A	Cross-sectional area of reactor, m^2
a	Interfacial area
atm	Atmosphere
^0C	Celsius
Cg inlet	Inlet concentration of VOCs
$C_{g(out)}$	Outlet concentration of VOCs in gas phase
C_L	Concentration of VOCs in liquid phase
C_L^S, C_{Lsat}	Saturated concentration VOCs in liquid phase
cm	Centre meter
CMC	Critical Micelle Concentration
D_{AB}	Diffusion coefficient
D_B	Bubble diameter
%Eff	Efficiency removal
^0F	Fahrenheit
f_B	Bubble formation frequency
g	Acceleration due to gravity
H_L	Liquid height
HLB	Hydrophile - lipophile balance
K	Kelvin
K_L	Liquid-film mass transfer coefficient
K_La	Overall mass transfer coefficient in liquid phase
kg	Kilogram
L	Liter
M	Molecular weight
m	Meter
m^2	Square meter
m^3	Cubic meter
min	Minute
mg	Milligram

ml	Milliliter
mol	Mole
N	Molar flux
N_B	Number of bubbles generated
N_{OR}	Number of orifice
ρ	Liquid density
ΔP	Pressure drop
p	Patial pressure
Pa	Pascal
ppm	Part per million
q	Heat flux
Q_g	Gas flow rate
R	Gas constant
Re_o	Orifice Reynolds number
s	Second
S_B	Total bubble surface
Se	Surface coverage ratio
SFT	Surface Tension
T	Temperature
Γ_∞	Surface concentration when it is saturated
Tween80	Non-ionic surfactant
U_B	Bubble rising velocity
V_L	Liquid volume
V_B	Bubble volume
V_{total}	Total volume in reactor
VOCs	Volatile Organic Compounds
x	Mole fraction of solute in liquid
σ_L	Liquid surface tension

CHAPTER I

INTRODUCTION

1.1 Statement of problem

Volatile Organic Compounds (VOCs) are well-known atmospheric pollutants that are emitted from numerous activities (printing, surface cleaning, coating, production of coating preparations, inks, and adhesives, manufacturing of pharmaceutical products) (A. Dubray, 2003) Their emissions can effect on human health, pose a serious environmental problem and entail large financial loss. Normally, such emissions may be reduced by different methods: adsorption, thermal and catalytic oxidation, absorption in a liquid, membrane separation, bio-treatment, etc. These techniques have their pluses and minuses (Poddar T. K. *et al*., 1996). Up to now, there is a continue research for the techniques, which do not suffer from any limitations. The absorption process, which allows the transfer of a pollutant from the gas phase to a liquid phase (absorbent), with or without any chemical reaction, is one of the well-known methods. From De Nevers, N. (2000), the VOCs removal efficiencies obtained with the absorption process can be greater than 98%. Moreover, this method is also used to remove odorous compounds from gaseous stream and thus suited to plants that already have an oversized wastewater treatment plant or to pollutants that can be removed by simple chemical reaction with little effect on the chemical composition of the liquid stream (Mycock *et al.,* 1995). Generally, the absorbent should have the following properties (Heymes *et al.,* 2005)

- High capacity to absorb the VOCs gases;

- Low viscosity and a high diffusion coefficient to control absorption kinetics;

- Low vapor pressure to reduce loss of absorbent by stripping and to prevent unwanted air pollution by the absorbent;

- Low toxicity;

- Low cost

Due to the hydrophilic and hydrophobic VOCs emission normally generated in real operating conditions, it can be noted that, in the case of hydrophobic VOCs, the normal absorbent used (water) can not be used due to the corresponding solubility of hydrophobic VOCs in water. Therefore, other kinds of absorbents are required. From Peeva *et al.,* (2001) an absorption reactor filled with the surfactant solutions can provide more hydrophobic VOCs removal than that filled with water. Surfactants composed of a hydrophilic head group and a hydrophobic tail can be well solubilized in water forming a micelle. The hydrophilic groups are headed to water while the hydrophobic tail aggregates in the middle of the micelle. As hydrophobic VOCs are captured in the hydrophobic tails due to the hydrophobic interaction, their solubility in the surfactant solution is much larger than that in pure water (Vane *et al.,* 2002). Moreover, from Dumont *et al.,* (2006), the presence of organic phase in the absorbent can possibly enhance the VOCs transfer rate and thus improve the VOC abatement capacity. Therefore, it can be stated that the aqueous solutions with surfactants and also oily wastewater obtained in environment can be applied in order to reduce the VOCs emission problem.

In order to transfer VOCs from large gas volumes to small absorbent volumes, a wide range of absorption apparatuses is accordingly available on the market: stirred tank, bubble column, packed bed column, plate column and static or dynamic mixer. The choices of the best absorption system are difficult and have to take into account various parameters to achieve the optimal design (Cotte *et al.,* 1995). Up to now, a few studies have been focused to the absorption process based on the bubbles column, which is one type of absorption technology possibly applied in the real operating conditions (Heymes *et al.,* 2006). Theoretically, bubble columns are usual gas-liquid chemical reactors especially for kinetically slow reactions such as oxidations or chlorinations. In bubble column, gas sparger (gas diffuser) is a device for introducing a stream of gas in the form of small bubbles into a liquid. Normally, porous plates made of ceramics, plastics, or sintered metals are applied, but their fine pores are more readily plugged with solids which may be present in the gas or the liquid. With punctured flexible rubber membranes, uniform size distribution of small bubbles is produced leading to large mass transfer area, without the usual clogging problems

encountered with a porous disk (rigid) diffuser (Rice & Lakhani, 1983). Concerning to the bubble column application, the gas phase dispersion (hydrodynamic) and the bubble size distribution are important factors affecting the obtained VOCs removal efficiency as defined in term of gas-liquid interfacial area available for mass transfer and therefore the reaction rate. In addition, the literatures about VOCs absorption process in bubble column shows that there is a very limited number of qualitative data related to the effect of bubble hydrodynamic (bubble diameter, bubble rising velocity, bubble formation frequency and interfacial area) and mass transfer parameter (Volumetric mass transfer coefficient and local film mass transfer coefficient) on the VOCs removal efficiency (Painmanakul *et al.,* 2004)

Based on a variety of literatures (Rice *et al.,* 1981; Loubière and Hébrard, 2003; Hébrard *et al.,* 1996; Couvert *et al.,* 1999; Painmanakul *et al.,* 2004); the bubble hydrodynamic and mass transfer parameters can be significantly affected by both types of gas diffusers and different contaminants (surfactants and organic substances) presence in the liquid phases: these phenomena relate surely to the associated removal efficiency by absorption process in bubble column. Loubière and Hébrard, (2004) have studied the influence of surfactants on the bubble hydrodynamic parameters at different gas spargers, especially on the generated bubble diameter (D_B), the associated bubble frequency (f_B) and the interfacial area (a). In this study, the liquid phases were characterized in terms of static and dynamic surface tensions, Critical Micelle Concentration (CMC) and characteristic adsorption parameters (surface coverage ratio at equilibrium (Se), adsorption constant at equilibrium (K) and surface concentration when it is saturated (Γ_∞)). These authors have observed that the effect of surface tension on the bubble generated depends on the type of orifice (flexible and rigid) and should be analyzed in terms of dynamic surface tension and of kinetics of surfactant molecule adsorption and diffusion. Concerning to the study of mass transfer parameters, the volumetric/overall mass transfer coefficient (K_La) which is the product of the local film mass transfer coefficient (K_L) and the interfacial area (a), is generally used in order to analyze the global mass transfer mechanism and also compare the different treatment methods. However, this overall mass transfer coefficient is often global and thus insufficient to understand the mass transfer

mechanism relating to the effect of gas diffusers and liquid phase contamination used in VOCs absorption in bubble column (Vazquez *et al.,* 1997; Akosman *et al.,* 2004) In this purpose, it becomes essential to separate the parameters, especially the liquid-side mass transfer coefficient (K_L) and the interfacial area (a) (Bouaifi *et al.,* 2001; Zhao *et al.,* 2003a,b); however, there is a lack of studies dealing with this separation in the presence of surfactants and organic substances (Vasconcelos *et al.,* 2003; Vazquez *et al.,* 2000; Cents *et al.,* 2001). Sardeing *et al.,* (2006) have focused on the effect of surfactants on the interfacial area developed by the air bubbles generated and on the mass transfer parameters (volumetric mass transfer coefficient k_La and liquid-side mass transfer coefficient k_L). Moreover, the model for predicting the k_L coefficient has been proposed over the whole bubble diameter range. Thus, it is interesting to apply these methodologies for analyzing the VOCs mass transfer mechanism.

To fill this gap, this research is mainly focused on the study of hydrophobic VOCs absorption in terms of bubble hydrodynamic and mass transfer parameters. Moreover, the effect of bubble hydrodynamic conditions (gas diffuser and gas flow rate) and also the non-ionic surfactant and oil-in-water emulsion as absorbents are investigated in order to understand the hydrophobic VOCs removal mechanism. The local experimental methods for measuring the bubble hydrodynamic (Painmanakul *et al.,* 2005) and mass transfer coefficient (Painmanakul *et al.,* 2004) are applies in order to facilitate the dissociation of various parameters which enables the VOCs mass transfer efficiency to be effectively controlled whatever the operating conditions.

1.2 Objectives

The purposes of this research is to study and apply the dissociation method for analyzing the VOCs removal mechanism in term of bubble hydrodynamic and mass transfer parameters obtained in a small bubble column. The scope of this work is as follows:

1. Study the effect of bubble hydrodynamic obtained with gas diffuser (rigid orifice) and different gas flow rates on the hydrophobic VOCs removal efficiency;

2. Investigate the effect of aqueous solutions with non-ionic surfactant and concentrations on the hydrophobic VOCs absorption process;

3. Study the effect of oil-in-water emulsion with non-ionic surfactants at Critical Micelle Concentration (CMC) on the hydrophobic VOCs absorption process;

1.3 Hypothesis

In the case of hydrophobic VOCs emission in environments, the classical pure water can not be used as high efficient absorbents: other kinds of absorbents (aqueous solution with surfactants and lubricant oily emulsion with/without surfactants) should be considered. Due to the application of bubble column in VOCs absorption process, this can enhance the overall system performance based on the small bubble size and thus high interfacial area generated by gas diffusers. Therefore, the local experimental methods for determining the bubble hydrodynamic and mass transfer coefficient are necessary to provide a better understanding of the VOCs mass transfer mechanisms and thus effectively control the absorption process whatever the operating conditions.

1.4 Scope of study

1. This experiment is carried out in laboratory scale with a glass bubble column of 4.4 cm in diameter and 30 cm in height, and remain constant room conditions;

2. In this study, benzene is chooses as hydrophobic VOCs gas emission. Gas diffuser used in this study is rigid orifice with 0.65 mm in diameter and different flow rate (0.5, 1.3, 2.2, and 3.0 ml/s);

3. The liquid absorbents used in this study are the tap water, the aqueous solutions with non-ionic surfactant and concentrations at 0.1, 0.5, 1, 3, and 5

CMC and the lubricant oil-in-water emulsion (50 and 300 mg/L) containing non-ionic surfactant at Critical Micelle Concentration (CMC);

4. The Critical Micelle Concentration (CMC) is determined by using the experimental values of surface tension obtained with tensiometer and then applied in order to prepare the different types of absorbents used in this study;

5. Based on the concentration of VOCs determined by Raoult's law and Ideal gas law, the experimental results of VOCs concentration and related loading can be obtained in order to create the calibration curve between the experimental values and the area under curve from analyzing equipment;

6. In this study, the overall mass transfer coefficients ($K_L a$) are determined by using the experimental data based on the variation of VOCs concentration in gas phase with time. Noted that the VOCs concentrations obtained in this study are measured by the Gas Chromatography using a flame ionization detector;

7. The calculation of interfacial area (a) is based on the experimental results of the bubble diameter (D_B), the bubble frequency (f_B) and the bubble rising velocity (U_B). The high speed camera (100 images/s) and image analysis program will be used;

8. The liquid-film mass transfer coefficients (K_L) are calculated as the ratio between the ($K_L a$) and (a) obtained experimentally.

CHAPTER II

BACKGROUND AND LITERATURE REVIEW

2.1 Volatile organic compounds

Volatile organic compounds (VOCs) are a class of substances in which organic carbon is boned to hydrogen or to other elements. As an approximate rule, VOCs may be defined as organic liquids or solids whose room temperature vapor pressure are greater than about 0.0007 atm, or 70 Pa and whose atmospheric boiling point are up to about 500 ^{0}F (260 ^{0}C, 533 K). The effect of these substances on human health range from a simple nuisance to a serious hazard, and regulations have been enacted to limit their emissions. VOCs represent a ubiquitous problem in indoor and outdoor air pollution. They are emitted from virtually all industrial sources in one form or another. In the atmosphere, they combine with oxides of nitrogen and sunlight to form ozone, an oxidant that has harmful effects on plant and animal life.

The physical and chemical properties of volatile organic compound play an important role in both the selection and proper operation of an absorption system. If the solubility of the gaseous contaminant is very high, then high removal efficiencies can be achieved by almost any absorption device. For a relatively insoluble contaminant only certain systems may be able to achieve the required removal efficiency.

In this work, Benzene was chosen as a model of a VOC with low solubility in water. If VOCs are insoluble, it may be leak and emitted to the atmosphere. Therefore, the water cannot be used as an absorbent. Other kinds of absorbent are required. Hence, an absorption reactor filled with the emulsion and surfactant solution is more efficient than one with pure water. The solubility of compounds can be defined by Henry's law as shown in next section.

- **Vapor-Liquid Equilibrium Relations (Raoult's Law)**

As in the gas-liquid systems, the equilibrium in vapor-liquid systems is restricted by the phase rule, as $F = C - P + 2$ where P is the number of phase at equilibrium, C

the number of total components in the two phases when no reactions are occurring, and F the number of variants or degrees of freedom of the system. As an example we shall use the ammonia-water, vapor-liquid system. For two components and two phases, F from above equation is 2 degrees of freedom. The four variables are temperature, pressure, and the composition y_A of NH_3 in the vapor phase and x_A in the liquid phase. The composition of water (B) is fixed if y_A or x_A is specified, since $y_A + y_B = 1.0$ and $x_A + x_B = 1.0$. If the pressure is fixed, only one more variable can be set. If we set the liquid composition, the temperature and vapor composition are automatically set. An ideal law, Raoult's law, can be defined for vapor-liquid phases in equilibrium.

$$p_A = P_A x_A \qquad (2.1)$$

where p_A is the partial pressure of component A in the vapor in Pa(atm), P_A is the vapor pressure of pure A in Pa(atm), and x_A is the mole fraction of A in the liquid. This law holds only for ideal solutions, such as benzene-toluene, hexane-heptane, and methyl alcohol-ethyl alcohol, which are usually substances very similar to each other. Many systems that are ideal or nonideal solutions follow Henry's law dilute solutions.

Table 2.1 Vapor-Pressure and Equilibrium-Mole-Fraction Data for Benzene-Toluene system.

Vapor pressure							
Temperature		Benzene		Toluene		Mole fraction benzene at 101.325 kPa	
K	C°	kPa	mmHg	kPa	mmHg	x_A	y_A
353.3	80.1	101.32	760			1.000	1.000
358.2	85	116.9	877	46.0	345	0.780	0.900
363.2	90	135.5	1016	54.0	405	0.581	0.777
368.2	95	155.7	1168	63.3	475	0.411	0.632
373.2	100	179.2	1344	74.3	557	0.258	0.456
378.2	105	204.2	1532	86.0	645	0.130	0.261
383.8	110.6	240.0	1800	101.32	760	0	0

- **Determination of VOCs concentration and Loading**

The concentration of VOCs can be determined by using Raoult's law and Ideal gas law. From Raoult's law, the partial pressure is obtained with the identified values of P_A and x_A as shown in equation (2.1). Then, we substitute the partial pressure into the ideal gas law as shown in equation (2.2):

$$pV = nRT \qquad (2.2)$$

where p is the partial pressure, V is the volume, n is the amount of gas (moles), R is the gas constant, 8.314 $J\cdot K^{-1} mol^{-1}$, and T is the absolute temperature. Thus, the initial VOCs concentration from the VOCs generator is achieved. If we multiply the concentration with flow rate, the loading can be obtained as shown in equation (2.3):

$$Loading = Q_g *[C] \qquad (2.3)$$

Note that, the experimental results of VOCs concentration and loading, obtained in this study, can be applied in order to create the calibration curve between the experimental values and the area under curve from analyzing equipment.

2.2 Control of gaseous and volatile organic compounds

The control of gaseous and volatile organic compounds depends on their properties. The methods of control include:

- **Combustion**

Combustion processes like flame combustion or catalytic combustion can be utilized to greatest advantage when the gases or vapors to be controlled are organic in nature. Equipment employing the principle of flame combustion includes:

  o Fume and vapor incinerators
  o After-burners
  o Flares, either with steam injection or venture flare

The method is too expensive. However, combustion control equipment has been used with advantage, in petrochemical, paint and varnish and fertilizer industries.

- **<u>Adsorption</u>**

Adsorption is a surface phenomenon and requires very large solid surface areas to be effective. In almost all cases these areas are internal as with porous material and may be almost unbelievably great per unit of adsorber volume. Adsorption is primarily a physical phenomenon. In this process the effluent gases are passed through adsorbers which contain solids of porous structure. The commonly used adsorbers include activated carbon, silica gel, activated alumina, lithium chloride, activated bauxite, etc. Active carbon appears to be the adsorbent most suitable for recovering organic solvent vapors. Adsorption as a means of air pollution control, offers certain advantages for some classes of contaminant. It includes gases and vapors for which other means of collection are uneconomical, hazardous or impossible. The efficiency of removal of gases by adsorbents depends on (a) The physical and chemical characteristics of the adsorbent and (b) The concentration and nature of gas to be adsorbed.

- **<u>Absorption</u>**

In this process, effluent gases are passed through absorbers which contain liquid absorbents that remove one or more of the pollutants in the gas stream. Absorption systems are capable of VOCs removal efficiencies greater than 98% show in Table 2.2. Because of their high efficiencies, they are frequently used to remove odorous compounds, from gaseous streams. (Application for indoor air treatment has also been described in the literature). Water is commonly used as the scrubbing liquid, or sorbent. For example, scrubbers are used at rendering plants to remove contaminants in the plant exhaust before it is released into the atmosphere. In some cases, seawater, chlorine, hypochlorite, hydrochloric acid, sodium hydroxide, or sodium bicarbonate is added to enhance the scrubbing efficiency. Absorption systems are most suited to plants that already have an oversized wastewater treatment plant or to pollutants that liquid stream. Simple absorber designs are also useful for streams that contain large amounts of particulate because the particulate can more easily foul a packed bed. It is not usually possible to optimize removal of both particulate and gaseous compounds in the same vessel.

Note that absorption efficiency depends upon the amount of surface contact between the gas and the liquid, time of contact between gas and liquid, concentration of the absorbing liquid, and the rate of reaction between the gas and the absorbent. Therefore, due to the high performances in VOCs treatment process, the absorption process will be studied and also locally analyzed in order to provide a better understanding of the process mechanism and thus well control the optimal operating conditions.

Table 2.2 Technology for removal volatile organic compounds (VOCs)

Device	Inlet Conc. PPMV	Efficiency	Advantages	Disadvantages
Absorption	250 1,000 5,000	90% 95% 98%	Especially good for inorganic acid gasses	Limited applicability
Adsorption	200 1,000 5,000	50% 90-95% 98%	Low capital investment good for solvent recovery	Selective applicability moisture and temperature constraints
Condensation	500 10,000	50% 95%	Good for product or solvent recovery	Limited applicability
Thermal incineration	20 100	95% 99%	High destruction efficiency Wide applicability can recover heat energy	No organics can be recovered Capital intensive
Catalytic incineration	50	90%	High destruction efficiency	No organics can be recovered
Flares	100	>95% >98%	Can be less expensive than thermal High destruction efficiency	Technical limitations that can poison No organics can be recovered Large emissions only

2.3 Absorption process

Absorption is a diffusional mass-transfer operation by which a soluble gaseous component is removed from a gas stream by dissolution in a solvent liquid. The driving force for mass transfer is the concentration difference of the solute between the gaseous and liquid phases. Some common terms used when discussing the absorption process as follows:

- Absorbent: the liquid, usually water, into which the contaminant is absorbed.
- Absorbate or solute: the gaseous contaminant being absorbed.
- Carrier gas: the inert portion of the gas stream, usually air, from which the contaminant is to be removed.
- Interface: the area where the gas phase and the absorbent contact each other.
- Solubility: the capability of a gas to be dissolved in a liquid.

2.3.1 Absorption mechanism

To remove a gaseous contaminant by absorption, the contaminant-laden exhaust stream must be passed through (contact with) a liquid. In the first step of the absorption process, the pollutant (or solute) diffuses from the bulk area of the gas phase to the gas-liquid interface. In the second step, gaseous pollutants transfer across the interface to the liquid phase. In the third step, the pollutants diffuse into the bulk area of the liquid, making room for additional gas molecules to be absorbed.

The purpose of analyzing these three steps is to determine which variables control the process. The most efficient system can be designed by knowing these variables. It is assumed that once the solute arrives at the interface area, transfer across it occurs simultaneously. This second step in the absorption mechanism is extremely rapid. Therefore, it does not need to be considered when deriving absorption efficiency equations. The rate of mass transfer (absorption) is dependent upon the diffusion rate in either the gas phase or the liquid phase.

Normally, two terms are used to describe mass transfer rates: gas phase controlled absorption and liquid phase controlled absorption. Each mechanism depends on the rate of diffusion in both phases and upon the solubility of the pollutant in the liquid phase. The gas phase controlled systems absorb pollutants more readily than do the liquid phase controlled systems. Thus, absorption systems used in the field of air pollution control are usually designed to be gas phase controlled.

2.3.2 Gas solubility in liquid phase

A very important factor affecting the amount of a contaminant that can be absorbed is the solubility of the contaminant. Solubility is a function of both the

temperature and, to a lesser extent, the pressure of the system. As temperature increase, the amount of gas that can be absorbed by the liquid decreases. Pressure affects the solubility of a gas in the opposite manner. By increasing the pressure of a system the amount of gas absorbed generally increases. The solubility of a specific gas in a given liquid is normally defined at a designated temperature and pressure. Under certain conditions, the portion of a compound that partitions between an aqueous and a gas phase, the partition coefficient is called *Henry's law coefficient*. Table 2.3 provides some examples of Henry's law coefficients for common compounds. Henry's law is expressed as:

$$p^* = Hx \qquad (2.4)$$

where: p^* =   Partial pressure of solute at equilibrium, units of pressure

         x =   Mole fraction of solute in the liquid

        H =   Henry's law constant, pressure/mole fraction

If the partial pressure is low, there is very little tendency for the component to leave the liquid phase; thus there is high solubility. Henry's law can be used to predict solubility only in the low concentration range, where the relationship between partial pressure and concentration is essentially a straight line. The slope of that line is the Henry's law constant. Another restriction is that Henry's law can be used as a predictive technique only for those gases that essentially do not change molecular form upon being dissolved: the permanent gases, some of the light hydrocarbons, etc. Any gas which dissociates or reacts on dissolution no linger exists as a simple molecule. In such situations, Henry's law does not hold exactly because the equilibrium relationship is curved rather than straight. Solubility predictions must then be based on experimentally derived data. One other aspect of solubility is that the strongest solution that can be made in an absorber is that which corresponds to equilibrium.

Compounds that have high Henry's law coefficients are the compounds that have high vapor pressures and low solubility. The normal classification for compounds is that if they have a Henry's law coefficient of above 0.01 (milligrams per liter over

milligrams per liter), they are considered volatile. If Henry's law coefficient is between 0.0001 and 0.01, the compounds are considered semi-volatile. If Henry's law coefficient is below 0.0001, the compound is generally considered nonvolatile from the aqueous phase.

Table 2.3 Relative solubility in water (Henry's law coefficients) for some common compounds.

Compound	Gas-phase concentration [ppm/(mg/L)]
Octane	33,900
Oxygen	22,600
Hydrogen sulfide	255
Benzene	71
PCBs	2.96
Ammonia	0.78
Ethanol	0.66

2.3.3 Equipment description for absorption process

The primary function of an absorber is to remove gaseous contaminants from an exhaust air stream. To accomplish this, absorption equipment is designed to maximize the mass transfer rate. In absorption, the rate of mass transferred depends largely on the surface areas of the air and liquid stream exposed to each other. Absorption proceeds at a finite rate. Increasing the time the two streams are in contact will increase the potential for absorption to occur.

Normally, the absorbers are designed to provide the necessary surface area and sufficient contact time between the gas and liquid streams. Absorption is conducted in tray towers (plate columns), packed columns, spray towers, bubble columns, and centrifugal contactors, as shown schematically in Figure 2.1.
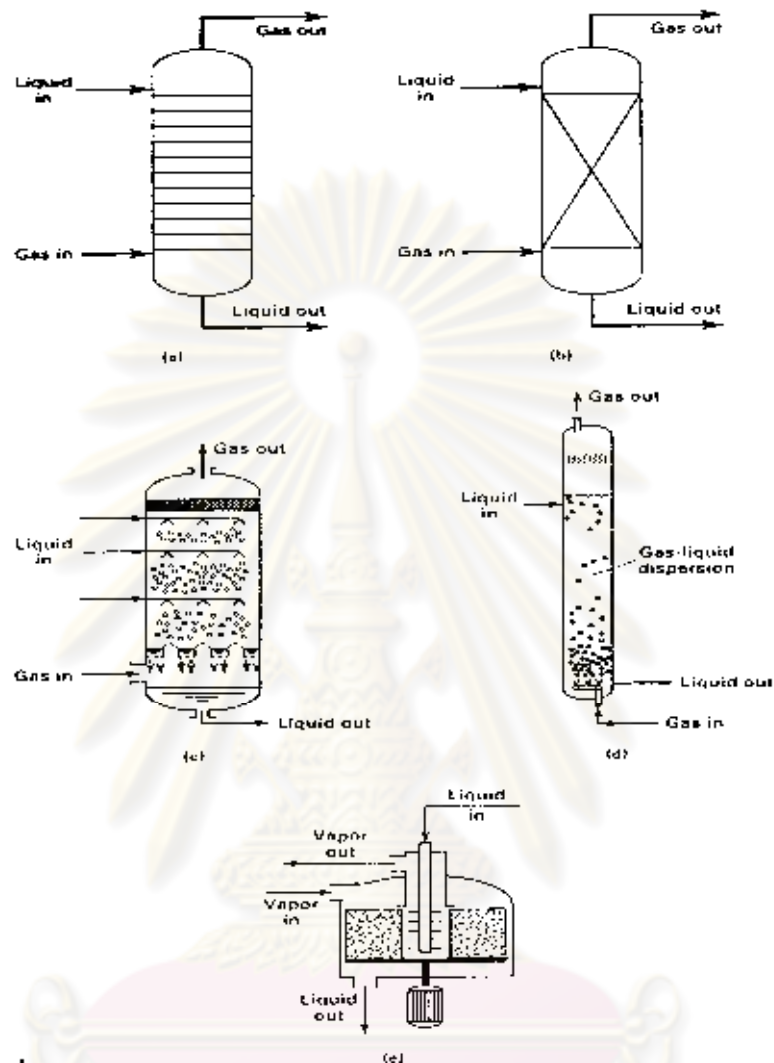
Figure 2.1 Equipment for absorption process: (a) trayed tower; (b) packed column; (c) spray tower; (d) bubble column; (e) centrifugal contactor.

A trayed tower is a vertical, cylindrical pressure vessel in which gas and liquid, is obtained by forcing the gas to pass upward through small orifices, bubbling through a liquid layer flowing across a plate. The bubble cap tower is a classical contacting device. A variation is the valve tray, which permits greater variations in gas flow rate without dumping the liquid through the gas passages. Example of which is shown in Figure 2.2
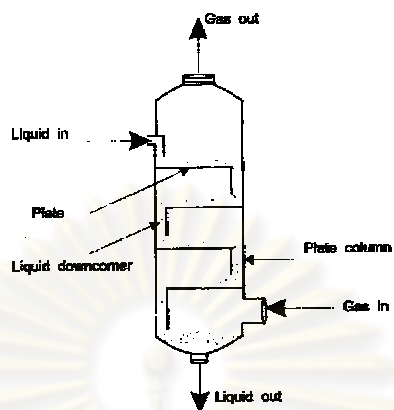
Figure 2.2 Trayed tower or plated column

Packed columns (tower), the most common scrubber used for gas absorption. Packed columns disperse the scrubbing liquid over packing material which provides a large surface area for continuous gas-liquid contact. Packed column are classified according to the relative direction of gas-to-liquid flow. Normally, the most common packed tower is the countercurrent (gas-to-liquid) flow tower, shown in Figure 2.3. The gas stream being treated enters the bottom of the tower and flows upward over the packing material. Liquid is introduced at the top of the packing by sprays or weirs and flows downward over the packing material. This flow arrangement results in the highest theoretically achievable efficiency. The most dilute gas is contacted with the purest absorbing liquor, providing a constant, maximized concentration difference (driving force) for the entire length of the column.
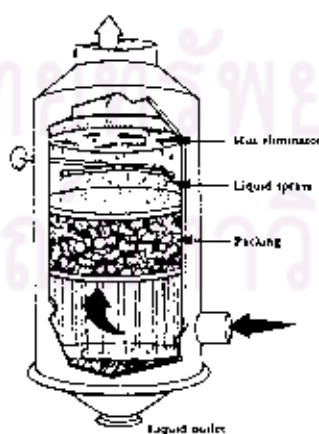
Figure 2.3 Packed columns

Spray towers, the simplest devices used for gas absorption, consist of an empty tower and a set of nozzles to spray liquid. A spray tower is similar in operation to spraying water in an open barrel. Typically, the contaminant gas stream enters the bottom of the tower and passes up through the device while liquid is being sprayed at one or more levels by nozzles. The flow of liquid and gas streams in opposite directions is referred to as countercurrent flow. Figure 2.4 illustrates the operation of a typical countercurrent flow spray tower. The main advantage of spray towers is that they are completely open; they have no internals except for the spray nozzles. Therefore, they have a very low pressure drop.
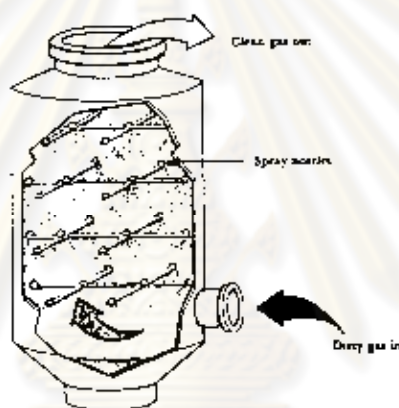
Figure 2.4 Spray columns

Bubble columns, as shown in Figure 2.1(d), consists of a vertical cylindrical vessel partially filled with liquid into which the vapor is bubbled. Vapor pressure drop is high, and only one or two theoretical stages can be achieved. Such a device has a low vapor throughput and should not be considered unless the solute has a very low solubility in the liquid and/or a slow chemical reaction takes place in the liquid phase, thus requiring an appreciable residence time. For this reason, the bubble column can be achieved the efficiency removal of benzene.

Centrifugal contactors, as shown in Figure 2.1(e), consist of a stationary ringed housing, intermeshed with a ringed rotating section. The liquid phase is fed near the center of the packing, from which it is caused to flow outward by centrifugal force. The vapor phase flows inward by a pressure driving force. Very high mass transfer rates can be achieved with only moderately high rotation rates. It is possible to obtain

the equivalent of several equilibrium stages in a very compact unit. This type of contact is favored when headroom for a trayed tower or packed column is not available or when a short residence time is desired.

2.4 Mass transfer theory

Mass transfer is the net movement of a component in a mixture from one location to another where the component exists at a different concentration. Thus, the absorption by a solvent liquid of a solute from a carrier gas involves mass transfer of the solute through the gas to the gas-liquid interface, across the interface, and into the liquid. Normally, mass transfer mechanism occurs by two basic mechanisms:

(1) Molecular diffusion by random and spontaneous microscopic movement of individual molecules in a gas, liquid, or solid as a result of thermal motion;

(2) Eddy (turbulent) diffusion by random, macroscopic fluid motion. Both molecular and/or eddy diffusion frequently involve the movement of different species in opposing directions. When a net flow occurs in one of these directions, the total rate of mass transfer of individual species is increased or decreased by this bulk flow or convection effect, which may be considered a third mechanism of mass transfer.

Molecular diffusion is extremely slow, whereas eddy diffusion is orders of magnitude more rapid. Therefore, if industrial separation processes are to be conducted in equipment of reasonable size, fluids must be agitated and interfacial areas maximized. If mass transfer in solids is involved, using small particles to decrease the distance in the direction of diffusion will increase the rate. Mass transfer of VOCs such as methanol in the solution is absorbed to the absorbate that is the mass transfer between phases and the convective mass transfer. Mass transfer between the fluid and area are depended on the movement properties and the dynamics. The equation of the convective mass transfer can be written from Newton's law:

$$N_A = k_C \Delta C_A \tag{2.5}$$

Note that N_A is Molar flux of specie A with respect to coordinates that are fixed in space. C_A and k_C are the different of concentration of specie A between the area and average of fluid and the convective mass transfer coefficient, respectively. Mass transfer occurs in the direction that is decrease the concentration. The equation (2.5) illustrated the relation between flux of diffusion substance and gradients of concentration, because of fluid through the area have a layer that are occur near the laminar flow thus the particles near the area of solid are fix in space. The mechanism of mass transfer between area and fluid are related to diffusion of molecule in a layer of fluid fix flow or laminar flow. The mass transfer are control by fluid film so the case of k_C is Film coefficient that depended on the system, fluid properties, and flow.

The laws of mass transfer show the relation between the flux of the diffusing substance and the concentration gradient responsible for this mass transfer. Since diffusion occurs only in mixtures, its evaluation must involve an examination of the effect of each component. For example, it is often desired to know the diffusion rate of a specific component relative to the velocity of the mixture in which it is moving. Since each component may possess a different mobility, the mixture velocity must be evaluated by averaging the velocities of all the components present.

2.4.1 Mass transfer fluxes

The mass (or molar) flux of a given species is a vector quantity denoting the amount of the particular species, in either mass or molar units, that passes per given unit time through a unit area normal to the vector. The flux may be defined with reference to coordinates that are fixed in space, coordinates which are moving with the mass-average velocity, or coordinates which are moving with the molar-average velocity. The mass flux of species i with respect to coordinates that are fixed in space can be defined by:

$$n_i = \rho_i v_i \qquad (2.6)$$

The molar flux of species i with respect to coordinates that are fixed in space is given by

$$N_i = \rho_i v_i \qquad (2.7)$$

The mass diffusion flux of species i with respect to the mass-average velocity is given by

$$j_i = \rho_i(v_i - v) \qquad \text{and} \qquad \sum_{i=1}^{n} j_i = 0 \tag{2.8}$$

The molar diffusion flux of species i with respect to the molar-average velocity is given by

$$J_i = c_i(v_i - V) \qquad \text{and} \qquad \sum_{i=1}^{n} J_i = 0 \tag{2.9}$$

The mass flux n_i is relate to the mass diffusion flux as

$$n_i = j_i + \rho_i v_i = j_i + \omega_i n \tag{2.10}$$

The molar flux n_i is relate to the mass diffusion flux as

$$N_i = J_i + c_i V = J_i + y_i N \tag{2.11}$$

2.4.2 Fick's law of diffusion

The above observations were quantified by Fick in 1855, who proposed an extension of Fourier's 1822 heat-conduction theory. Fourier's first law of heat conduction is

$$q_z = -k \frac{dT}{dz} \tag{2.12}$$

where q_z is the heat flux by conduction in the positive z-direction, k is the thermal conductivity of the medium, and dT/dz is the temperature gradient, which is negative in the direction of heat conduction. Fick's first law of molecular diffusion also features proportionality between a flux and a gradient. For a binary mixture of A and B,

$$J_{Az} = -D_{AB} \frac{dc_A}{dz} \tag{2.13a}$$

and

$$J_{Bz} = -D_{BA} \frac{dc_B}{dz} \tag{2.13b}$$

where, in (2.13a), J_{Az} is the molar flux of A by ordinary molecular diffusion relative to the molar-average velocity of the mixture in the positive z direction, D_{AB} is the

mutual diffusion coefficient of A in B, c_A is the molar concentration of A, and dc_A/dz is the concentration gradient of A, which is negative in the direction of ordinary molecular diffusion. Similar definitions apply to (2.13b). The molar fluxes of A and B are in opposite directions. If the gas, liquid, or solid mixture through which diffusion occurs is isotropic, then values of k and D_{AB} are independent of direction. Nonisotropic (anisotropic) materials include fibrous and laminated solids as well as single, noncubic crystals. The diffusion coefficient is also referred to as the *diffusivity* and the mass diffusivity (to distinguish it from thermal and momentum diffusivities). Many alternative forms of (2.13a) and (2.13b) are used, depending on the choice of driving force or potential in the gradient. For example, we can express (2.13a) as

$$J_A = -cD_{AB}\frac{dx_A}{dz} \tag{2.14}$$

where, for convenience, the z subscript on J has been dropped, c = total molar concentration or molar density $(c = 1/\upsilon = \rho/M)$, and x_A = mole fraction of species A. Note that the equation (2.14) can also be written in the following equivalent mass form, where j_A is the mass flux of A by ordinary molecular diffusion elative to the mass-average velocity of the mixture in the positive z-direction, ρ is the mass density, and w_A is the mass fraction of A:

$$j_A = -\rho D_{AB}\frac{dw_A}{dz} \tag{2.15}$$

2.4.3 Diffusion coefficient

The chemical properties that have the most control over microscale mass transfer are the liquid- and gas-phase diffusion coefficients. The diffusion coefficient depends upon the pressure, temperature, and composition of the system. As one might expect from consideration of the mobility of the molecules, the diffusivities are generally higher for gases (in the range of 0.5 x 10^{-5} to 1.0 x 10^{-5} m²/s) than for liquids (in the range of 10^{-10} to 10^{-9} m²/s) which are higher than the values reported for solids (in the range of 10^{-14} to 10^{-10} m²/s). In the absence of experimental data, semi theoretical

expressions have been developed which give approximations, sometimes as valid as experimental values due to the difficulties encountered in their measurement.

Due to the absorption process which relate to the solubility of gaseous molecules in liquid phase, it can be stated that the knowledge about the molecular diffusion coefficients in liquid phase is one of the important parameters. Normally, the Stokes-Einstein equation is a purely theoretical method of estimation:

$$\left(D_{AB}\right)_{\infty} = \frac{RT}{6\pi\mu_B R_A N_A} \tag{2.16}$$

where R_A is the radius of the solute molecule and N_A is Avagadro's number. Although (2.16) is very limited in its application to liquid mixtures, it has long served as a starting point for more widely applicable empirical correlations for the diffusivity of solute (A) in solvent (B), where both A and B are of the same approximate molecular size. Unfortunately, unlike the situation in binary gas mixture, $D_{AB} = D_{BA}$ in binary liquid mixtures can vary greatly with composition. Because the Stokes Einstein equation does not provide a basis for extending dilute conditions to more concentrated conditions, extensions of (2.16) have been restricted to binary liquid mixtures dilute in A, up to 5 perhaps 10 mol%.

2.5 Interphase mass transfer mechanism

Many mass-transfer operations, however, involve the transfer of material between two contacting phases. These phases may be a gas stream contacting a liquid, two liquid streams if they are immiscible, or a fluid flowing past a solid. In this section, we shall consider the mechanism of steady-state mass transfer between phases.

2.5.1 Two-resistance theory

Interphase mass transfer involves three transfer steps, the transfer of mass from the bulk conditions of one phase to the interfacial surface, transfer across the interface into the second phase, and finally transfer to the bulk conditions of the second phase. A two-resistance theory, initially suggested by Whitman (1923), is often used to explain this process. The theory has two principal assumptions: the rate of mass

transfer between the two phases is controlled by the rates of diffusion through the phases on each side of the interface, and no resistance is offered to the transfer of the diffusing component across the interface. The transfer of component A from the gas phase to the liquid phase may be graphically illustrated as in Figure 2.5, with a partial pressure gradient from the bulk gas composition, $p_{A,G}$, to the interfacial gas composition, $p_{A,i}$, and a concentration gradient in the liquid from, $c_{A,i}$, at the interface to the bulk liquid concentration, $c_{A,L}$. If no resistance to mass transfer exists at the interfacial surface, $p_{A,i}$ and $c_{A,i}$ are equilibrium concentrations; these are the concentration values which would be obtained if the two phases had been in contact for an infinite period of time. The concentrations $p_{A,i}$ and $c_{A,i}$ are related by thermodynamic relations. The interfacial partial pressure, $p_{A,i}$, can be less than, equal to, or greater than $c_{A,i}$ according to the equilibrium conditions at the temperature and pressure of the system. When the transfer is from the liquid phase to the gas phase, $c_{A,L}$ will be greater than $c_{A,i}$ and $p_{A,i}$ will be greater than $p_{A,G}$.
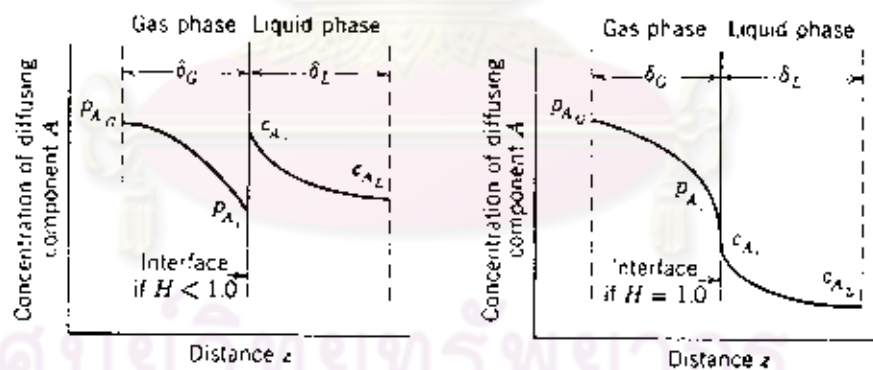
Figure 2.5 Concentration gradients between two contacting phases.

2.5.2 Individual mass transfer coefficients

Restricting our discussion to the steady-state transfer of component *A*, we can describe the rates of diffusion in the z direction on each side of the interface by the equations

$$N_{A,z} = k_G \left(p_{A,G} - p_{A,i} \right) \qquad (2.17)$$

and

$$N_{A,z} = k_L \left(c_{A,i} - c_{A,G} \right) \tag{2.18}$$

where k_G is the convective mass-transfer coefficient in the gas phase, in [moles of A transferred/(time) (interfacial area) (Δp_A units of concentration)]; and k_L is the convective mass-transfer coefficient in the liquid phase, in [moles of A transferred/(time) (interfacial area) (Δc_A units of concentration)]. The partial pressure difference, $p_{A,G} - p_{A,i}$, is the driving force necessary to transfer component A from the bulk gas conditions to the interface separating the two phases. The concentration difference, $c_{A,G} - c_{A,i}$, is the driving force necessary to continue transfer of A into the liquid phase. Under steady-state conditions, the flux of mass in one phase must equal the flux of mass in the second phase. Combining equations (2.17) and (2.18), we obtain

$$N_{A,z} = k_G \left(p_{A,G} - p_{A,i} \right) = k_L \left(c_{A,i} - c_{A,L} \right) \tag{2.19}$$

The ratio of the two convective mass-transfer coefficients may be obtained from equation (2.19) by rearrangement, giving

$$-\frac{k_L}{k_G} = \frac{p_{A,G} - p_{A,i}}{c_{A,L} - c_{A,i}} \tag{2.20}$$
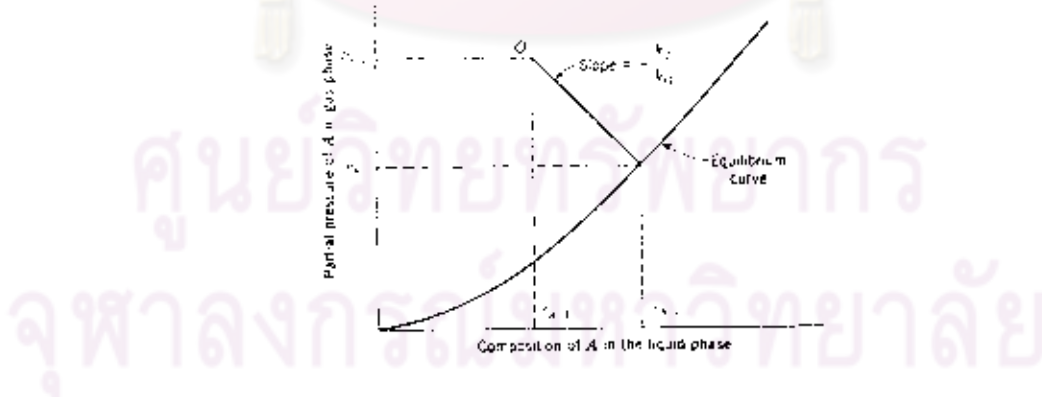
Figure 2.6 Interfacial compositions as predicted by the two-resistance theory.

2.5.3 Overall mass transfer coefficients

It is quite difficult to measure physically the partial pressure and concentration at the interface. It is therefore convenient to employ overall coefficients based on an overall driving force between the bulk compositions, $p_{A,G}$ and $c_{A,L}$. An overall mass transfer coefficient may be defined in terms of a partial pressure driving force. This coefficient, K_G, must account for entire diffusional resistance in both phases; it is defined by

$$N_A = K_G \left(p_{A,G} - p_A * \right) \tag{2.21}$$

where $p_{A,G}$ is the bulk composition in the gas phase; $p_A *$ is the partial pressure of A in equilibrium with the bulk composition in the liquid phase, $c_{A,L}$, and K_G is the overall mass-transfer coefficient based on a partial pressure driving force, in moles of A transferred/(time) (interfacial area) (pressure). Since the equilibrium distribution of solute A between the gas and liquid phases is unique at the pressure and temperature of the system, then $p_A *$, in equilibrium with $c_{A,L}$, is as good a measure of $c_{A,L}$ as $c_{A,L}$ itself, and it is on the same basis as $p_{A,G}$. An overall mass transfer coefficient, K_L, including the resistance to diffusion in both phases in terms of liquid phase concentration driving force, is defined by

$$N_A = K_L \left(c_A * - c_{A,L} \right) \tag{2.22}$$

where $c_A *$ is the concentration of A in equilibrium with $p_{A,G}$ and is accordingly, a good measure of $p_{A,G}$; K_L is the overall mass-transfer coefficient based on a liquid concentration driving force, in [moles of A transferred/(time) (interfacial area) (moles/volume)]. Figure 2.7 illustrates the driving forces associated with each phase and the overall driving forces. The ratio of the resistance in an individual phase to the total resistance may be determined by:

$$\frac{\text{resistance in gas phase}}{\text{total resistance in both phases}} = \frac{\Delta p_{A,gasfilm}}{\Delta p_{A,total}} = \frac{1/k_G}{1/K_G} \tag{2.23}$$

$$\frac{\text{resistance in liquid phase}}{\text{total resistance in both phases}} = \frac{\Delta c_{A,liquidfilm}}{\Delta c_{A,total}} = \frac{1/k_L}{1/K_L} \tag{2.24}$$
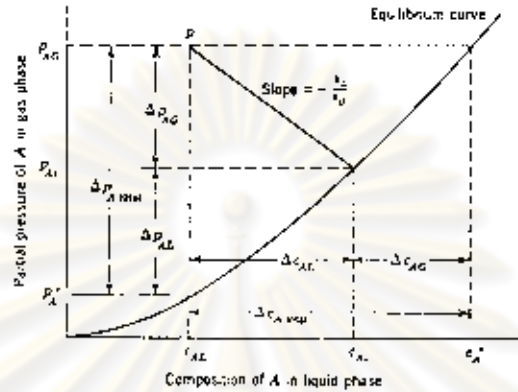
Figure 2.7 Concentration driving forces for two-resistance theory.

A relation between these overall coefficients and the individual phase coefficients can be obtained when the equilibrium relation is linear as expressed by

$$p_{A,i} = mc_{A,i} \tag{2.25}$$

This condition is always encountered at low concentrations, where Henry's law is obeyed; the proportionality constant is then the Henry's law constant, H. Utilizing equation (2.25), we may relate the gas- and liquid-phase concentrations by:

$$p_{A,G} = mc*$$
$$p_A* = mc_{A,L}$$
$$y_{A,G} = mx_A*$$

Rearranging equation (2.21),

$$\frac{1}{K_G} = \frac{p_{A,G} - p_A*}{N_{A,z}} = \frac{p_{A,G} - p_{A,i}}{N_{A,z}} + \frac{p_{A,i} - p_A*}{N_{A,z}}$$

or, in terms of m,

$$\frac{1}{K_G} = \frac{p_{A,G} - p_{A,i}}{N_{A,z}} + \frac{m(c_{A,i} - c_{A,L})}{N_{A,z}} \tag{2.26}$$

The substituting of equation (2.17) in (2.18) into the above relation relates K_G to the individual phase coefficients by

$$\frac{1}{K_G} = \frac{1}{k_G} + \frac{m}{k_L} \qquad (2.27)$$

A similar expression for K_L may be derived as follows:

$$\frac{1}{K_L} = \frac{c_A * - c_{A,L}}{N_{A,z}} = \frac{p_{A,G} - p_{A,i}}{m N_{A,z}} + \frac{(c_{A,i} - c_{A,L})}{N_{A,z}}$$

or

$$\frac{1}{K_L} = \frac{1}{m k_G} + \frac{1}{k_L} \qquad (2.28)$$

Equation (2.27) and (2.28) stipulate that the relative magnitudes of the individual phase resistances depend on the solubility of the gas, as indicated by the magnitude of the proportionality constant.

- For a system involving a soluble gas, such as ammonia in water, m is very small. From equation (2.27), we may conclude that the gas-phase resistance is essentially equal to the overall resistance in such a system. When this is true, the major resistance to mass transfer lies in the gas phase, and such a system is said to be *gas phase controlled*.

- Systems involving gases of low solubility, such as carbon dioxide in water, have such a large value of m that equation (2.28) stipulates that the gas-phase resistance may be neglected, and the overall coefficient, K_L, is essentially equal to the individual liquid phase coefficient, k_L. This type of system is designated *liquid-phase controlled*. In many systems, both phase resistances are important and must be considered when evaluating the total resistance.

2.6 Overall mass transfer coefficient in liquid phase ($K_L a$)

Concerning to the VOCs with low solubility in water, it can be note that the mass transfer process is controlled by the liquid phase. Therefore, the $K_L a$ coefficient is

used in order to analyse the absorption process and the K_La determination procedure can be described as follows;

- Measuring the variation of gas concentration in the outlet of bubble column with time: if the outgoing gas concentration are followed until the saturated condition, for this small bubble column, the mass balance equation can be applied:

$$Q_g C_{g,in} = Q_g C_{g,out}(t) + V_L \frac{dC_L(t)}{dt} \tag{2.29}$$

where Q_g is the flow rate and V_L is the absorbent volume, $C_{g,in}$ and $C_{g,out}$ are the inlet and outlet concentration of hydrophobic VOCs in the gas phase, respectively.

- Then, the concentration of VOCs in the liquid phase $C_L(t)$ can be expressed by:

$$C_L(t) = \frac{Q_g}{V_L} \left(C_{g,in} t - \int C_{g,out}(t) dt \right) \tag{2.30}$$

From this equation, the variation of the VOCS concentration in the liquid phase with the time and also the saturated VOCs concentration (C_L^S) can be obtained.

- Based on the Non-stationary or dynamic method (Deckwer, 1992), the overall mass transfer coefficient in liquid phase (K_La) is given by the following equation;

$$\frac{dC_L}{dt} = k_L a (C_L^S - C_L) \tag{2.31}$$

or, in its integral from by:

$$\ln[C_L^S - C_L] = \ln(C_L^S) - k_L a \cdot t \tag{2.32}$$

where C_L and C_L^S are the hydrophobic VOCs concentration and the saturation VOCs concentration in the liquid phase, respectively. Thus, the K_La coefficient can be deduced from the slope of the curve relating the variation of $\ln(\Delta C)/C_L^S$ with time.

2.7 Bubble hydrodynamic parameter

Since bubble hydrodynamic parameters is one of the parameters that effect to the treatment efficiency of hydrophobic VOCs by absorption process. Thus, this part will describe the determination method based on these parameters in order to understand their effect on VOCs bubble characteristics on absorption mechanism and also to calculate the associated interfacial area.

2.7.1 Bubble diameter (D_B)

In practice, the measurement of bubble diameter at any flow rate (Q_g) can be performed by Image Treatment Techniques. Normally, 200-300 bubbles obtained with any gas flow rate were captured and analyzed to be a good statistical representative. In this research, the average diameter (d_{avg}) and Sauter diameter (d_{32}) were calculated from equation (2.33) and (2.34) respectively.

$$d_{avg} = \frac{\sum_{i=1}^{N} d_i}{N} \tag{2.33}$$

$$d_{32} = \frac{\sum_{i=1}^{N} d_i^3}{n \sum_{i=1}^{N} d_i^2} \tag{2.34}$$

Moreover, size of gas bubbles depends upon the rate of flow through the orifices, the orifice diameter, the fluid properties, and the extent of turbulence prevailing in the liquid. What follows is for cases where turbulence in the liquid is solely that generated by the rising bubbles and when orifices are horizontal and sufficiently separated to prevent bubbles from adjacent orifices from interfering with each other.

- **Very slow gas flow rate**: For water-like liquids, the diameter can be computed by equating the buoyant force on the immersed bubble, which tends to lift the bubble away from orifice, to the force due to surface tension, which tends to retain the bubble at the orifice. This provides the correlation as:

$$d_B = \left(\frac{6d_o \sigma g_e}{g \, \Delta p} \right)^{1/3} \tag{2.35}$$

- **Intermediate flow rates**: The bubbles generated in this zone are larger than those described above, although still fairly uniform, they form in chains rather than separately.

For air-water,

$$d_P = 0.0287.d_o^{1/2} \, Re_e^{1/3} \tag{2.36}$$

For other gases and liquids,

$$d_P = \left(\frac{72 \text{pL}}{\pi^2 g \Delta p} \right)^{1/4} \cdot Q_{G0}^{0.4} \qquad (2.37)$$

- **Large gas rates:** In this zone, jets of gas which rise from orifice break into bubbles at some distance from the orifice. The bubbles smaller than those described above and non-uniform in size. For air-water orifice diameters 0.4 to 1.6 m

$$d_{B(m)} = 0.0071 \cdot Re_e^{-0.05} \qquad (2.38)$$

For the transition range (Re_o = 2,100 to 10,000) there is no correlation of data. It is suggested that d_B for air-water can be approximated by the straight line on log-log coordinates between the points given by d_B at Re_o = 2,100 and Re_o = 10,000.

2.7.2 Bubble rising velocity (U_B)

Typically, the steady-state rising velocity of single gas bubbles, which occurs when the buoyant force equals the drag force on the bubbles, varies with the bubble diameter as shown in Figure 2.8
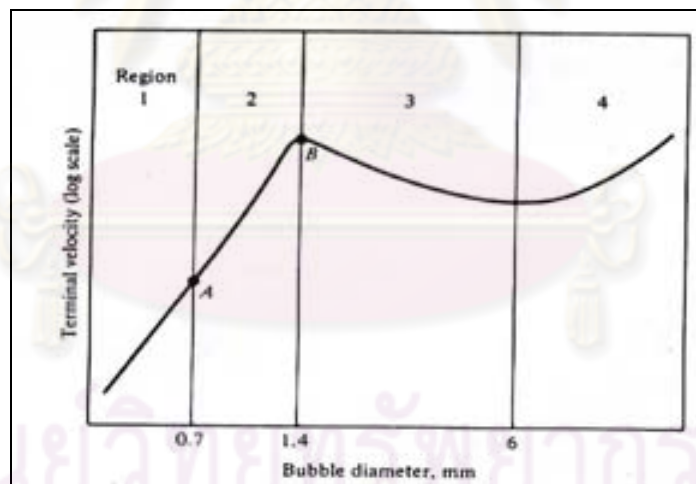
Figure 2.8 Rising (terminal) velocity of single gas bubbles.

- **Region 1, d_p < 0.7 mm:** The bubbles are spherical, and they behave like rigid spheres, for which the terminal velocity is given by Stokes' law:

$$V_T = \frac{g d_p^2 \Delta p}{18 \mu L} \qquad (2.39)$$

- **Region 2, 0.7 mm < d_p < 1.4 mm:** The gas within the bubble circulates, so that the surface velocity is not zero. Consequently the bubble rises faster than rigid

spheres of the same diameter. There is no correlation of data; it is suggested that V_t may be estimated as following the straight line on Fig. 2.8 drawn between points A and B.

- **Regions 3, (1.4 mm < d_p < 6 mm) and 4 (d_p > 6 mm):** The bubbles are no longer spherical and in rising follow a zigzag or helical path. For region 4 the bubbles have a spherically shaped cap. In both these regions for liquids of low viscosity.

$$V_T = \sqrt{\frac{2\sigma g_e}{d_p \rho L} + \frac{gd_p}{2}} \qquad (2.40)$$

However the behavior of large numbers of bubbles crowded together is different from that of isolated bubbles. Rising velocities are smaller because of crowding, and bubble diameter may be altered by liquid turbulence, which causes bubble breakup, and by coalescence of colliding bubbles. From Painmanakul *et al.,* (2005) bubble rising velocity were calculated by taking picture of bubble in reactor to analyze its distance at any time frame (t_{frame}), thus, the bubble rising velocity were calculated from equation (2.41)

$$U_B = \frac{\Delta D}{t_{frame}} \qquad (2.41)$$

U_B = bubble rising velocity (cm/s)

ΔD = the distance between two frames (cm)

t_{frame} = time frame (s)

2.7.3 Bubble formation frequency (f_B)

Bubble formation frequency is the number of bubble generated within one second. From Painmanakul *et al.,* (2005), it can be calculated from the number of orifice multiply with gas flow rate of each orifices, then divided by volume of bubble as shown in equation (2.42):

$$f_B = \frac{N_{OR} \times q}{V_B} \qquad (2.42)$$

where	f_B	=	Bubble formation frequency, s^{-1}
	N_{OR}	=	Number of orifices
	q	=	Gas flow rate through the orifice, m^3/s
	V_B	=	Bubble volume, m^3

2.8 Interfacial area (a)

Interfacial area is the ratio of interfacial area of bubble and capacity of reactor at a certain time. Since there are limitation of data analysis such as Chemical Method, size of reactor, type of bubble generator, and condition, thus interfacial area (a) normally is included with mass transfer coefficient.

To understand the mechanism of mass transfer of bubble generator, this research will determine experimentally the value of a based on the bubble hydrodynamic parameters. Normally, the interfacial area is defined as the ratio between the total bubble surfaces (S_B) and the total volume in reactor (V_{Total}). Note that the values of S_B is the product of number of bubbles and bubble surface. The number of bubbles (N_B) is deduced from the terminal rising bubble velocities (U_B) and the bubble formation frequency (f_B) as:

$$N_B = f_B \times \frac{H_L}{U_B} \qquad (2.43)$$

$$a = N_B \times \frac{S_B}{V_{total}} = f_B \times \frac{H_L}{U_B} \times \frac{\pi D_B^2}{AH_L + N_B V_B} \qquad (2.44)$$

Where	a	=	Interfacial area, m^{-1}
	N_B	=	Number of bubbles generated
	S_B	=	Total bubble surface, m^2
	V_{total}	=	Total volume in reactor, m^3
	f_B	=	Bubble formation frequency, s^{-1}
	H_L	=	Liquid height, m
	U_B	=	Bubble rising velocity (cm/s)
	D_B	=	Bubble diameter, m
	A	=	Cross-sectional area of reactor, m^2
	V_B	=	Bubble volume, m^3

2.9 Liquid-side mass transfer coefficient (K_L)

Normally, the product of the liquid-film (side) mass transfer coefficient (K_L) and interfacial area (a) is know as the overall volumetric mass transfer coefficient (K_La). Note that the subscribe L related with the K coefficient correspond to the mass transfer resistances obtained with the liquid phase. Thus, in the case of hydrophobic VOCs, the liquid-film mass transfer coefficient can be determined by:

$$K_L = \frac{K_L a}{a} \qquad (2.45)$$

K_L =   Liquid-film mass transfer coefficient (m/s)

K_La =   The overall mass transfer coefficient in liquid phase (s^{-1})

a   =   specific interfacial area (m^{-1})

2.10 Surfactant

Surfactants are one of the most widely used class of chemicals in the chemical process industry under a variety of names such as detergents, coagulants, dispersants, emulsifiers, de-emulsifiers, foaming agents, and defoamers. They are used in diverse products such as detergents, paints, pharmaceuticals, and motor oil. Of late, surfactants have found application in such high technology areas as magnetic recording, microelectronics, biotechnology, and viral research. At the molecular level, a surfactant is an organic compound (Figure 2.9) that contains at least one lyophilic ("solvent-loving") and one lyophobic ("solvent-fearing) group in the molecule. If the solvent in which the surfactant is to be used is water or an aqueous solution, the respective terms are hydrophilic and hydrophobic.

Surfactants reduce the surface tension of water by adsorbing at the liquid-gas interface. They also reduce the interfacial tension between oil and water by adsorbing at the liquid-liquid interface. Many surfactants can also assemble in the bulk solution into aggregates. Examples of such aggregates are vesicles and micelles. The concentration at which surfactants begin to form micelles is known as the critical micelle concentration or CMC. When micelles form in water, their tails form a core

that can encapsulate an oil droplet, and their (ionic/polar) heads form an outer shell that maintains favorable contact with water. When surfactants assemble in oil, the aggregate is referred to as a reverse micelle. In a reverse micelle, the heads are in the core and the tails maintain favorable contact with oil.
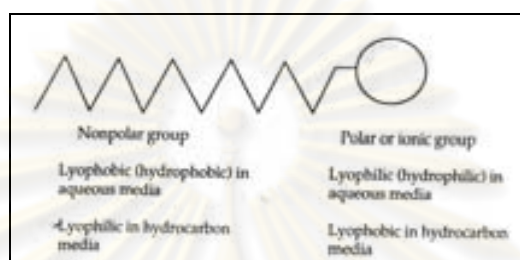
Figure 2.9 Generalized surfactant structures.

2.10.1 Classification of surfactant

A surfactant can be classified by the presence of formally charged groups in its head as shown in Figure 2.10. A non-ionic surfactant has no charge groups in its head. The head of an ionic surfactant carries a net charge. If the charge is negative, the surfactant is more specifically called anionic; if the charge is positive, it is called cationic. If a surfactant contains a head with two oppositely charged groups, it is termed zwitterionic. Some commonly encountered surfactants of each type include:

- **Cationic surfactant** is the surfactant that the surface-active part is cation. It is usually salt of quaternary ammonium hydroxide, which its hydrogen of the ammonium ion have been replaced with alkyl groups. Cationic surfactants are quite expensive. But they are noted for their disinfecting property. The symbol of the surfactant contains "plus" sign**.**

- **Anionic surfactant** is the surfactant that ionizes to yield a positive charge, free ion and a negative charge which localizes at the interface. Its symbol contains a "minus" sign in the head. This type of surfactant is relatively cheap and widely used in industries. Common anionic surfactants are, i.e.,Soaps, dodecyl or lauryl alcohol.

- **Non-ionic surfactant** is the surfactant that does not ionize and have to depend on groups in the molecule to make it soluble. The groups are usually polymers of

ethylene oxide (C_2H_4O). The symbol of the surfactant, in this case, contains no sign. Examples of the surfactants are polyethyleneglycol monooleate, nonylphynol ethoxylene of ethylene oxides. The surfactants are noted for adjustable hydrophil-lipophil properties.

- **Amphoteric surfactant** is the surfactant that contains both positive and negative surface-active part. Its symbol contains 2 circles, one with minus sign, and another with plus sign**.**
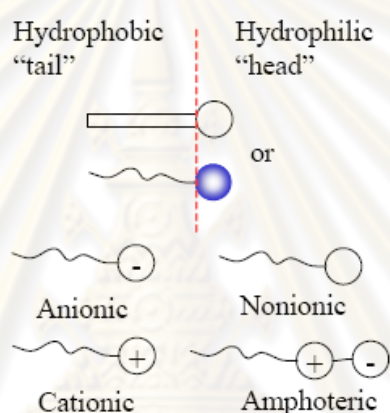
Figure 2.10 Symbols of surface active agent

2.10.2 Micelle

A micelle is an aggregate of surfactant molecules dispersed in a liquid colloid. A typical micelle in aqueous solution forms an aggregate with the hydrophilic "head" regions in contact with surrounding solvent, sequestering the hydrophobic tail regions in the micelle centre as shown in Figure 2.11. This type of micelle is known as a normal phase micelle (oil-in-water micelle). Inverse micelles have the head groups at the centre with the tails extending out (water-in-oil micelle). Micelles are approximately spherical in shape. Other phases, including shapes such as ellipsoids, cylinders, and bilayers are also possible. The shape and size of a micelle is a function of the molecular geometry of its surfactant molecules and solution conditions such as surfactant concentration, temperature, pH, and ionic strength. The process of forming micelle is known as micellisation and forms part of the phase behavior of many lipids according to their polymorphism.
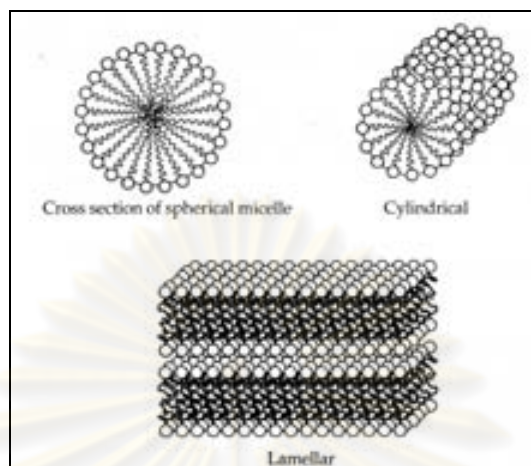
Figure 2.11 Micella shapes.

Micelles only form when the concentration of surfactant is greater than the critical micelle concentration (CMC), and the temperature of system is greater than the critical micelle temperature, or Krafft temperature. The formation of micelles can be understood using thermodynamics: micelles can form spontaneously because of a balance between entropy and enthalpy. When surfactants are present above the CMC, they can act as emulsifiers that will allow a compound normally insoluble (in the solvent being used) to dissolve. This occurs because the insoluble species can be incorporated into the micelle core, which is itself solubilized in the bulk solvent by virtue of the head groups' favorable interactions with solvent species. The most common example of this phenomenon is detergents, which clean poorly soluble lipophilic material (such as oils and waxes) that cannot be removed by water alone. Detergents also clean by lowering the surface tension of water, making it easier to remove material from a surface. Normally, the mechanisms of absorption organics are depend on the form of aggregation of surfactant as show in Figure 2.12. The surfactant is form to micelle that is monolayer as in Figure 2.12A, thus the surfactant is form to admicelle that is bi-layer as in Figure 2.12B.
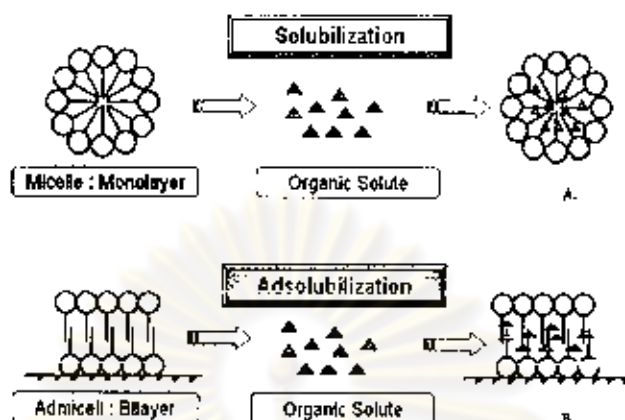
Figure 2.12 The mechanism of absorption of surfactant

Moreover, the surfactant can be absorbed VOCs. The capabilities of VOCs absorption are depend upon the concentration of surfactant. If the concentration is increase, the aggregation of surfactant to form micelle is increase; the capable of absorb is increase too, thus, the tail part of surfactant are absorbed the VOCs due to the non-polar part or hydrophobic part.

2.11 Emulsions

Emulsions are colloidal dispersions in which a liquid is dispersed in a continuous liquid phase of different composition. The dispersed phase is sometimes referred to as the internal (disperse) phase and the continuous phase as the external phase. Practical emulsions may well contain droplets that exceed the classical size range limits given above, sometimes ranging upwards to tens or hundreds of micrometers. In most emulsions, one of the liquids is aqueous while the other is hydrocarbon and referred to as oil.

2.11.1 Emulsion type

Two types of emulsion are readily distinguished in principle, depending upon which kind of liquid forms the continuous phase.

Whether an O/W emulsion (oil-in-water for oil droplets dispersed in water) or a W/O emulsion (water-in-oil for water droplets dispersed in oil) is mainly determined by the relative hydrophobicity of the surfactant tail and the hydrophilicity of the head

group. According to Bancroft's rule (1913), a rough guide is that the continuous phase will be that in which the surfactant is preferentially soluble. A more quantitative prediction is provided by the HLB (hydrophilic-lipophilic balance) of the surfactant. The HLB can be determined from the chemical formula of the surfactant using empirically determined 'group numbers'. Table 2.4 summarizes the classification of emulsifiers according to this scale.

Table 2.4 Classification of emulsifiers according to HLB values

Range of HLB values	Application
3-6	W/O emulsifier
7-9	Wetting agent
8-18	O/W emulsifier
12-15	Detergent
15-18	Solubilising agent

Even the HLB method is only semi-empirical and other factors can have a considerable influence on the type of emulsion formed. The most important is the relative phase-volume of oil and water. A more general relation would be one that expressed the phase-volume of oil, at which an emulsion inverts from O/W to W/O, as a function of the HLB of the surfactant. Examples of emulsions include butter and margarine, milk and cream, espresso, mayonnaise, the photo-sensitive side of photographic film, magmas and cutting fluid for metal working. In butter and margarine, oil surrounds droplets of water (a water-in-oil emulsion). In milk and cream, water surrounds droplets of oil (an oil-in-water emulsion). In certain types of magma, globules of liquid NiFe may be dispersed within a continuous phase of liquid silicates.

Practical situations are not always so simple and one may encounter double emulsions, that is, emulsions that are oil-in-water-in-oil (O/W/O) and water-in-oil-in-water (W/O/W). For example, O/W/O denotes a double emulsion, containing oil phase. The double emulsion droplets can be quite large (tens of μm) and can contain many tens of droplets of the ultimate internal phase.

2.11.2 Formation and stability of emulsions

Emulsions, that are dispersions of one liquid in another immiscible liquid, are of immense importance in many areas of technology as well as in nature. Milk is an emulsion and the process of emulsification plays an important part in the digestion of dietary fats. Many food products, such as butter, low-fat spreads and mayonnaise are emulsions and their rheological and stability behavior are important to their aesthetic as well as their storage properties. Many products, in addition to foods, are formulated as emulsions. These include agrochemicals, pharmaceuticals, cosmetics, paints, and drilling fluids. There are many different reasons for formulating such products as emulsions and, in most cases, surfactants play a central role. Because of their practical importance as well as their great scientific interest, a considerable amount of literature has appeared in the area of emulsions. In stead, the role played by the surfactant, especially dynamic aspects relevant to the stability and rheology of emulsions, will be examined.

For the effect to prevail, the interfacial tension between oil and water phases must be very low. Provided that sufficient surfactant is present, subdivision continues until a droplet size is reached that is controlled mainly by the preferred interface curvature; otherwise the droplet size is governed by the ratio of surfactant to disperse phase. Microemulsions are therefore transparent since such tiny droplets are usually an order of magnitude smaller than the wavelength of visible light. In contrast, in conventional emulsions, the interfacial tension is not usually so low, and mechanical energy has to be supplied in order to produce the desired droplet-size distribution. As a consequence, emulsions are not thermodynamically stable and it is the role of the surfactants adsorbed at the interface to create sufficient ' kinetic stability' to be useful on a time scale appropriate to the particular product or process.

Clues as to how surfactants produce stability are provided by examining some of the rules for good emulsion formulation that have been established by practical experience, before which it is necessary to define various aspects of stability as applied to emulsions, and these are depicted in Figure 2.13. A detailed description of each of these processes can be summarized briefly as follows:

1.   Creaming is caused by the action of gravity or a centrifugal field and produces a vertical gradient in concentration of the droplets without changing the droplet size distribution.

2.   Flocculation is the aggregation of droplets due to attractive van der Waals forces, again with no change in size distribution. At low volume fraction of dispersed phase, flocculation can assist creaming and at high volume fraction can retard it by establishing a structured network within the emulsion.

3.   Coalescence is the fusion of droplets to produce larger droplets with the elimination of some liquid/liquid interface. This irreversible change would require the input of further mechanical energy to restore the original size distribution.

4.   Ostwald ripening is the growth of large droplets at the expense of smaller ones and occurs when the dispersed phase has a finite solubility in the continuous phase. The driving force is the higher internal pressure (and hence higher chemical potential) in the smaller drops due to the interfacial tension.
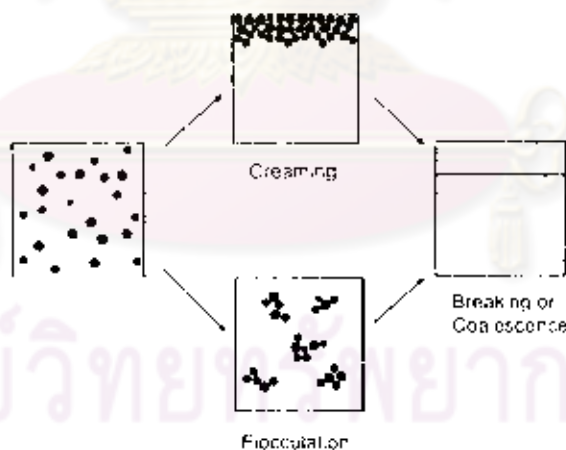
Figure 2.13 Schematic diagram showing the various types of instability in emulsions

The two irreversible changes are coalescence and Ostwald ripening. Other than reducing the interfacial tension, surfactants can do little to alter the rate of increase of mean particle size due to Oswald ripening and it is by their influence on the process of coalescence that they have the greatest impact on emulsion stability.

2.12 Literature review

1. Study of bubble hydrodynamic behavior in bubble column

Loubière and Hébrard, (2002) have investigated the bubble formation in an inviscid liquid for different flexible orifices (industrial membrane spargers) and gas flow rates. The results shown that increasing gas flow rate intensifies the phenomenon of the bubble spread on the membrane surface. The variation in the bubble diameter at detachment as a function of gas flow rate is logarithmic. The industrial membranes produce bubbles of comparable sizes. Nevertheless, significant differences in the bubble frequencies between membranes are observed, involving different gas hold-up.

Loubière and Hébrard, (2003) have studied the influence of surfactants on the bubble hydrodynamic parameters at different gas spargers, especially on the generated bubble diameter (D_B), the associated bubble frequency (f_B) and the interfacial area (a). These authors have observed that the effect of surface tension on the bubble generated depends on the type of orifice (flexible and rigid) and should be analyzed in terms of dynamic surface tension and of kinetics of surfactant molecule adsorption and diffusion.

Painmanakul *et al.,* (2004) compared two flexible membranes used in waste water treatment. The bubble generations at the membranes with a single orifice and with four orifices have been studied and their performances have been compared in terms of interfacial area and power consumption. This study has shown that the membranes used in industrial work can be characterized and can be compared by considering their physical properties, the bubble generation process and their performances. However, the hole number and the membrane operating life which is linked to its elasticity should also be taken into account when comparing membranes.

2. Mass transfer enhancement of gas absorption

Peeva *et al.* (2001) have used the water-silicone oil as absorbent and made several emulsion composition varying from zero to 90% water. It was established that the volumetric mass transfer coefficient based on the emulsion volume is independent of the emulsion composition. A small fraction of silicone oil may be enough to provide a strong enhancement of VOCs absorption.

Painmanakul *et al.* (2005) study the effect of surfactants (cationic and anionic) on bubble generation phenomenon, interfacial area and liquid-side mass transfer coefficient. The local liquid-side mass transfer coefficient (K_L) was obtained from the volumetric mass transfer coefficient (K_La) and the interfacial area (a) was deduced from the bubble diameter (D_B), the bubble frequency (f_B) and the terminal bubble rising velocity (U_B). They report that the volumetric mass transfer coefficient increases with the gas flow rates whatever the liquid phases and the K_La and K_L values for both surfactants are significantly smaller. Also the liquid-side mass transfer coefficient remains roughly constant for a given liquid phase whatever the bubble diameters.

Heymes *et al.* (2006) have provided the hydrophobic absorption more competitive by selecting an efficient absorbent. Note that they have studied the efficiency and mass transfer parameters in a packed column. Four chemical classes were tested (i) polyethylene glycols, (ii) phthalates (iii) adipates and (iv) silicon oil. They discover that di(2-ethylhexyl) adipate can be the best suits the requirements to be used as an absorbent.

Dumont *et al.* (2006) have studied the mass transfer coefficients of styrene and oxygen into silicone oil emulsion at a constant gas flow rate for the whole range of emulsion composition (0-10% v/v). In the case of styrene absorption, it was found that the volumetric mass transfer coefficient based on the emulsion volume is roughly constant with the increase in the emulsion composition. Moreover, water–silicone oil emulsions remain relevant to treat low-solubility volatile organic compounds, such as styrene, in low-concentration gas streams.

Franck L. *et al.* (2007) have developed the technique of VOCs treatment by using a bioscrubber and tested a washing agent made up of water and cutting oil in order to optimize the VOCs mass transfer. The results show that the addition of oil strongly increases the quantity of transferred aromatics. For these compounds, the apparent mass transfer coefficient k_La is lower than with water alone. In term of bioscrubbing performances, comparison of the results obtained with the water–oil mixture and water alone showed that the removal efficiency for aromatics is enhanced: from 12% to 36% (applied load of 852 gVOCs m^{-3}.h^{-1}); the elimination of chlorinated compounds is slightly improved.

3. Research focuses

Based on various literature reviews, it can be stated that the bubble hydrodynamic behaviors and also the mass transfer mechanisms are the important factors that can affect the absorption performance. Therefore, in order to enhance the absorption of hydrophobic gases (VOCs in this study), it is essential to determine and associate both parameters for well understanding the mechanism. Moreover, the complexities of solutions with surfactants and organic substances (oily emulsion), used as absorbents in this work, should be considered in terms of bubble hydrodynamic and mass transfer parameters.

Therefore, this research is mainly focused on the study of hydrophobic VOCs absorption in terms of bubble hydrodynamic and mass transfer parameters. Moreover, the local experimental methods for measuring the bubble hydrodynamic and mass transfer coefficient are used in order to enables the VOCs mass transfer efficiency to be effectively controlled whatever the operating conditions.

CHAPTER III

METHODOLOGY

3.1 Research overview

The objective of this research was to study the absorption mechanism for removing the hydrophobic Volatile Organic Compounds (VOCs) in small bubble column. The bubble hydrodynamic and mass transfers parameters from the gas phase to the liquid phase were the key parameters of this study. Research flow chart can be illustrated in Figure 3.1.
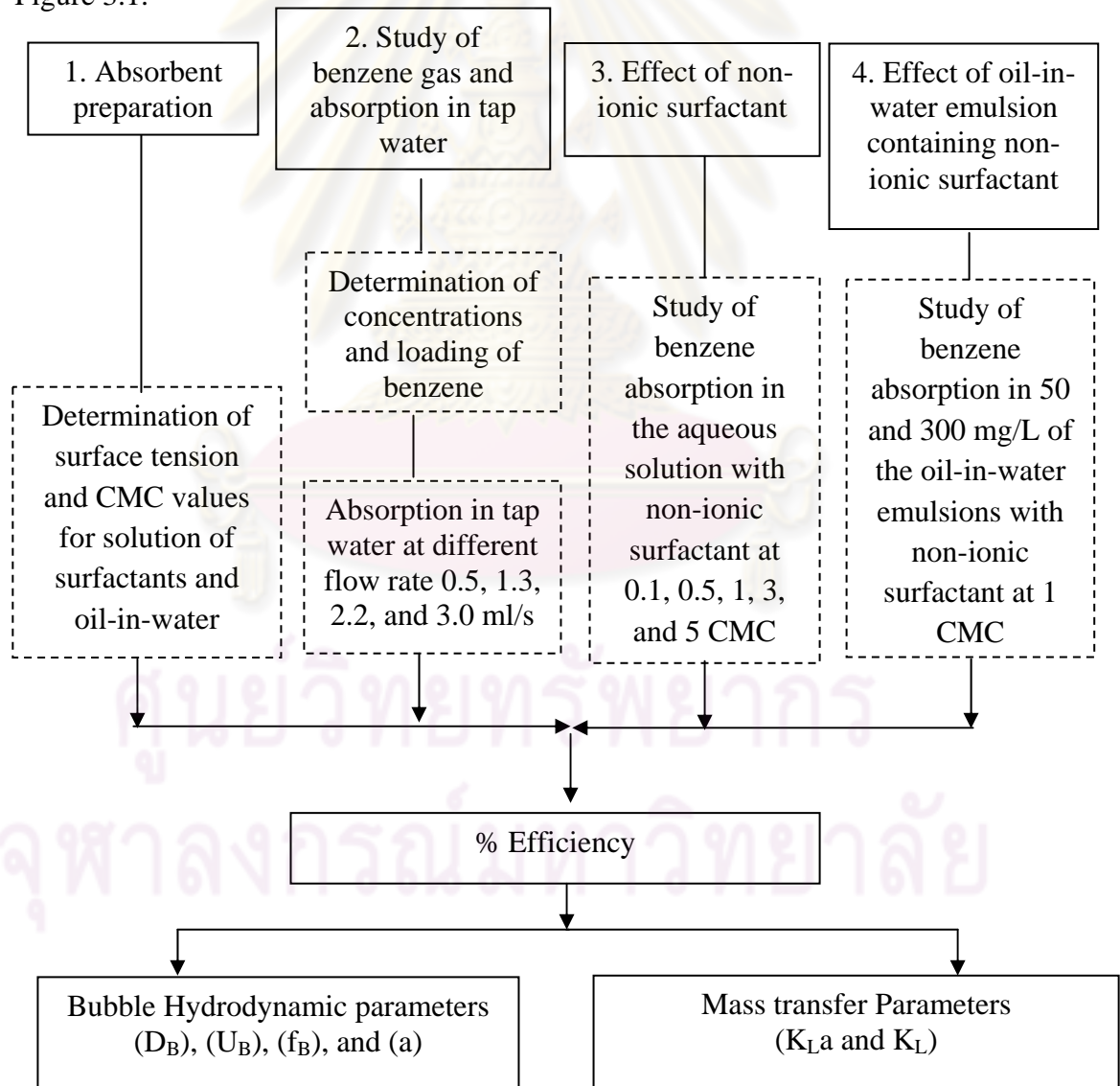
Figure 3.1 Flow chart of the research

3.2 Experimental set-up

The experiment set up was schematically represented in Figure 3.2. The experiments were carried out in a small bubble column 4.4 cm in diameter and 30 cm in height. Tap water, aqueous solution with non-ionic surfactant, and stabilized oil-in-water emulsion were used as liquid absorbents. Benzene (hydrophobic VOCs) was applied as absorbate. Moreover, the hot plate was used for generating the VOC gases at T = $85\pm3^{o}C$. In this study, the air tank was used for injecting the mixture of VOCs gas and air through the bubble column. The average gas flow rate from air tank was measured by using the soap film meter.
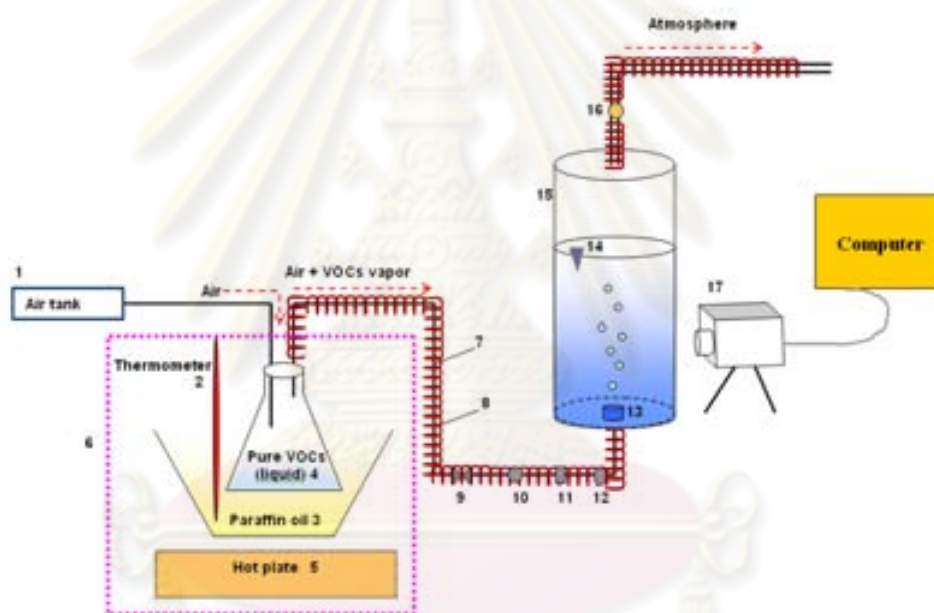
Figure 3.2 Schematic diagram of the experimental set up.

1) Air zero tank

2) Thermometer

3) Paraffin oil

4) Pure VOCs (liquid)

5) Hot plate

6) VOC generator

7) Stainless steel

8) Heating tape

9) Valve control flow rate

10) Septum for sampling gas (in)

11) Soap film meter

12) Manometer

13) Bubble generator

14) Absorbent

15) Bubble column

16) Septum for sampling gas (out)

17) Acquisition computer & Camera

In order to generate the VOCs bubbles, the single puncture rigid orifice made from PVC plastic was applied and located at the centre at bottom column: the rigid orifice was 0.65 mm in diameter. In this study, the bubble column reactor was a closed system. The bottom of reactor was drilled for installing the orifice diffuser in order to inject the VOCs gas bubble. Moreover, the top and bottom of reactor have the septum (sampling point) for collecting the inlet and outlet VOC gases, respectively. Then, the associated VOCs concentrations (in gas phase) were measured by using gas chromatography with a Flame Ionisation Detector (FID). In order to analyze the bubble hydrodynamic mechanism, the high speed camera (100 images/second) and image analysis program were used to determine the bubble hydrodynamic parameters.
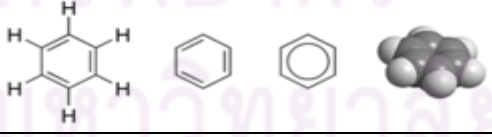
3.3 Materials

3.3.1 Chemical agents

3.3.1.1 Volatile Organic Compounds (VOCs)

In this study, Benzene, purchased from S.R.LAB Company, was used as hydrophobic VOCs. Frequently, it was encountered in industrial gaseous emissions (as in printing or in transportation industries). The major interest of these molecules was the very low solubility in water, which enables us to study the absorption efficiency in alternative operating conditions. Note that, Henry's constant reported for benzene was equal to 11.32×10^5 Pa and confirms its low solubility in water.

Table 3.1 Physical and chemical properties of benzene

Property	Characteristic
Structure	
Molecular formula	C_6H_6
Molar mass	78.1 g/mol
Density	0.8786 g/cm^3, liquid
Boiling point	80.1 ^{o}C
Solubility in water	1.8 g/L (25 ^{o}C)
Viscosity	0.652 cP at 20 ^{o}C

Source: Wikipedia (2008), http://en.wikipedia.org/wiki/Benzene.

<u>3.3.1.2 Absorbents used in this study</u>

In order to study the absorption mechanism of benzene in small bubble column, the different chemical agents can be summarized as follows:

- Tap water;

- Tween80 (Carlo Erba Co., Ltd): it was used as non-ionic surfactant with different concentrations at 0.1, 0.5, 1, 3, and 5 Critical Micelle Concentration, CMC;

- Lubricant oil (PTT V-120 manufactured by Petroleum Authority of Thailand (PTT). Stabilized oil-in-water emulsions were containing non-ionic surfactants at Critical Micelle Concentration (CMC).

3.3.2 Equipments

1. Tensiometer K10T, Kruss, Germany
2. Gas chromatography Detector FID, Agilent Technologies 6890N
3. Motor stirrer, Becthai, Thailand
4. Basler camera and Image acquisition
5. Cylinder
6. Hot plate
7. Impinger

3.4 VOCs gas generator and measuring equipments

For generating the VOCs (benzene) gas in this study, an impinger 500 ml. contained with pure benzene VOCs (300 ml) was set in paraffin oil and controlled the temperature condition at T = 85 ± 3 °C. Then, the preliminary runs were carried out to verify the conditions required the generation of the concentration of VOCs gas. Moreover, the air zero was injected at different gas flow rates (0.5, 1.3, 2.2 and 3.0 ml/s) in order to obtain the different inlet VOC gases and study the effect of bubble hydrodynamic related with different gas flow rates.

3.4.1 Gas Chromatography Detector FID, Agilent Technologies 6890N

In this study, the Agilent Technologies gas chromatograph 6890N equipped with flame ionization detector (FID) and a split injector, operated in split ratio (10:1) was used for quantification of Benzene.

A fused-silica, HP-5 column (5% Phenyl Methyl Siloxane; 25 m x 0.32 mm i.d., 0.17 μm film thickness), supplied by J&W Scientific, USA was employed, with helium (purity 99.995%) as carrier gas at flow rate of 2.1 mL.min^{-1}. The column temperature was programmed as follows: 40 ^{0}C for 5 min, then post run to 200 ^{0}C and holding time for 1 min. The injection port and detector were operated at 250 and 300 ^{0}C, respectively. Moreover, the sampling system was carried out independently before and after the process in a continuous mode. Therefore, the VOCs gas inlet and outlet concentrations were measured every 30 minutes and allow us to determine the process efficiency. Normally, this parameter can be defined as the ratio between the amounts of VOCs concentration in gas phase transferred and injected to the liquid phase.

Note that, in this study, the area under curve of VOC gas obtained with gas chromatography was applied to calculate the VOCs removal efficiency. Based on the concentrations of VOCs determined by Raoult's law and Ideal gas law, the experimental results of VOCs concentration and loading, obtained in this study, can be applied in order to create the calibration curve between the experimental values and the area under curve from analyzing equipment.

3.4.2 High speed camera and Image analysis program

In this work, the VOCs bubbles generated by rigid orifice were captured with a Basler camera 100 image/sec (Figure 3.3). Then, the images were visualized on the acquisition computer through the PylonViewer vision software and analyzed by the Bubble measuring software (Figure 3.4).

Figure 3.3 High speed camera   **Figure 3.4** Software with License Dongle
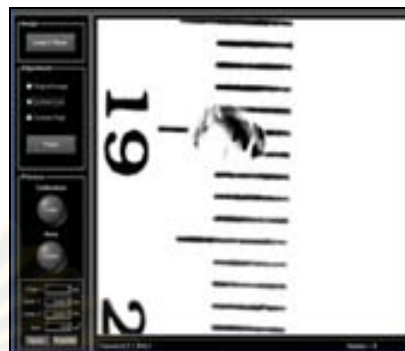
Figure 3.5 presents a typical sequence of image treatment. This treatment was based on a transformation of the acquired image into a binary image, followed by different arithmetical and geometrical operations. Then, the images were given uniform surface treatment (bubble area) and superfluous images were removed. In this study, the bubble diameter can be thus calculated from this obtained bubble area. Normally the bubbles were spherical at low gas flow rates but become ellipsoidal at high gas flow rates.
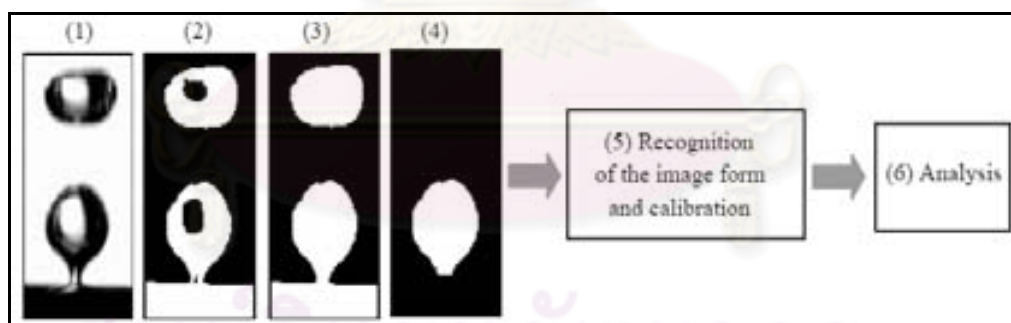
Figure 3.5 Typical sequence of image treatment: (1) image acquisition; (2) image binarization; (3) image completion; (4) border image delation;

3.5 Analytical methods

In this part, the applied method for determining the various parameters in order to provide a better understanding on hydrophobic VOCs absorption mechanism in small bubble column were used.

3.5.1 VOCs removal efficiency

The VOCs removal efficiency (%Eff) indicated the performance of the absorption process occurred in the small bubble column. It was defined as the ratio between the amounts of VOCs transferred and injected to the liquid phase. Note that the area under curve obtained with gas chromatography was used in this study.

$$Eff\,(\%) = \frac{C_{inlet(area)} - C_{outlet(area)}}{C_{inlet(area)}} \times 100 = \frac{A_{inlet(area)} - A_{outlet(area)}}{A_{inlet(area)}} \times 100 \qquad (3.1)$$

3.5.2 Overall mass transfer coefficient

3.5.2.1 Overall mass transfer coefficient in liquid phase ($K_L a$)

Concerning to the VOCs with low solubility in water, it can be noted that the mass transfer process was controlled by the liquid phase. Thus, the $K_L a$ coefficient was used and the determination procedure can be described as follows:

-   Measuring the variation of gas concentration in the outlet of bubble column with time: if the outgoing gas concentrations were followed until the saturated condition, for this small bubble column, the mass balance equation can be written as:

$$Q_g C_{g(in)} = Q_g C_{g(out)}(t) + V_L \frac{dC_L(t)}{dt} \qquad (3.2)$$

    where Q_g is the flow rate and V_L is the absorbent volume, $C_{g\,(in)}$ and $C_{g\,(out)}$ are the inlet and outlet concentration of benzene in the gas phase.

-   Therefore, the concentration of VOCs in the liquid phase $C_L(t)$ can be express by:

$$C_L(t) = \frac{Q_g}{V_L}(C_{g(in)}t - \int C_{g(out)}(t)dt) \qquad (3.3)$$

    From this equation, the variation of the VOCs concentration in the liquid phase with the time and also the saturated VOCs concentration (C_s) can be obtained.

- Based on the Non-stationary or dynamic method (Deckwer, 1992) the overall mass transfer coefficient in liquid phase $K_L a$ was given by the following equation;

$$\frac{dC_L}{dt} = k_L a (C_L^{\,s} - C_L) \qquad (3.4)$$

or, in its integral form by:

$$\ln[C_L^S - C_L] = \ln(C_L^S) - k_L a \cdot t \qquad (3.5)$$

where C_L and C_L^S were the dissolved VOCs concentration and the saturation VOCs concentration in the liquid phase, respectively. Thus, the $k_L a$ coefficient can be deduced from the curve relating the variation of $\ln(\Delta C)/C_L^S$ with time.

3.5.2.2 Liquid film mass transfer coefficient (K_L)

The liquid film mass transfer coefficient was the proportions of the overall mass transfer coefficient and interfacial area obtained experimentally in this study. Therefore, the local film mass transfer coefficient in gas phase and also liquid phase can be determined by:

$$K_L = \frac{K_L a}{a} \qquad (3.6)$$

K_L = Liquid-film mass transfer coefficient (m/s)

$K_L a$ = The overall mass transfer coefficient in liquid phase (s^{-1})

a = Specific interfacial area (m^{-1})

3.5.3 Bubble hydrodynamic and interfacial area

In this present part, the method for determining the bubble hydrodynamic parameters and also local interfacial area (a) provided by a single rigid orifice diffuser was described. It can be note that the values of (a) obtained can be applied in order to separate the overall mass transfer coefficient ($K_L a$) which is global and the insufficient to understand the VOCs gas-liquid mass transfer mechanism. Therefore, the liquid film mass transfer coefficient (K_L) was obtained.

3.5.3.1 <u>Bubble diameter (D_B)</u>

Measurement of bubble diameter at any flow rate (Q_g) can be performed by Image Treatment Techniques. 150-200 bubbles at any flow rate were photo. Images were visualized on the acquisition computer through the soft ware. This bubble was based on a geometrical operation. Then, the images were given uniform surface (bubble area A_B) and superfluous images were removed. The bubbles were spherical at low gas flow rates but become ellipsoidal at high gas flow rates as shown in Figure 3.6. For the bubble diameter were follow by equation 3.7 and 3.8, respectively.

Spherical bubble	Ellipsoidal bubble
$D_B = \sqrt{\dfrac{4 \times A_B}{\pi}}$ (3.7)	$D_{Bm} = \sqrt[3]{a^2 \times h}$ (3.8)
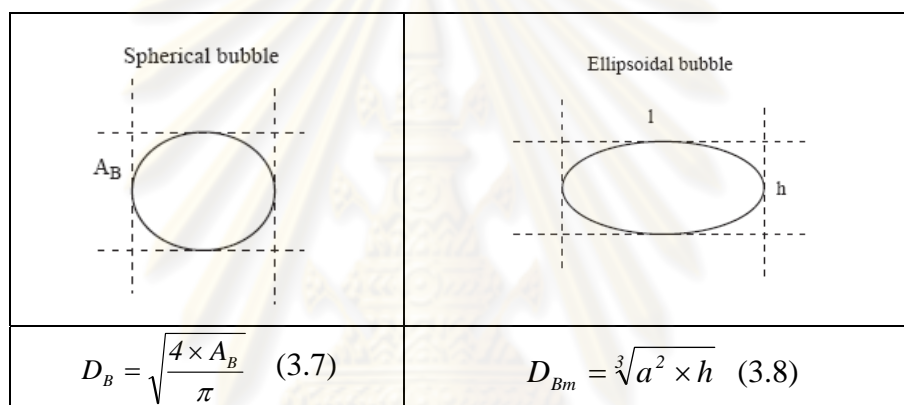
Figure 3.6 Typical bubble generation shape photographs.

3.5.3.2 <u>Bubble rising velocity (U_B)</u>

The bubble rising velocity were calculated by taking picture of bubble in reactor to analyze its distance at any time frame (t_{frame}), thus, the bubble rising velocity were calculated from equation (3.9)

$$U_B = \frac{\Delta D}{t_{frame}}$$ (3.9)

U_B = bubble rising velocity

ΔD = the distance between two frames

t_{frame} = time frame

Moreover, the bubble rising velocity can be determined from Grace and Wairegi, (1986) as shown in Figure 3.7 that was the graph of relationship between bubble rising velocity and bubble diameter.
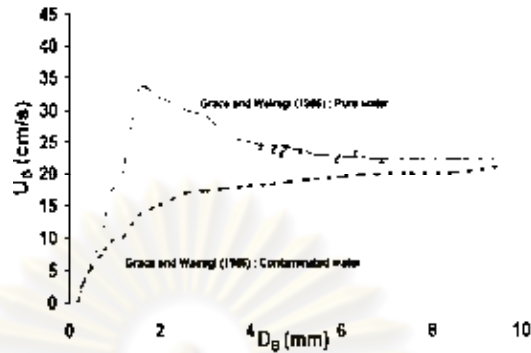
Figure 3.7 The relationship between bubble rising velocity and bubble diameter.

3.5.3.3 <u>Bubble formation frequency (f_B)</u>

Bubble formation frequency was the number of bubble formed with in 1 second. It can be calculated from the number of orifice multiply with gas flow rate of each orifices, then divided by volume of bubble as shown in equation (3.10)

$$f_B = \frac{N_{OR} \times q}{V_B} \tag{3.10}$$

N_{OR} and q are the number of orifices and the gas flow rate through the orifice, respectively. V_B is the bubble volume generated in bubble column.

3.5.3.4 <u>Specific interfacial area (a)</u>

The interfacial area can be determined by several methods: although the chemical methods were the most frequently used the interfacial area can also be estimated by taking into account the bubble size and the gas hold-up. In this work, the local interfacial area was defined as the ratio between the bubble surface (S_B) and the total volume in reactor (V_{total}). The number of bubbles (N_B) was deduced from the terminal rising bubble velocities (U_B) and the bubble formation frequency (f_B) as:

$$N_B = f_B \times \frac{H_L}{U_B} \tag{3.11}$$

The velocities, determined have been validated by the experimental curves of consequently; the interfacial area was expressed as:

$$a = N_B \times \frac{S_B}{V_{total}} = f_B \times \frac{H_L}{U_B} \times \frac{\pi D_B^2}{A H_L + N_B V_B} \tag{3.12}$$

H_L and A are the liquid height and cross-sectional area of reactor, respectively.

3.6 Experimental Procedure

3.6.1 Preparation of absorbents (Tap water, aqueous solution of non-ionic surfactant and oil-in water emulsion with non-ionic surfactant)

```
┌──────────────────────────────┐   ┌──────────────────────────────┐
│   Tap water prepared for     │   │  Lubricant oil was added into │
│  producing the aqueous       │   │  tap water in order to produce │
│  solution of non-ionic       │   │  the 50 and 300 mg/l oil-in-   │
│  surfactant                  │   │  water                        │
└──────────────────────────────┘   └──────────────────────────────┘
```

Non ionic surfactant was added at different concentrations ranged between $1.0 \times 10^{-6} – 1.0 \times 10^{-2}$ mol/l

Mixing with 200 rpm for 20 minutes

Measuring the surface tension and thus determining the CMC values

The aqueous solution of non ionic surfactant at concentration equal to 0.1, 0.5, 1, 3, and 5 CMC

Oil-in-water emulsion with non ionic surfactant at concentration equal to 1 CMC

Figure 3.8 Preparation of synthetic oil-in-water emulsion

The aim of this part was to generate the absorbents used in this study. Therefore, the aqueous solution of non ionic surfactant and also the stabilized oil droplets presented in term of oil-in-water emulsion with non ionic surfactant were prepared and compared with each others. Moreover, the different parameters were investigated, for example, surface tension and the Critical Micelle Concentration (CMC). Note that the surface tension decreases when stability of oil droplet increases.

Moreover, the summary variables concerning to the preparation of absorbents (tap water, aqueous solution of non-ionic surfactant and oil-in-water emulsion with surfactant) can be summarized and shown in Table 3.2 and 3.3.

Table 3.2 Variable for measured the surface tension and the CMC values of the aqueous solution of non-ionic surfactant

Fixed Variables	Parameter
Temperature	Room temperature
Mixed rate	Mixing until its homogenized
Type of surfactant	Non-ionic surfactant
Independent Variables	**Parameter**
Non-ionic surfactant concentrations	0.1, 0.5, 1, 3, and 5 CMC
Dependent Variables	**Parameter**
Surface tension	Value depend on tensiometer
	CMC

Table 3.3 Variable for measured the surface tension and the CMC values of emulsion with non-ionic surfactant

Fixed Variables	Parameter
Temperature	Room temperature
Mixed rate	200 rpm for 20 minutes
Type of surfactant	Non-ionic surfactant
Independent Variables	**Parameter**
Non-ionic surfactant concentrations	0.1, 0.5, 1, 3, and 5 CMC
Concentrations of emulsion	50 and 300 mg/l
Dependent Variables	**Parameter**
Surface tension	Value depend on tensiometer
	CMC

3.6.2 Study of benzene and absorption process in tap water

3.6.2.1 Study of Benzene as hydrophobic VOCs gas

The objective of this study was to evaluate benzene concentrations and their loadings associated with the different applied gas flow rates. The outline of this study was presented in Figure 3.9. Moreover, the summary variables concerning to this study can be presented in Table 3.4.
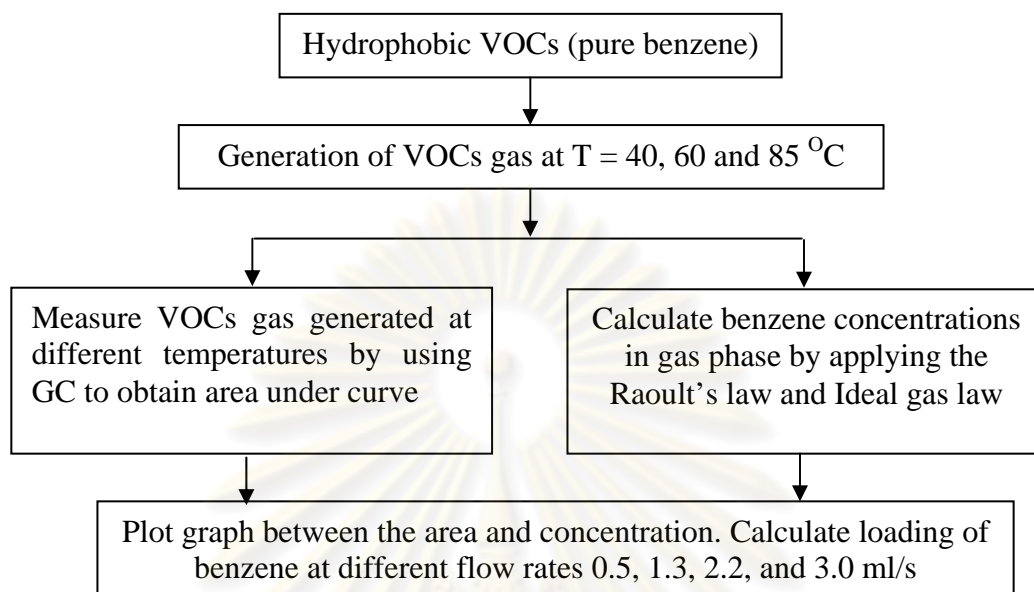
Figure 3.9 Flow diagram for studying benzene concentration and loading

Table 3.4 Variable of study benzene concentration and loading

Fixed Variables	Parameter
Volatile organic compounds	Benzene
Volume of absorbent	300 cm^3
Liquid phase (absorbent)	Tap water
Independent Variables	**Parameter**
Gas flow rates	0.5, 1.3, 2.2, 3.0 ml/s.
Temperature in VOCs generator	40, 60, 85 °C
Dependent Variables	**Parameter**
Peak area	Value depend on the GC
VOCs concentration	n/v=P/RT
Loading	Loading = Q_g * concentration

3.6.2.2 Study of Benzene absorption process in water

The objective of this study was to evaluate inlet and outlet concentration of benzene on the VOCs removal efficiency, bubble hydrodynamic and mass transfer parameters. The outline of this study was presented in Figure 3.10. Moreover, the summary variables concerning to this study can be present in Table 3.5.
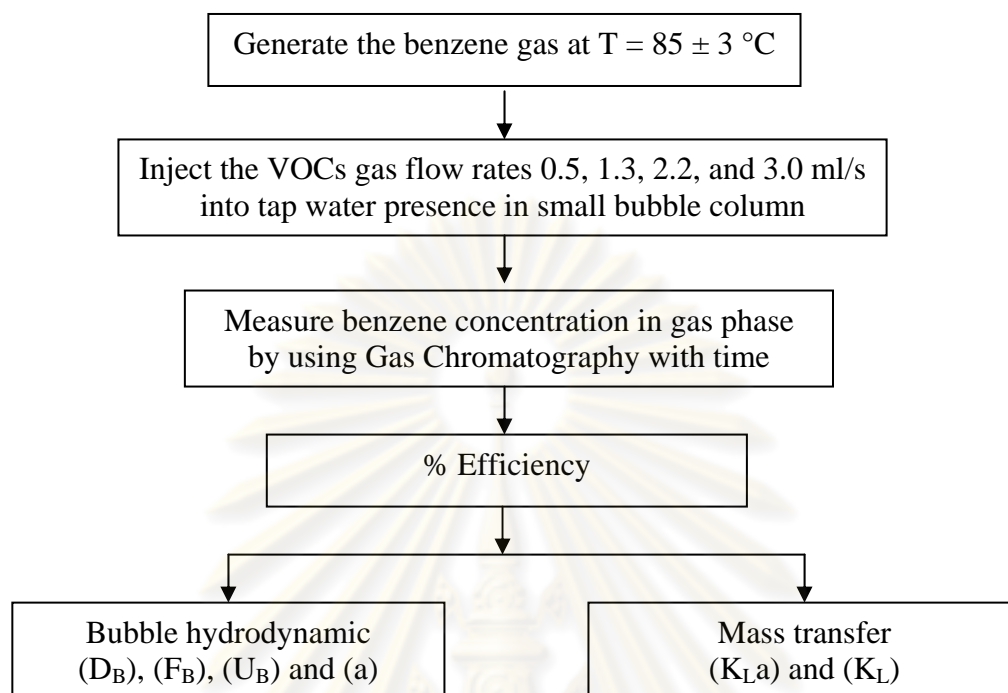
Figure 3.10 Flow diagram for study benzene absorption in water

Table 3.5 Variable of study benzene absorption in water

Fixed Variables	Parameter
Volatile organic compounds	Benzene
Temperature in VOCs generator	85 °C
Liquid phase (absorbent)	Tap water
Independent Variables	**Parameter**
Gas flow rates	0.5, 1.3, 2.2, 3.0 ml/s.
Dependent Variables	**Parameter**
VOCs removal efficiency	VOCs removal efficiency (%Eff)
Mass transfer parameters	$K_L a$, K_L
Bubble hydrodynamic parameters	a, D_B, f_B, U_B

3.6.3 Study the effect of non-ionic surfactant at difference concentrations

The objective of this present study was to evaluate the effect of non-ionic surfactant on the VOCs removal efficiency, bubble hydrodynamic and mass transfer parameters. The outline of this study was presented in Figure 3.11. Moreover, the summary variables concerning to this study can be present in Table 3.6.
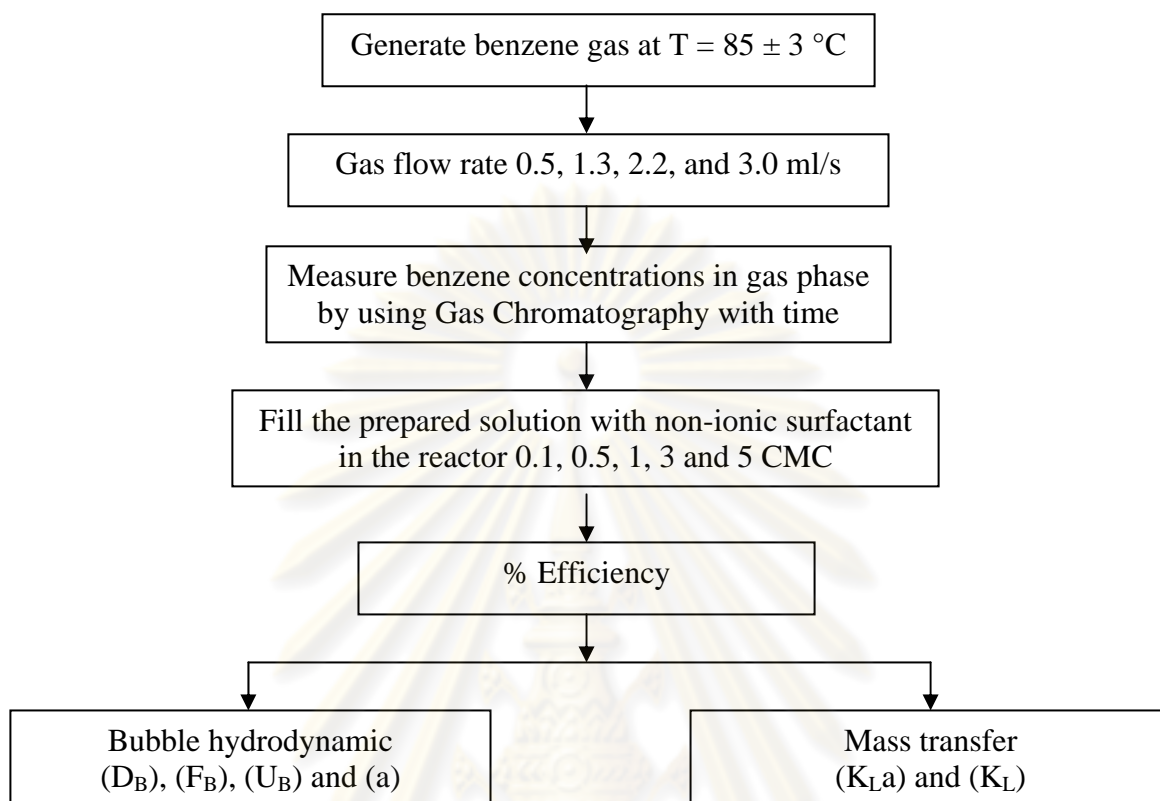
Figure 3.11 Flow diagram for study the effect of non-ionic surfactant at difference concentrations

Table 3.6 Variable of study the effect of non-ionic surfactant at difference

concentrations

Fixed Variables	Parameter
Volatile organic compounds	Benzene
Temperature in VOCs generator	85 °C
Independent Variable	**Parameter**
Gas flow rates	0.5, 1.3, 2.2, 3.0 ml/s.
Liquid phase (absorbent)	Aqueous solution with non-ionic surfactant 0.1, 0.5, 1, 3 and 5 CMC
Dependent Variables	**Parameter**
VOCs removal efficiency	VOCs removal efficiency (%Eff)
Mass transfer parameters	K_La, K_L
Bubble hydrodynamic parameters	a, D_B, f_B, U_B

3.6.4 Study the effect of oil-in-water emulsion with non-ionic surfactant at CMC
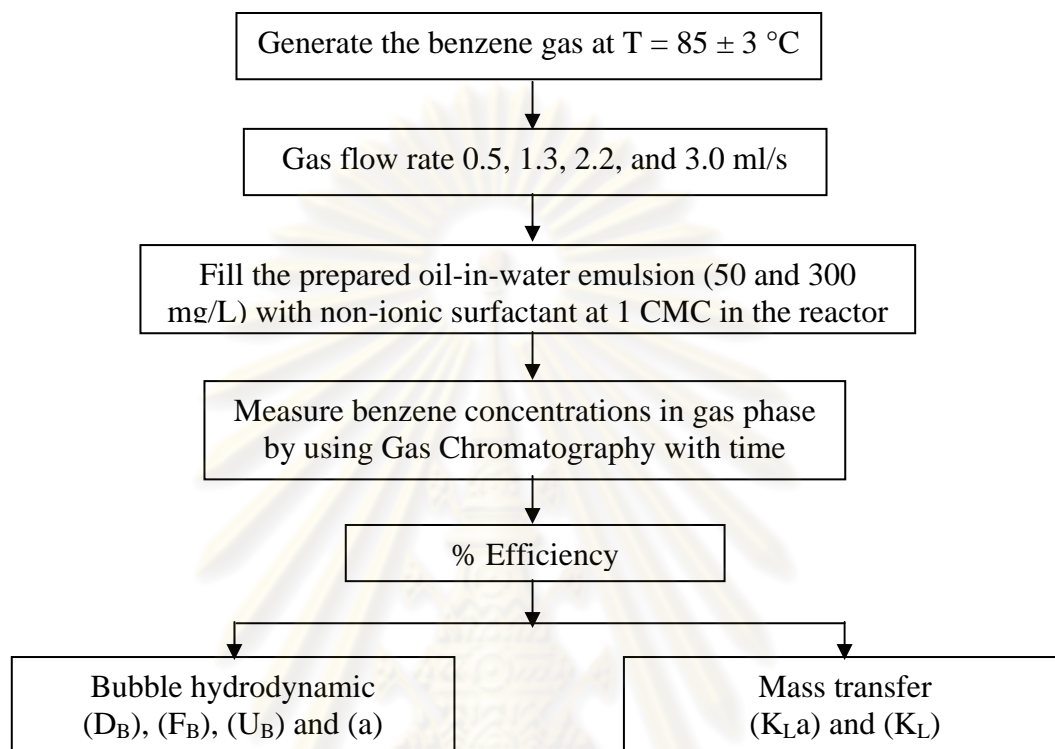
Figure 3.12 Flow diagram for study the effect of oil-in-water emulsion with non-ionic surfactant at CMC

The objective of this present study was to study the effect of oil-in-water emulsion containing with non-ionic surfactant at 1 CMC on the VOCs removal efficiency, bubble hydrodynamic and mass transfer parameters. The outline of this study was presented in Figure 3.12. Moreover, the summary variables concerning to this study can be present in Table 3.7.

Table 3.7 Variable of study the effect of oil-in-water emulsion with non-ionic surfactant at CMC

Fixed Variables	Parameter
Volatile organic compounds	Benzene
Temperature in VOCs generator	85 °C
Size of reactor	Diameter 4.4 cm. and height 30 cm.
Volume of absorbent	300 cm^3
Size of rigid orifices	0.65 mm
Independent Variable	**Parameter**
Gas flow rates	0.5, 1.3, 2.2, 3.0 ml/s.
Liquid phase (absorbent)	1. Emulsion 50 mg/L with non-ionic surfactant at CMC 2. Emulsion 300 mg/L with non-ionic surfactant at CMC
Dependent Variables	**Parameter**
VOCs removal efficiency	VOCs removal efficiency (%Eff)
Mass transfer parameters	K_La, K_L

CHAPTER IV

RESULTS AND DISCUSSIONS

The objectives of this research were to study the absorption mechanism for removing the hydrophobic Volatile Organic Compounds (VOCs) in small bubble column. The bubble hydrodynamic and mass transfers parameters from the gas phase to the liquid phase were the key parameters of this study. The results were consists of 4 parts as follow:

1. Analyze the injected VOCs gas and liquid phase characteristic;
2. Study the effect of different gas flow rates on the inlet VOCs concentrations and the hydrophobic VOCs removal efficiency;
3. Study the effect of aqueous solutions with surfactants (non-ionic surfactant and concentrations) on the hydrophobic VOCs absorption process;
4. Study the effect of oil-in-water emulsion containing non-ionic surfactant at Critical Micelle Concentration (CMC) on the hydrophobic VOCs absorption process.

4.1 VOCs concentrations determination and liquid phase characteristic

The aim of this part was to determine the inlet VOCs concentrations and the liquid phase characteristics. Therefore, the VOCs concentrations were calculated by applied Henry's law and Raoult's law. Also the aqueous solution of non-ionic surfactants and also the stabilized oil droplets (presented in term of oil-in-water emulsion with non ionic surfactant) were prepared and compared with each others.

4.1.1 Determination of VOCs concentrations and loading

In the VOCs gas generator, it was applied in order to generate the VOCs gas at T = 85±3 ^{0}C. Due to the boiling point of benzene was 80.1 ^{0}C and it maked sure that the VOCs was evaporated already. So, the impinger has the saturated of benzene vapor at the roughly constant partial pressure. In this case, the concentrations at

equilibrium of two phases written in term of thermodynamic relation can be founded. For the ideal gas or liquid (such as benzene), Raoult's law was chosen, in this study, to find the partial pressure (p_A) of substance as:

$$p_A = P_A x_A \qquad (4.1)$$

where p_A is the partial pressure of component A in the vapor in Pa (atm), P_A is the vapor pressure of pure A in Pa (atm), and x_A is the mole fraction of A in the liquid. From (4.1), the partial pressure is obtained with the identified values of P_A and x_A. Then, substitute the partial pressure into the ideal gas law as shown in equation (4.2) in order to calculate the initial VOCs concentration:

$$pV = nRT \qquad (4.2)$$

where V is the volume, n is the amount of gas (moles), R is the gas constant, 8.314 J·K^{-1}mol^{-1}, and T is the absolute temperature. Moreover, the relation between the concentration and gas flow rate can be used to define the loading as shown in equation (4.3):

$$Loading = Q_g * [C] \qquad (4.3)$$

Note that, the experimental results of inlet VOCs concentration and loading obtained in this study can be applied in order to create the calibration curve between the experimental values and the area under curve obtained with the analyzing equipment as shown in Appendices.

From table 4.1, it can be concluded that

- The concentrations of VOCs (benzene) from VOCs generator were related to temperatures. Due to the higher vapor pressure as follow equation (4.2)
- The different gas flow rates that were released from Air zero (pure air 99.9% and reduced the contaminated such as hydrocarbon, humidity, particulate, NOx, and SOx) were affected to higher loading as follow equation (4.3) (Tom R., 2009).
- The higher loadings can provide the higher inlet benzene gas in bubble column (at the same time). Moreover, it can be affected to the VOCs removal efficient including the mass transfer and bubble hydrodynamic parameters.

Table 4.1 Summary of inlet VOCs concentrations and loading

Temp (^{0}C)	Gas flow rate (Qg) (ml/s)	VOCs concentration in VOCs generator (mol/L of gas)	Loading (mol/s)	Inlet VOCs concentration (Cg^*_{in}) (mol/L)
40	0.5	0.00961	4.81×10^{-6}	Not use as the operating condition for this study
	1.3		1.25×10^{-5}	
	2.2		2.11×10^{-5}	
	3.0		2.88×10^{-5}	
60	0.5	0.01892	9.46×10^{-6}	
	1.3		2.46×10^{-5}	
	2.2		4.16×10^{-5}	
	3.0		5.68×10^{-5}	
85	0.5	0.03948	1.97×10^{-5}	0.004279
	1.3		5.13×10^{-5}	0.004357
	2.2		8.69×10^{-5}	0.004468
	3.0		1.18×10^{-4}	0.004501

4.1.2 The preparation of aqueous solution with non-ionic surfactant

In this study, Tween 80 was represented the non-ionic surfactant. Moreover, the different concentrations of non-ionic surfactant were varied into 0.1, 0.5, 1, 3, and 5 CMC. The characteristic of non-ionic surfactant was shown in Table 4.2.

Table 4.2 Characteristic of non-ionic surfactant

Liquid phase	Chemical name	M (kg.mol^{-1})	σ_L (mN.m^{-1})	CMC (mol.L^{-1})
Non-ionic surfactant	Tween 80	1310 x 10^{-3}	59.31	0.0000012 (0.1 CMC)
			50.04	0.000006 (0.5 CMC)
			45.21	0.000012 (1 CMC)
			42.48	0.000036 (3 CMC)
			40.14	0.00006 (5 CMC)

4.1.3 The preparation of lubricant oil-in-water emulsion

In this study, lubricant oil was chosen as the oil-in-water emulsion. SKG Bleder with 350 W, 13,000 rpm motor and maximum capacity of 1.5 L was used for preparing the stock oil-in-water emulsion. Due to the specific gravity of lubricant oil equal to 994 mg/L, the required oil concentrations (50 and 300 mg/L) can be prepared by adding distilled water. Note that, 1 mL of Oil (PTT V-120) was injected into the blender and mixed with 800 mL distilled water and 100 mL 0.1% emulsifier or non-ionic surfactant (Tween80) for 1 minute. The admixture was later stabilized by stirring for 10 minutes and diluted to 1 L with distilled water (PanPanit, 2001 and Kloet et al., 2001). The oil-in-water emulsion remains stable during the experimental run. In order to determine the CMC values, the different concentrations of non-ionic surfactant (ranging between $1.0 \times 10^{-7} - 1.0 \times 10^{-2}$ mol/l and mixing with 200 rpm for 20 minutes) were operated in order to measure the associated surface tensions. After that, the surface tension was used for determining the CMC values in order to perform the stabilized oil-in-water emulsion at 1 CMC. The surface tension and CMC values were presented in Table 4.3.

Table 4.3 Characteristic of oil-in-water emulsion

Liquid phase	Chemical name	[oil-in-water emulsion] (mg.L^{-1})	σ_L (mN.m^{-1})	[surfactant] at CMC (mol/L)
Oil-in-water emulsion	Lubricant oil	50	36.93	0.001
		300	35.81	0.0015

4.1.4 Calculation of the power consumption

In the case of a gas–liquid reactor equipped with rigid diffuser, the total specific power consumption (P_G) can be related to the total gas pressure drop according to the following equation (Bouaifi M. *et al.,* 2001);

$$P_G = Q \times (\rho_L g H_L + \Delta P) \qquad (4.4)$$

where Q_G and V_L are the applied gas flow rate at operating temperature and pressure (m^3/s) and liquid phase volume (m^3), respectively. ρ_L is liquid density (kg/m^3) and g is

acceleration due to gravity (m/s^2). Moreover, H_L is liquid height (m) and ΔP is pressure drop measured experimentally in this study (Pa).

Table 4.4 Power consumption required for generating the VOCs bubbles from rigid orifice diffuser with 0.65 mm in orifice diameter

Liquid phase	Qg (ml/s)	P$_G$ (Watt)
Tap water	0.5	0.00112
	1.3	0.00359
	2.2	0.00893
	3.0	0.01510
Non-ionic 0.1 CMC	0.5	0.00988
	1.3	0.02640
	2.2	0.04750
	3.0	0.06770
Non-ionic 0.5 CMC	0.5	0.00988
	1.3	0.02640
	2.2	0.04750
	3.0	0.06770
Non-ionic 1 CMC	0.5	0.00988
	1.3	0.02640
	2.2	0.04750
	3.0	0.06760
Non-ionic 3 CMC	0.5	0.00986
	1.3	0.02630
	2.2	0.04740
	3.0	0.06760
Non-ionic 5 CMC	0.5	0.00986
	1.3	0.02630
	2.2	0.04740
	3.0	0.06760
Emulsion 50 mg/L	0.5	0.00983
	1.3	0.02620
	2.2	0.04720
	3.0	0.06740
Emulsion 300 mg/L	0.5	0.00983
	1.3	0.02620
	2.2	0.04720
	3.0	0.06740

From Table 4.4, it can be noted that the power consumptions were increased with gas flow rate. Concerning to different liquid phase, the power consumptions are less pronounced due to their physical characteristics (density and volume). The variation of the power consumptions varied between 0.00112 – 0.0677 Watts. Therefore, it should be used, in practice, the suitable gas flow rate in order to achieve the high VOCs removal efficiency and save the related energy consumption. Moreover, in order to well understand the effect of gas flow rates and the various liquid phases on the VOCs removal efficiency, it is essential to analyze locally the bubble hydrodynamic parameters (bubble diameter, bubble formation frequency, bubble rising velocity and interfacial area) and also mass transfer parameters (overall and liquid-film mass transfer coefficients). The next part will present the effect of different gas flow rates on VOCs removal efficiency, mass transfer and bubble hydrodynamic parameters.

4.2 The effect of gas flow rate on the hydrophobic VOCs absorption process in small bubble column

The objective of this part was to study the effect of different gas flow rates related to the inlet VOCs loading values in bubble column. Moreover, the VOCs removal efficiency, bubble hydrodynamic and mass transfer parameters were determined.

4.2.1 Outlet VOCs concentrations in gas phase

Figure 4.1 presents the variation of outlet VOCs concentration in gas phase with times. The gas flow rates, used in this study, range between 0.5 - 3.0 ml/s.
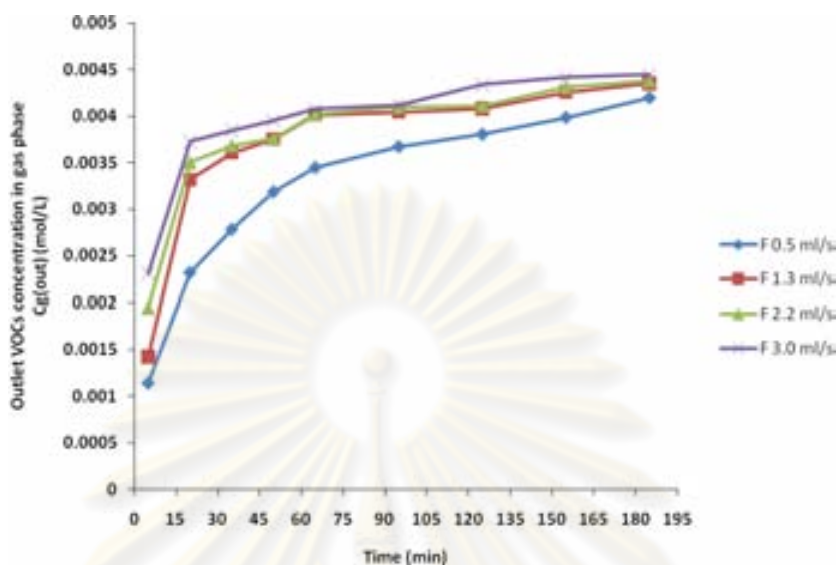
Figure 4.1 Outlet VOCs concentration in gas phase versus time

From Figure 4.1, the outlet gas concentrations were related to experimental times. The outlet VOCs concentrations were rapidly increase in first step, and then reach closely to the constant values with increasing times (second step). Due to the higher loading VOCs at high gas flow rate, it was founded that Cg (out) was used shorter times to reach the 2nd step. The final outlet gas concentrations obtained experimentally with 4 Qg values were different based on the mass balance equation: the $Cg_{(out)}$ values were increase continuously and reach finally the inlet concentrations ($Cg^*_{(in)}$) measured experimentally by GC-FID equipment as previously presented in Chapter 3. These confirm to those obtained with the study of the absorption process of hydrophobic VOCs (toluene) in tap water by Heymes *et al.,* (2006) as shown in Figure 4.2.
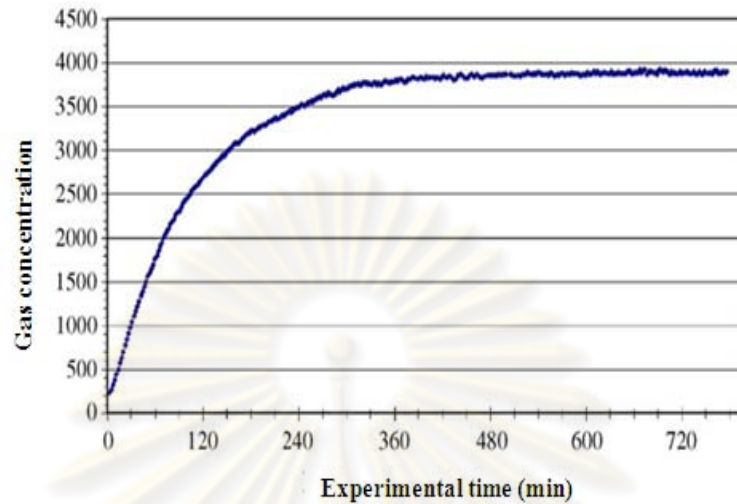
Figure 4.2 The outlet concentration in gas phase of hydrophobic VOCs (toluene) in
bubble column (Heymes *et at.,* 2006)

4.2.2 VOCs concentration in liquid phase (tap water)

Figure 4.3 presents the VOCs concentration in liquid phase (tap water) at
different experimental times. The gas flow rate used in this study ranges between 0.5-
3.0 ml/s. The experimental times were 185 minutes.

Due to the experimental results obtained with the outlet VOCs gas
concentration, the concentration of VOCs in liquid phase (tap water) was calculated
by applied the mass balance equation as shown in equation (4.5).

$$C_L(t) = \frac{Q_g}{V_L}[C_{g(in)}^* \times t - \int_0^t C_g \, dt] \tag{4.5}$$

The integrated term of $\int_0^t C_g \, dt$ can be determined by the area under curve obtained
from the Figure 4.1.
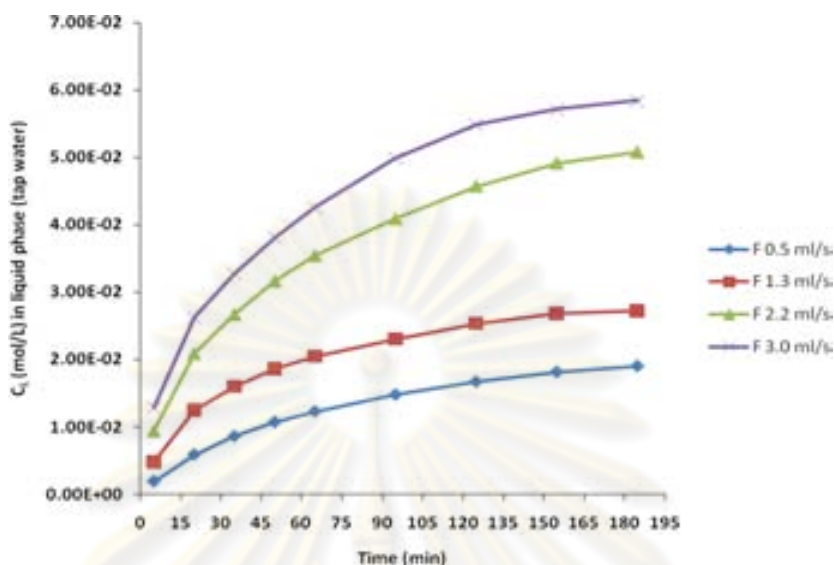
Figure 4.3 VOCs concentration in liquid phase (tap water) versus time

From Figure 4.3, it was founded that VOCs concentrations in liquid phase (C_L) increase with operating time. Concerning to the Henry law constant of benzene (11.32 x 10^5 Pa), low solubility of benzene gas in water can be thus defined. Therefore, it can be stated that the mass transfer mechanism, in this case, was controlled by liquid-film around the generated bubble (Lewis and Whitman, 1962). Moreover, it can be noted that C_L was rapidly increasing at high gas flow rate that were related to higher loading or inlet benzene gas as previous mention. However, at long operating times, the C_L values were finished and also equal for any gas flow rates (4 values at 0.5, 1.3, 2.2, and 3.0 ml/s). These values were related to the saturated concentrations at equilibrium (C_L^S) concerning to the chosen types of absorbent in liquid phase, temperature and pressure in the experimental system (Franck L. *et al.,* 2008). In this study, the experimental process was carried out at T = 85 ^{0}C and atmospheric pressure (1 atm). Therefore, in order to determine the C_L^S value, the experiment was operated for very long operating time (8 – 10 hrs) and for highest gas flow rate (3.0 ml/s) for confirming and thus well determining the saturated time (T_{SAT}). Then, this T_{SAT} values (140 minutes) were applied into the C_L determination equation for calculating finally the associated C_L^S value. The determining method can be described as follow: Firstly, the mass balance equation as shown in equation (4.5) was applied:

$$C_L(t) = \frac{Q_g}{V_L}[C^*_{g(in)} \times t - \int_0^t C_g \, dt \tag{4.5}$$

In order to simulate the variation of the Cg values with time and thus determine the integrated term of $\int_0^t C_g \, dt$, the Langmuir equation was chosen in this study:

$$C_g = \frac{C^*_{g(in)} \times (kt)}{1 + kt} \tag{4.6}$$

$$\int_0^t C_g \, dt = C^*_{g(in)}\left[t - \frac{1}{k}\ln(1 + kt)\right] \tag{4.7}$$

Substitute equation (4.7) in to equation (4.5):

$$C_L = \frac{Q_g}{V_L}\left[C^*_{g(in)} \times t - C^*_{g(in)}\left[t - \frac{1}{k}lm(1 + kt)\right]_0^t\right] \tag{4.8}$$

Rearranging equation (4.8):

$$C_L = \frac{Q_g}{V_L}\left[\left(C^*_{g(in)} \times t\right) - \left(C^*_{g(in)} \times t\right) + \frac{C^*_{g(in)}}{k}\ln(1 + kt)\right] \tag{4.9}$$

So, the VOCs concentration in liquid phase can be calculated as follow:

$$C_L = \frac{Q_g}{V_L}\left[\frac{C^*_{g(in)}}{k}\ln(1 + kt)\right] \tag{4.10}$$

where
C_L^S	=	Saturated concentration of VOCs in liquid phase
C_L	=	Concentration of VOCs in liquid phase
Q_g	=	Gas flow rate
V_L	=	Liquid volume (300 ml)
$C^*_{g\,(in)}$	=	Inlet concentration of VOCs in gas phase
k	=	Constant (the relation between the VOCs concentrations in gas phase and time in order to find the saturated time)

Note that, the value of k can be obtained due the experimental results of Cg = f(t) as previously presented in Figure 4.1. The rearranged term of equation (4.6) was applied:

$$k = \frac{1}{t} \times \left[\frac{C_g}{C^*_{g(in)} - C_g * t}\right] \tag{4.11}$$

At the equilibrium condition between gas and liquid phases, the value of C_L the saturated time in gas phase should be normally equal to the saturated time in liquid phase (tap water). Thus, the T_{SAT} values related with different gas flow rates can be thus determined by using equation (4.9). The results were shown in Table 4.5.

Table 4.5 The saturated concentration of VOCs in liquid phase (tap water) at different gas flow rates and the saturated time

Gas flow rate (ml/s)	The saturated time in liquid phase (T_{SAT}) (minute)	The saturated concentration in liquid phase, C_L^S (mol/L)
0.5	635	0.0695
1.3	290	0.0680
2.2	190	0.0708
3.0	140	0.0677

According to Table 4.5, it was founded that, for high gas flow rate, the saturated time was very short and the outlet gas concentration was increased quickly. Whereas, for low gas flow rate, the saturated time was very long and the outlet gas concentration was gradually increased. Moreover, the T_{SAT} values obtained were related to those obtained experimentally with the $Cg = f(t)$ as shown in Figure 4.1. Whereas, the calculating method was possibly responsible for the differences between the experimental results as shown in Figure 4.3 and also calculated results as in Table 4.5. In this study, the concentrations of VOCs in liquid phase (C_L) and the saturated concentration of VOCs in liquid phase (C_L^S) were important parameters for calculating the overall mass transfer coefficient (K_La) in next part.

As previously described, the mass transfer mechanism in case of hydrophobic VOCs (benzene) was controlled by the liquid film related to the significant decrease of benzene concentration in liquid film as shown in Figure 4.4 and 4.5.
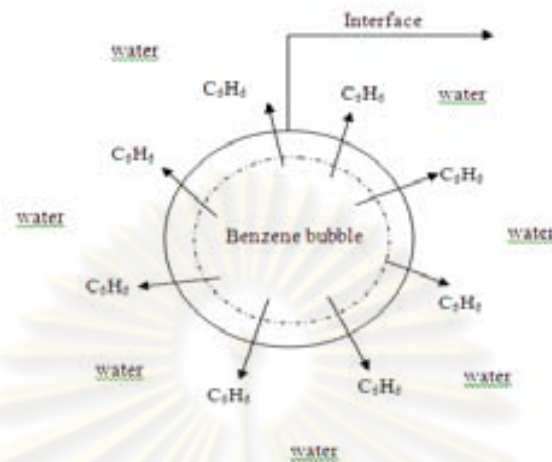
Figure 4.4 Mass transfer from bubble (benzene) to liquid phase (tap water)
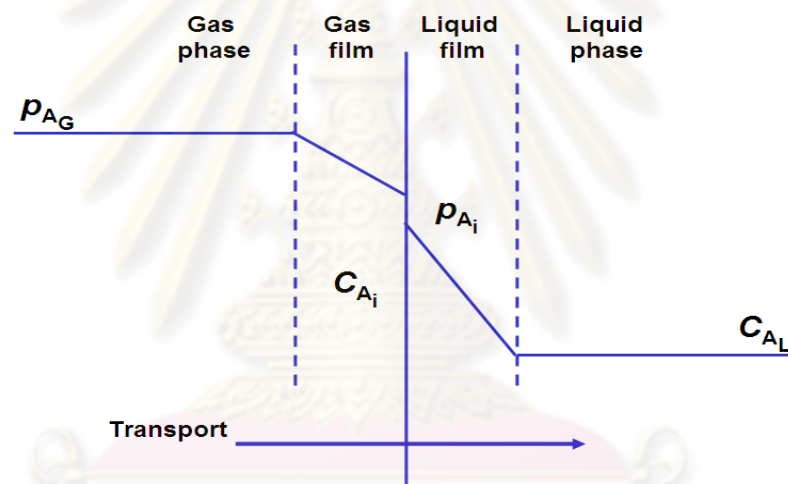
Figure 4.5 Mass transfer mechanism from bubble to liquid phase controlled by liquid film (Lewis and Whitman, 1962)

Due to two-film theory (Lewis and Whitman, 1962), the mechanism of gas-liquid mass transfer can be classified into three transferring steps. Firstly, the benzene gas in bubble was transferred from gas-film to the interface. Secondly, the transfer process will cross the interface. Finally, the benzene component will transfer through the liquid-film to the liquid phase (tap water). Concerning to Figure 4.5, it can be observed that longer time and higher concentration gradient for benzene transferring from liquid-film to liquid phase than that obtained with gas-film. Therefore, the mass transfer from gas phase (benzene in bubble) to liquid phase (tap water) depends on the concentration difference in each phase. Normally, the benzene gas in generated

bubbles was transferred from the higher concentration (bubble) to the lower concentration (tap water) until the concentrations of all components were equal or equilibrium. Then, the mass transfer process was thus stopped.

4.2.3 VOCs removal efficiency

Figure 4.6 presents VOCs removal efficiency (%Eff) in tap water used as the absorbent. The gas flow rates used in this study range between 0.5-3.0 ml/s. Note that, the VOCs removal efficiency was calculated at 185 minutes by the follow equation (4.12):

$$Eff(\%) = \frac{C_{inlet} - C_{outlet}}{C_{inlet}} \times 100 = \frac{A_{inlet} - A_{outlet}}{A_{inlet}} \times 100 \qquad (4.12)$$
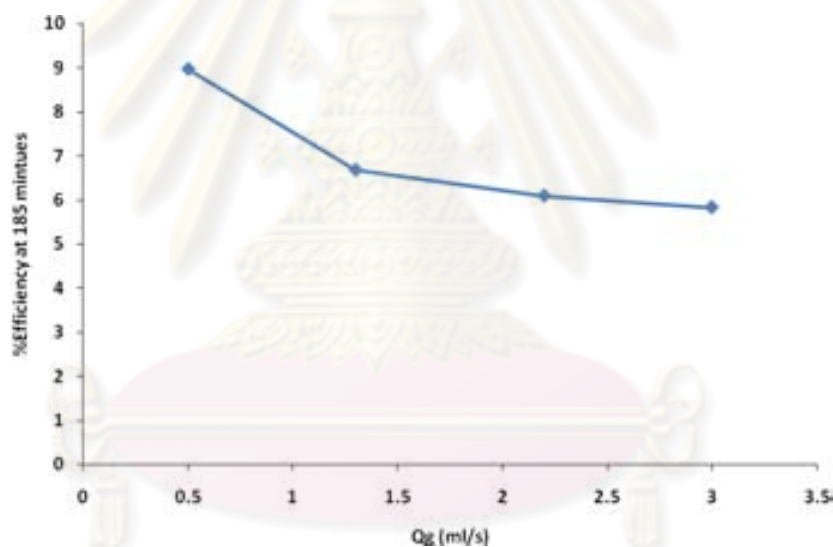
Figure 4.6 VOCs removal efficiency versus gas flow rate

According to Figure 4.6, it was shown that VOCs removal efficiencies vary between 5.83% - 8.97%. The highest value of VOCs removal efficiency was observed at gas flow rate 0.5 ml/s. Moreover, VOCs removal efficiency tends to decrease when gas flow rate was increased: higher outlet concentration in gas phase, as shown in Figure 4.1, was possibly responsible for this result. In addition, the %Eff values obtained at different operating time should be considered in order to understand the suitable operating time in the absorption process (Figure 4.7).
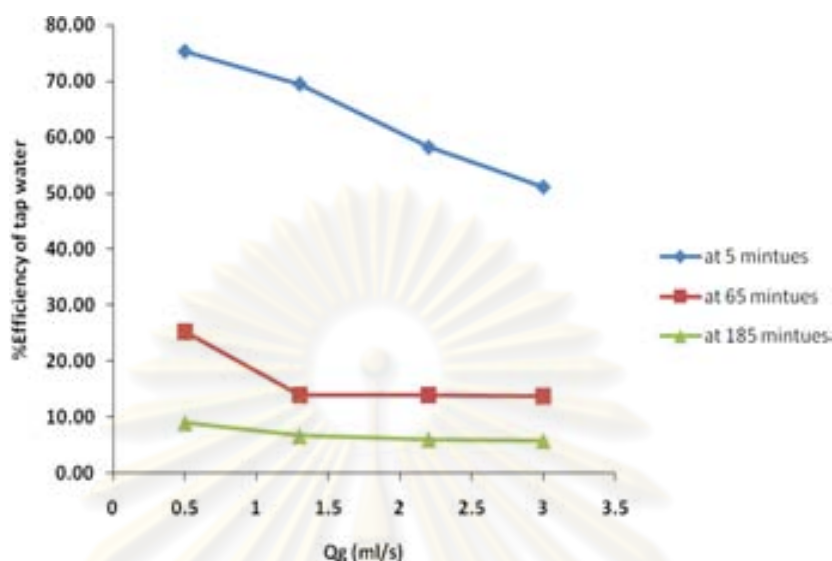
Figure 4.7 The VOCs removal efficiency at different time versus gas flow rate

According to Figure 4.7, it can be noted that the VOCs removal efficiencies at 5 minutes (51.18% - 75.27%) was higher than 65 minutes (13.71% - 25.25%) and 185 minutes (5.83% - 8.97%) comparable with different gas flow rates. Therefore, in order to achieve the highest VOCs removal efficiencies, it should be used the appropriated gas flow rate (0.5 ml/s) and operating times (5 minutes). In conclusion, the main factors that affect the absorption process were the characteristic of the absorbate and absorbent applied in this study. The chemical properties should be considered as: 1) Solubility (high solubility indicates the reaction of the absorbate and absorbent) and 2) Molecular polarity (polarity of absorbent can enhance the solubility of the absorbate in absorbent).

The next part was described about the K_La coefficient in order to understand the VOCs removal efficient. The C_L^S and C_L from previous results were applied for calculated the the K_La coefficient.

4.2.4 Overall mass transfer coefficient in liquid phase (K_La)

Figure 4.8 shows the overall mass transfer coefficient in liquid phase (K_La) at any gas flow rate. The gas flow rates vary between 0.5 – 3.0 ml/s. Note that, the K_La coefficients obtained in this study were given by the following equation:

$$\frac{dC_L}{dt} = k_L a(C_L{}^s - C_L) \tag{4.13}$$

or, in its integral form by:

$$\ln[C_L^S - C_L] = \ln(C_L^S) - k_L a \cdot t \tag{4.14}$$

where C_L and $C_L{}^S$ were the dissolved VOCs concentration and the saturation VOCs concentration in the liquid phase, respectively. Thus, the $k_L a$ coefficient can be deduced from the curve relating the variation of $\ln(\Delta C)/C_L{}^S$ with time.
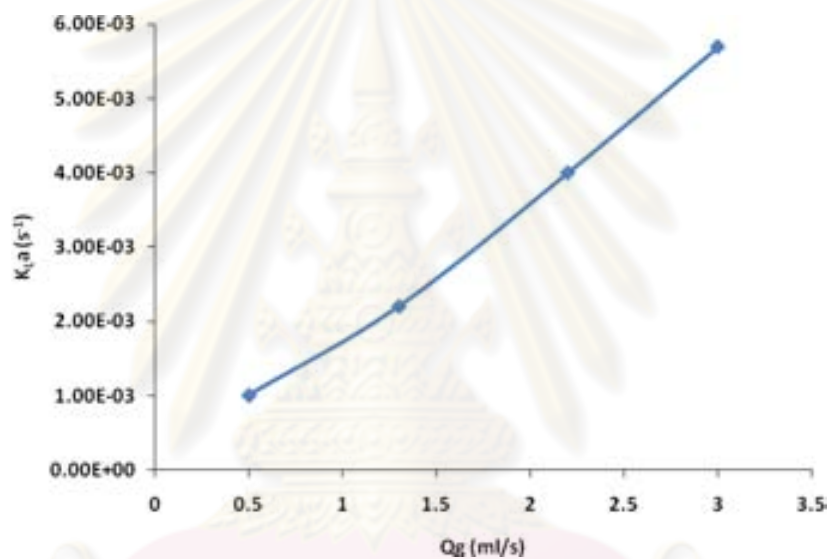
Figure 4.8 Overall mass transfer coefficient based on liquid phase ($K_L a$) versus gas flow rate

Concerning to Figure 4.8, the $K_L a$ coefficients vary between 0.0010 and 0.0057 s^{-1} for gas flow rates varying between 0.5 and 3.0 ml/s. Moreover, it can be noted that the $K_L a$ coefficients obtained with high gas flow rate was greater than low gas flow rate due to the difference in mass transfer capability (loading value). Therefore, it can be noted that the mass transfer performance was based on the concentration gradient related to gas flow rate as shown in Table 4.1. However, at high gas flow rate, higher $K_L a$ coefficients were obtained, the desorption or stripping phenomena can be occurred due to the turbulent condition and thus reduce the associated VOCs removal efficiency as shown in Figure 4.6 and 4.7.

Therefore, the absorption process should be operated with the suitable gas flow rate in order to obtain the high VOCs removal efficiency and also save the power

consumption. In order to provide a better understanding the effect of gas flow rate on mass transfer mechanism which enables the absorbed amount to be effectively controlled whatever the operating condition, the interfacial area (a) was considered. Note that, the bubble hydrodynamic parameters including bubble diameter, bubble formation frequency, and bubble rising velocity have to be locally measured.

4.2.5 Hydrodynamic parameters

Bubble diameter (D_B)

Figure 4.9 demonstrates the variation of the generated bubble diameter (D_B) with gas flow rate. These results can be obtained by using the Image Treatment Techniques by high speed camera (100 image/s).
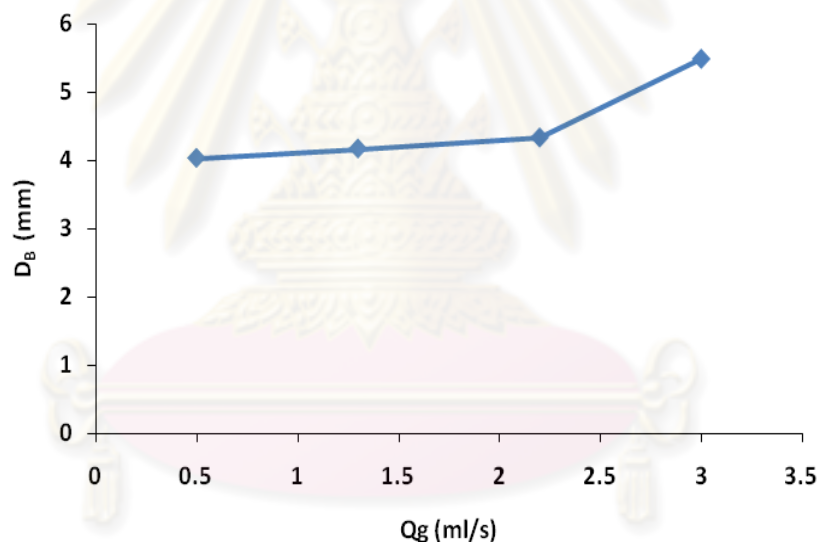
Figure 4.9 Bubble diameter versus gas flow rate

According to Figure 4.9, the bubble diameters obtained experimentally vary between 4.03 -5.49 mm while gas flow rates can change between 0.5 - 3.0 ml/s. The bubble diameter increases with gas flow rate. The results have shown that, at low gas flow rate 0.5 – 2.2 ml/s, the bubble diameters were constant: the orifice size applied (OR 0.65 mm) was the main parameter that controls the generated bubble diameter in bubble column. However, at higher gas flow rate (>2.0 ml/s), the bubble diameter was increasing due to the coalescence phenomena of many small bubbles suspended in the reactor, and thus reduction of removal efficiency as previously described. Hence, it

can be concluded that high gas flow rates should not be applied due to the generation of large bubble size inducing the high power consumption, the turbulent condition, and also desorption process as discussed in previous part.

Bubble formation frequency (f_B)

Figure 4.10 demonstrates the variation of the bubble formation frequency (f_B) with gas flow rate. Note that, the bubble formation frequency can be calculated as the ratio between the gas flow rate (Q_G) and the bubble volume (V_B):

$$f_B = \frac{N_{OR} \times q}{V_B} \tag{4.15}$$
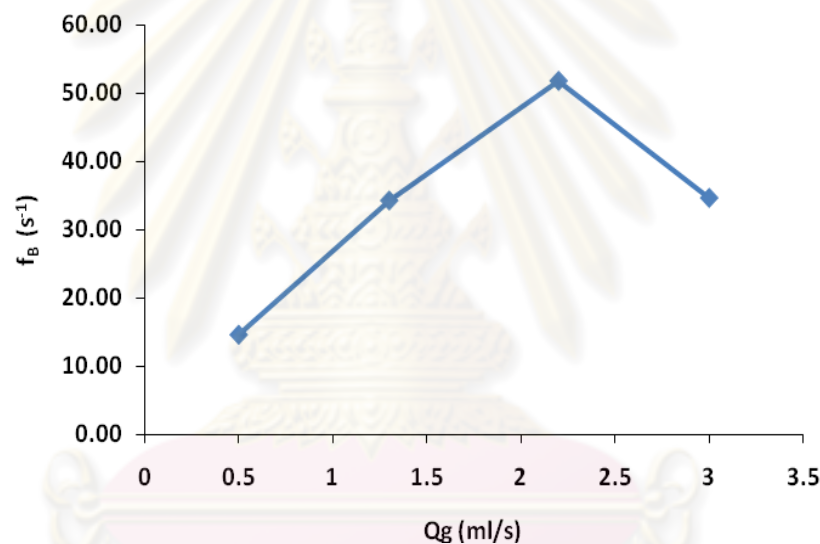
Figure 4.10 Bubble formation frequency versus gas flow rate

Concerning to Figure 4.10, the bubble formation frequency obtained experimentally vary between 14.58 - 51.74 s^{-1} while gas flow rates can change between 0.5 - 3.0 ml/s. For gas flow rate between 0.5 and 2.2 ml/s, the bubble formation frequency was obviously increased until the gas flow rate 3.0 ml/s: the bubble formation frequency starts decreasing. Moreover, it can be noted that the small f_B value obtained with 3.0 ml/s gas flow rate corresponds to the highest bubble size and thus volumes generated in bubble column. Therefore, the highest bubble formation frequencies (high gas flow rate and small bubble diameter) were not the controlled factor for the removal efficiency of hydrophobic VOCs. Thus, the control

of turbulent from bubble hydrodynamic condition should be well considered for the VOCs absorption.

<u>Bubble rising velocity (U_B)</u>

Figure 4.11 shows the relation between the bubble rising velocity (U_B) with the generated bubble diameter.
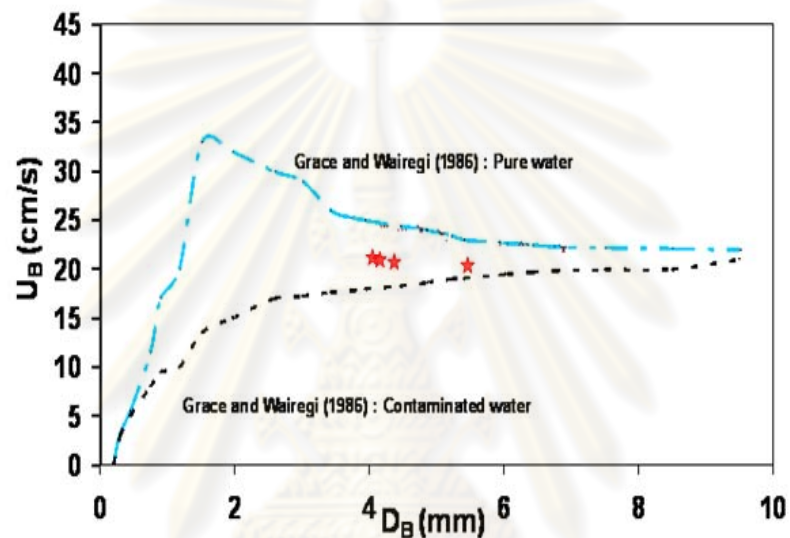
Figure 4.11 Bubble rising velocity versus bubble diameter

According to Figure 4.11, over the whole bubble diameter range (4.03 -5.49 mm), the U_B values were nearly constant which vary between 19 - 21 cm.s^{-1}. The similar figure also presents the experimental U_B values obtained by Grace and Wairegi, (1986) in the average value between pure and contaminated water. The results show that the bubble rising velocity were nearly constant at different bubble diameters although it has high bubble diameter at high gas flow rate. In this study, the addition of gas flow rates were less pronounced to the bubble rising velocity and thus the retention time of bubble in column. Therefore, the bubble rising velocity may be less affected to the bubble hydrodynamic parameters, interfacial area, and the VOCs removal efficiencies obtained in this work.

<u>Specific interfacial area (a)</u>

Figure 4.12 presents the variation of the interfacial area (a) with the gas flow rate. Normally, this value was the ratio of interfacial area of bubble and capacity of

reactor at a certain time. Since there were limitation of data analysis such as Chemical Method, size of reactor, type of bubble generator, and condition, thus interfacial area (a) normally was included with mass transfer coefficient. To understand the mechanism of mass transfer of bubble generated, this research was determine experimentally the value of a based on the bubble hydrodynamic parameters. Normally, the interfacial area was defined as the ratio between the total bubble surfaces (S_B) and the total volume in reactor (V_{Total}). Note that the value of S_B was the product of number of bubbles and bubble surface. The number of bubbles (N_B) was deduced from the terminal rising bubble velocities (U_B) and the bubble formation frequency (f_B) as previously presented:

$$a = N_B \times \frac{S_B}{V_{total}} = f_B \times \frac{H_L}{U_B} \times \frac{\pi D_B^2}{AH_L + N_B V_B} \qquad (4.16)$$
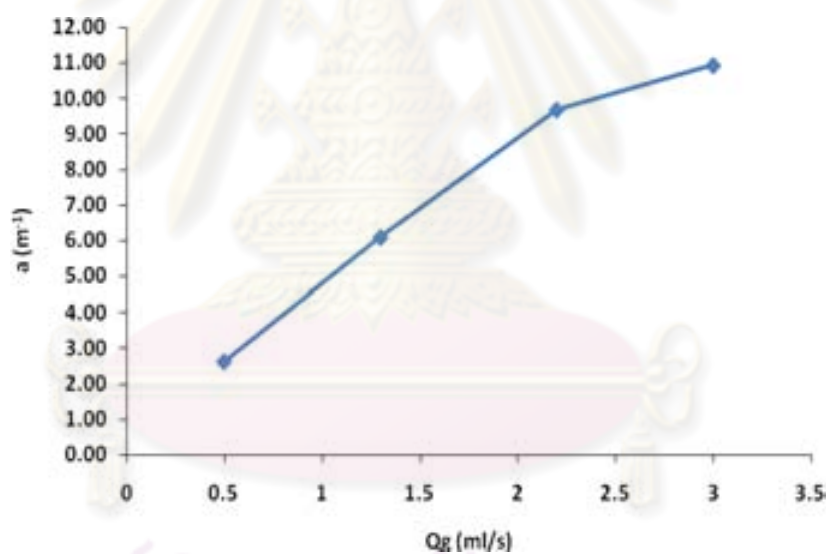
Figure 4.12 Specific interfacial area versus gas flow rate

From the results presented in Figure 4.12, the values of a vary between 2.61 – 10.93 m^{-1} for gas flow rates varying between 0.5 - 3.0 ml/s. Moreover, it can be noted that the values of a increase linearly with the gas flow rates and then become slowly increase at higher gas flow rate: the interfacial areas obtained with flow rate 3.0 ml/s greater than those obtained with another. These results were directly correlated with the experimental results of D_B, f_B and U_B as presented in Figure 4.9 – 4.11, respectively.

Concerning to the augmentation of values of K_La and a with gas flow rate as presented in Figure 4.8 and 4.12, these provide, however, the low efficiency removal. Therefore, the generation of small bubble size and also operation of absorption process with high gas flow rate for acquiring the highest value of a and K_La coefficient were not the best choice. Power consumption, turbulent condition and desorption phenomena should be taken into account: these negative effect can be possibly presented in term of the Liquid – film mass transfer coefficient (K_L).

4.2.6 Liquid – film mass transfer coefficient (K_L)

Figure 4.13 shows the variation of liquid–film mass transfer coefficient (K_L) with gas flow rate. Normally, the product of the liquid-film (side) mass transfer coefficient (K_L) and interfacial area (a) was know as the overall volumetric mass transfer coefficient (K_La). Note that, the subscribe L related with the K coefficient correspond to the mass transfer resistances obtained with the liquid phase. Thus, in the case of hydrophobic VOCs, the liquid-film mass transfer coefficient can be determined by:

$$K_L = \frac{K_L a}{a} \qquad (4.17)$$
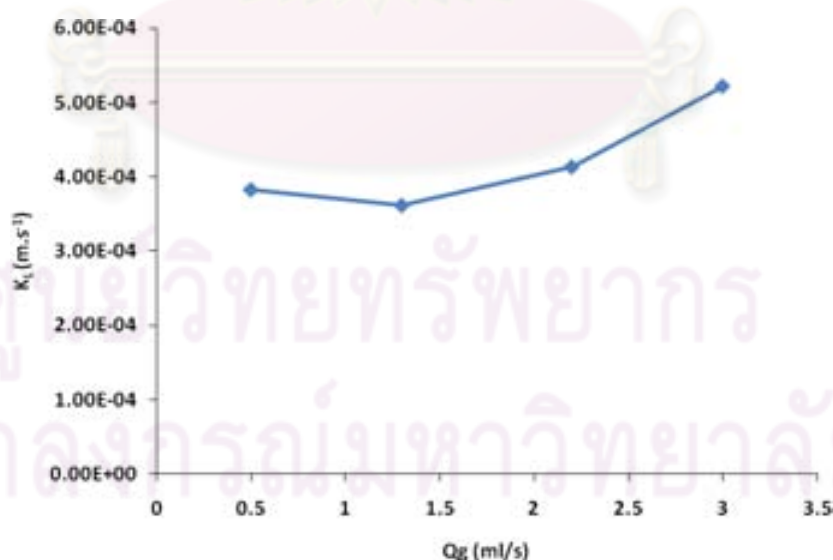
Figure 4.13 Liquid – film mass transfer coefficient versus gas flow rate

According to Figure 4.13, it can be expressed that the values of K_L obtained were roughly constant ($\approx$ 0.0004 m.s^{-1}) for gas flow rates varying between 0.5 – 2.5 ml/s: this confirm to the value obtained with mass transfer coefficient in the case of surfactant (Painmanakul *et al.,* 2005). Note that, the values of K_L were independence with gas flow rate, thus the mass transfer was controlled by liquid film around the bubble as previous described and the turbulent condition generated high gas flow rate was not affected to the mechanism of mass transfer, in this study. However, the augmentation of K_L coefficients was observed at high gas flow rates ($Q_G > 2.5$ ml/s): the additional energy due to the mixing or turbulent condition should be the important factor for these results. Therefore, in general, the enhancement of mass transfer mechanism in term of K_La coefficient and thus of mass transfer rate (dC/dt) as presented in equation 4.13 can be possibly obtained at high gas flow rates. Nevertheless, concerning to high Q_G values, the VOCs removal efficiency was reduced due to the turbulent condition and desorption of benzene gas from bubble column. Therefore, in order to achieve the high VOCs removal efficiency and high mass transfer, the fine bubble size (high interfacial area) and optimal gas flow rate (low turbulence and moderated K_L coefficient) should be applied.
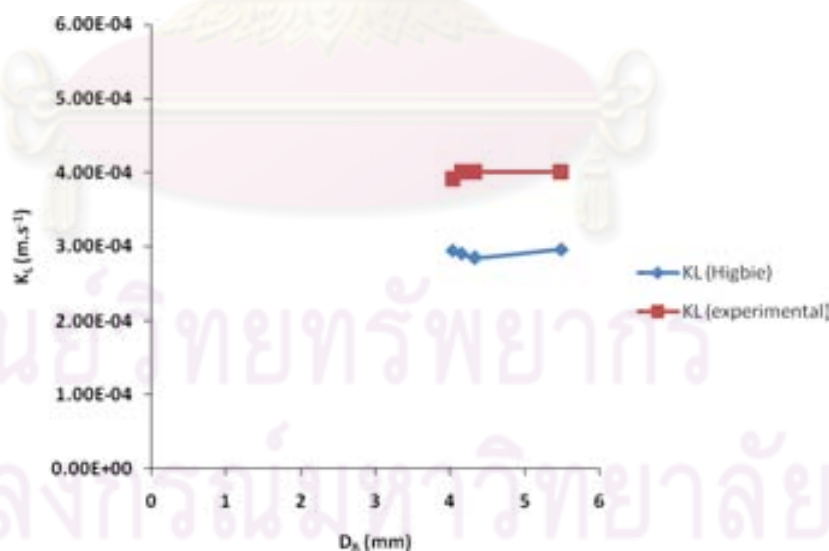
Figure 4.14 Liquid-film mass transfer coefficient based on (Eq. 4.18) versus bubble diameter

Figure 4.14 presents the variation of the liquid-side mass transfer coefficient (K_L) with the bubble diameter generated (D_B) for the different liquid phases. According to Fig. 14, the K_L values obtained were roughly constant 0.0003 m/s for bubble sizes varying between 4 and 5.5 mm. The K_L values for tap water did not depend on the bubble diameter. These results agree with those of Calderbank and Mooyong (1961): the authors have shown that the K_L values were constant for bubbles having diameters greater than 3 mm behaving usually like fluid particles with a mobile surface.

Comparison with existing model, the literature (Painmanakul *et al.,* 2005) related to K_L shows that the K_L values obtained with tap water were close to those obtained with Higbie's equation (90%) at bubble diameters for $3.5 < D_B < 6$mm (Treybal, 1980). However, the appropriate model for predicted the K_L values should be proposed.

$$K_L = 2\sqrt{\frac{D_{Benzene}.U_B}{\pi.D_B}} \qquad (4.18)$$

where $D_{benzene} = 1.1 \times 10^{-9}$ m^2/s

Table 4.6 Summary of different parameters concerning to the VOCs absorption

Qg (ml/s)	%Eff at 185 minutes	K_La (s^{-1})	D_B (mm)	f_B (s^{-1})	U_B (cm/s)	a (m^{-1})	K_L (m/s)
0.5	8.97	0.0010	4.03	14.58	19	2.61	0.00038
1.3	6.68	0.0022	4.17	34.23	20.5	6.08	0.00036
2.2	6.09	0.0040	4.33	51.74	21	9.68	0.00041
3.0	5.83	0.0057	5.49	34.61	20	10.93	0.00052

From table 4.6, it can be concluded that:

- At the higher gas flow rate, it can be caused the lower VOCs removal efficiency due to the turbulent condition in bubble column and also more energy consumption for generating the numerous bubble presence in bubble column;

- Concerning to the C_L and $C_L{}^S$, the K_La coefficient can be deduced. The values of K_La coefficient were increasing with gas flow rate.

- Due to the local analyzing method of bubble hydrodynamic parameters, the interfacial area (a) can be deduced. Moreover, the increase of a values were obtained with gas flow rate;

- According to the values of $K_L a$ and a obtained experimentally in this work. The K_L coefficient can be then determined. At low gas flow rates, the values of K_L coefficient were roughly constant around 0.0004 m/s and then increase with the Q_G values: the additional energy due to the mixing and turbulent condition was responsible for these results;

- In order to achieve the high values of mass transfer coefficients and VOCs removal efficiency by using low power consumption, the fine bubble (high interfacial area) and low gas flow rate (low turbulence and moderated K_L coefficient) should be applied.

In order to enhance the hydrophobic VOCs (benzene) removal efficiency, the next part was considered on the effect of non-ionic surfactant on VOCs removal efficiency, mass transfer and bubble hydrodynamic parameters.

4.3 The effect of non-ionic surfactant and concentrations on hydrophobic VOCs absorption process

The objective of this part was to study the effect of non-ionic surfactant at different concentrations (0.1, 0.5, 1, 3, and 5 CMC) on the VOCs removal efficiency, bubble hydrodynamic and mass transfer parameters. These results were compared with those obtained with tap water.

4.3.1 Outlet VOCs concentration in gas phase

Figure 4.15 presents the outlet VOCs concentration in gas phase with times. The gas flow rates used in this study ranges between 0.5-3.0 ml/s. Moreover, non-ionic surfactant at different concentrations was used as absorbent in this study.
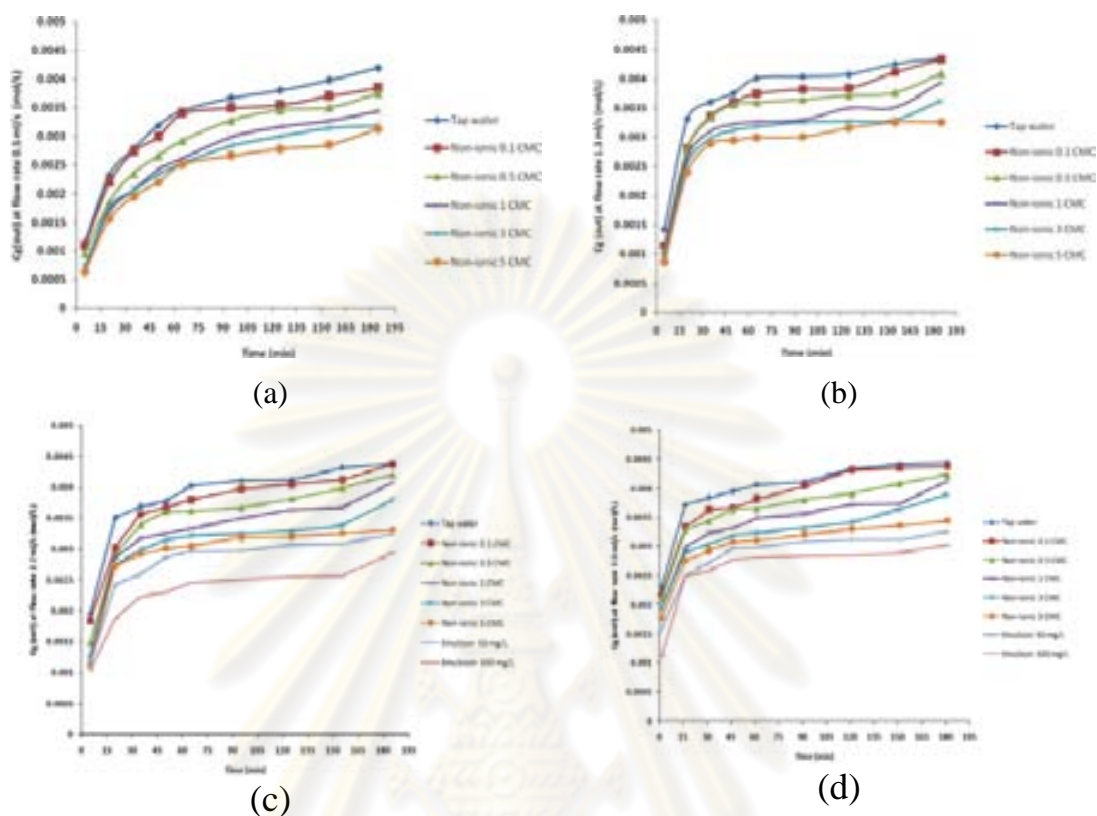
Figure 4.15 Outlet VOCs concentration in gas phase versus time: (a) gas flow rate 0.5, (b) gas flow rate 1.3 ml/s, (c) gas flow rate 2.2 ml/s, (d) gas flow rate 3.0 ml/s of tap water and aqueous solution of surfactant concentrations

From Figure 4.15, the outlet gas concentrations were increase with time due to the inlet concentrations and loadings as previously presented. The variation of outlet concentrations vary between 0.0005 – 0.0040 mol/L. Moreover, the outlet concentrations with non-ionic at any time were lower than those obtained with tap water: benzene was lower solubility in tap water. It can be noted that the influence of different surfactant concentrations (0.1, 0.5, 1, 3, and 5 CMC) was observed in this study. The outlet concentration with non-ionic 0.1 CMC was higher than the outlet concentration with non-ionic 5 CMC: these correspond to the surface tension as shown previously in Table 4.2. Therefore, the surface tension can be possibly considered as the important parameter in order to select the suitable absorbent.

In this study, it was founded that the outlet gas concentration at the last time was different. However, this value was increased continuously until the outlet concentrations were equal to the inlet concentrations (Cg(out) ≅ Cg(in)). Due to the

loading of benzene gas concentration, the outlet concentrations were increased comparable with others research such as Franck L. *et al.,* 2008 and the results as shown in Figure 4.16. The benzene gas can be absorbed to the absorbent (tap water) in a few amounts because it low solubility VOCs. Therefore, tap water should not be used as absorbent: the use of aqueous solution with non-ionic surfactant as absorbent was thus interesting point in order to enhance this absorption process.
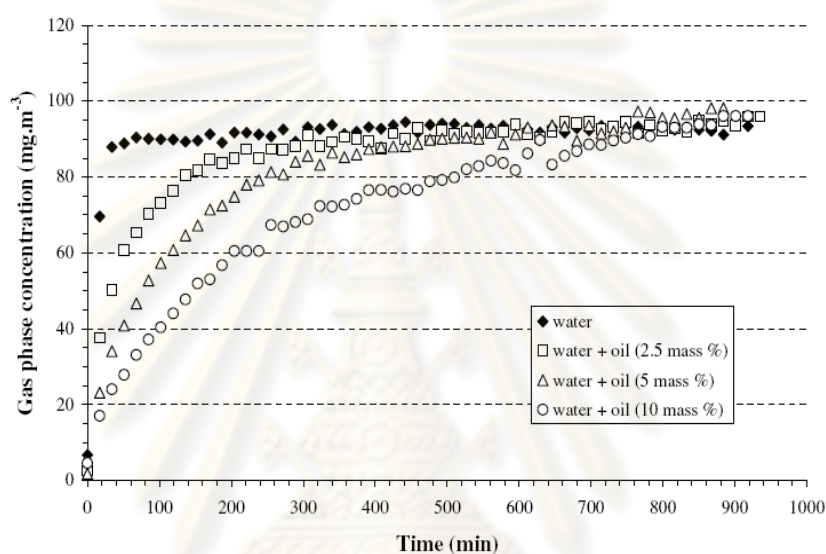
Figure 4.16 The outlet concentration in gas phase of VOCs absorption process corresponded to different liquid phase (Franck L. *et al.,* 2008)

4.3.2 VOCs concentration in liquid phase

Figure 4.17 presents hydrophobic VOCs (benzene) concentration in liquid phase with times. The gas flow rates used in this study ranges between 0.5-3.0 ml/s and the liquid phases were the aqueous solutions of non-ionic surfactants at different concentrations as absorbent. Note that, the calculation of the concentration of VOCs in different surfactant concentration (0.1, 0.5, 1, 3, and 5 CMC) was done by applying the mass balance equation as shown in equation (4.5).
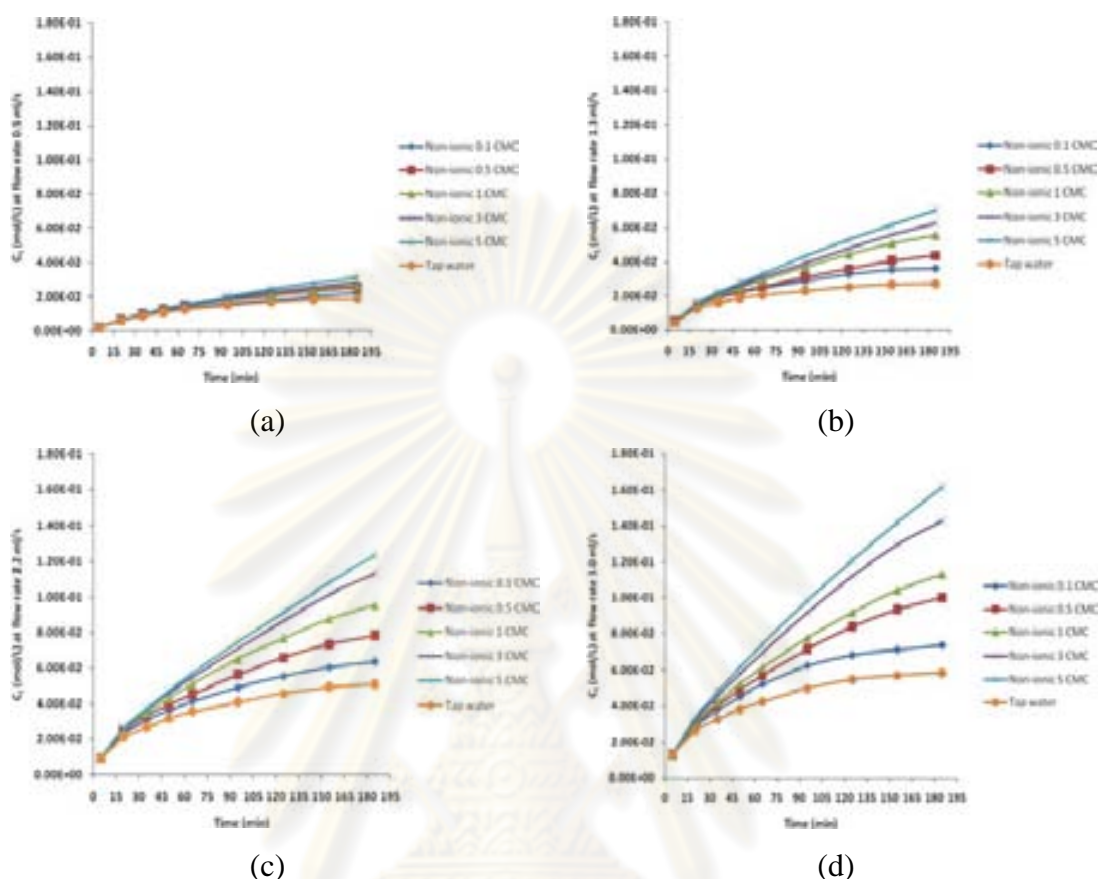
Figure 4.17 VOCs concentration in liquid phase versus time: (a) gas flow rate 0.5, (b) gas flow rate 1.3 ml/s, (c) gas flow rate 2.2 ml/s, (d) gas flow rate 3.0 ml/s of tap water and aqueous solution of surfactant concentrations

From Figure 4.17, it was founded that VOCs concentration in liquid phase increase with time. The values of C_L for surfactants were greater than those of tap water. Thus, the addition of non-ionic surfactants in order to reduced the surface tension in liquid phase and also increased the solubility of hydrophobic VOCs, up to 100 % compared with non-ionic 5 CMC and tap water. Moreover, the different concentrations of surfactant (different of surface tension) were effected to the C_L values. The C_L values were related to surfactant concentrations but independence with surface tension.

$$C_{L5\ CMC} > C_{L3\ CMC} > C_{L1\ CMC} > C_{L0.5\ CMC} > C_{L0.1\ CMC} > C_{LTap\ water}$$
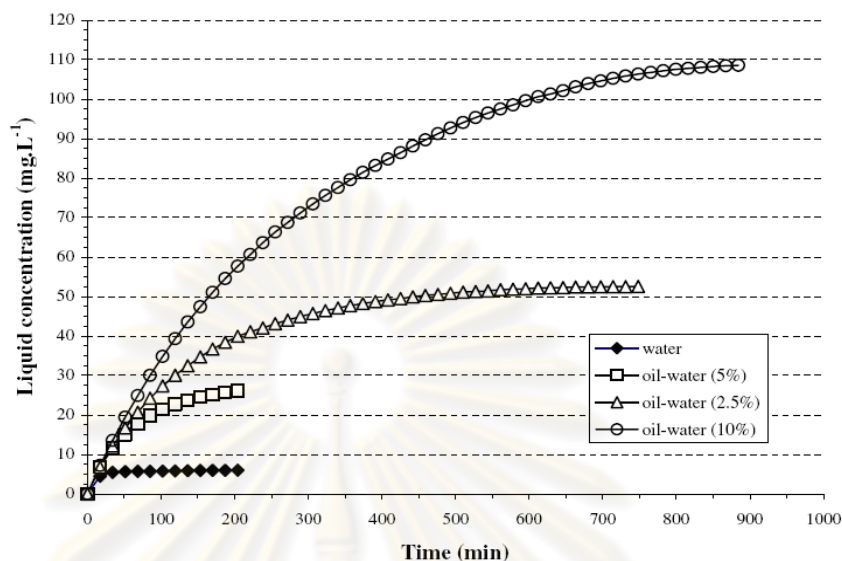
Figure 4.18 The concentration of hydrophobic VOCs in different liquid phases (Franck L. *et al.,* 2008)

At the equilibrium, the saturated time in gas phase should be equal to those obtained in liquid phase. In order to find the saturated concentration of VOCs in liquid phase (C_L^S), the experimental was run in the long time at high gas flow rate (3.0 ml/s) in order to get the saturated time. Then, it can be calculated the saturated concentrations in another gas flow rate because of the saturated concentrations were equal in the same absorbent: this phenomenon was confirmed by Franck L. *et al.,* (2008) as shown in Figure 4.18. Therefore, the results were shown in Table 4.7.

From Table 4.7, it was founded that the T_{SAT} values were related to the variation of the outlet gas concentration with time (Figure 4.15). Moreover, it can be observed that, at high gas flow rate, the saturated time was very short and the outlet gas concentration was increased quickly. But, at low gas flow rate, the saturated time was higher than high gas flow rate and the outlet gas concentration was gradually increased. Note that, consider in Henry law constant of benzene, it corresponds to low solubility in water and also in surfactant solution: mass transfer mechanism was controlled by liquid-film. Therefore, the concentration of VOCs in liquid phase and the saturated concentration of VOCs in liquid phase were important key parameters for the calculated the overall mass transfer coefficient (K_La).

Table 4.7 Saturated concentrations of VOCs in tap water, and aqueous solution of surfactant concentrations at different gas flow rate and the saturated time

Liquid phase	Qg (ml/s)	The saturated concentration in liquid phase (C_L^S) (mol/L)	The saturated time in liquid phase (T_{sat}) (minute)
Tap water	0.5	0.0695	635
	1.3	0.0680	290
	2.2	0.0708	190
	3.0	0.0697	140
Non-ionic 0.1 CMC	0.5	0.1035	640
	1.3	0.1030	425
	2.2	0.1026	265
	3.0	0.1039	200
Non-ionic 0.5 CMC	0.5	0.1246	770
	1.3	0.1252	430
	2.2	0.1244	310
	3.0	0.1250	240
Non-ionic 1 CMC	0.5	0.1440	910
	1.3	0.1430	460
	2.2	0.1435	335
	3.0	0.1443	245
Non-ionic 3 CMC	0.5	0.2280	1185
	1.3	0.2275	515
	2.2	0.2285	340
	3.0	0.2284	265
Non-ionic 5 CMC	0.5	0.2977	1405
	1.3	0.2982	575
	2.2	0.2981	345
	3.0	0.2982	270

4.3.3 VOCs removal efficiency

Figure 4.19 presents VOCs removal efficiency obtained with in different liquid phases (tap water and aqueous solutions of surfactants containing with 0.1, 0.5, 1, 3, and 5 CMC). The gas flow rate used in this study ranges between 0.5-3.0 ml/s. VOCs removal efficiency was calculated at 185 minutes by using the equation (4.12).
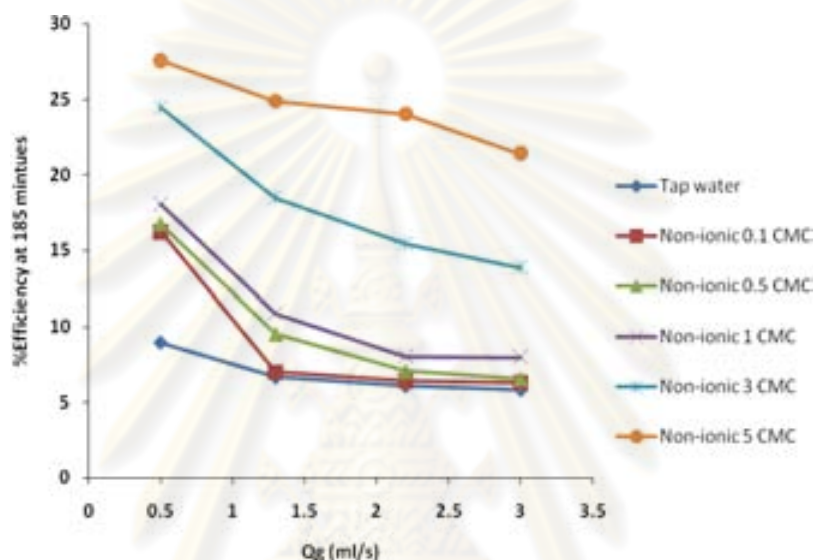
Figure 4.19 VOCs removal efficiencies versus gas flow rate for tap water and aqueous solution of surfactant with different concentrations

According to Figure 4.19, it was shown that VOCs removal efficiencies vary between 5.83% - 27.56%. The highest value of VOCs removal efficiency was observed at gas flow rate 0.5 ml/s and the desorption or stripping phenomenon can also be observed at high gas flow rate. In addition, the %Eff values were related to the concentration of surfactants and thus surface tension of applied liquid phases. When the surfactant concentrations increase and then the solubility of VOCs in liquid phases (C_L^S) and the associated %Eff values were increased due to the augmentation of the concentration gradient as previously described. Moreover, concerning to the liquid phase properties as shown in Table 4.2, it can be noted that the formation of surfactant molecules depends on the concentrations of surfactant (Painmanakul *et al.,* 2005). Thus, the formation of Admicelle and Micelle at high surfactant concentrations can affect the VOCs solubility and also absorption performance.

At the molecular level, a surfactant was an amphiphilic molecule that contains polar (hydrophilic head portion) and non polar (lipophilic tail portion) groups. Surfactants can reduce the surface tension by adsorbing at the liquid-gas interface. At higher concentration, the formation of micelles can be occurred: the non-polar tails form the core that encapsulates the benzene bubble, and the polar heads form an outer shell that maintains favorable contact with liquid phase (Vane L.M. and Giroux E.L., 2000). Therefore, the effect of surfactant concentrations presence in liquid phase can be concluded as follows:

- Hydrophobic VOCs (Benzene) removal efficiencies in tap water vary between 5.83% - 8.97% and were very low due to their low solubility.

- For the aqueous solution of surfactant with 0.1 CMC, the %Eff values vary between 6.27% – 16.24% and higher than those obtained with tap water. Small aggregate of surfactant molecules occurred on bubble surface as in Figure 4.20 (a) was responsible for these results.

- For the aqueous solution of surfactant with 0.5 CMC, the % Eff values vary between 6.58% – 16.74%. The numbers of surfactant molecule aggregation around the bubble were increased. Thus, the augmentation of hydrophobic part in both bubble and liquid phase as shown in Figure 4.20 (b) were the main reason for these results.

- The %Eff values obtained with the aqueous solution of surfactant at 1 CMC used as absorbent vary between 7.97% – 18.08%. The concentration of surfactant in this zone called the Critical Micelle Concentration (CMC): total surface of bubble was covered by the surfactant molecules and also the formation of Micelle was firstly observed (Vane L.M. and Giroux E.L., 2000). The phenomena can be presented as shown in Figure 4.20 (c).

- Concerning to the aqueous solution of surfactant with 3 CMC, the %Eff values increase and vary between 13.85% – 24.46%. The aggregation of surfactant molecule on bubble surface was similar to that obtained with surfactant concentration with 1 CMC. However, more surfactant micelles were found in the liquid phase and thus can capture the VOCs molecules dissolved as the adsolubiliization mechanism as shown in Figure 4.20 (d) (Vane L.M. and Giroux

E.L., 2000). Therefore, the VOCs removal efficiencies were higher than those obtained with the former cases.

- Finally, for the highest surfactant concentration (5 CMC) presence in liquid phase the %Eff values vary between 21.38% – 27.56%. The aggregation of surfactant molecule around the bubbles was as same as 1 and 3 CMC. Thus, the added surfactant molecules were form or increase the numerous micelles presences in liquid phase as shown in Figure 4.20 (e). These can provide the highest VOCs removal efficiencies in this case.

(a)   (b)   (c)

(d)   (e
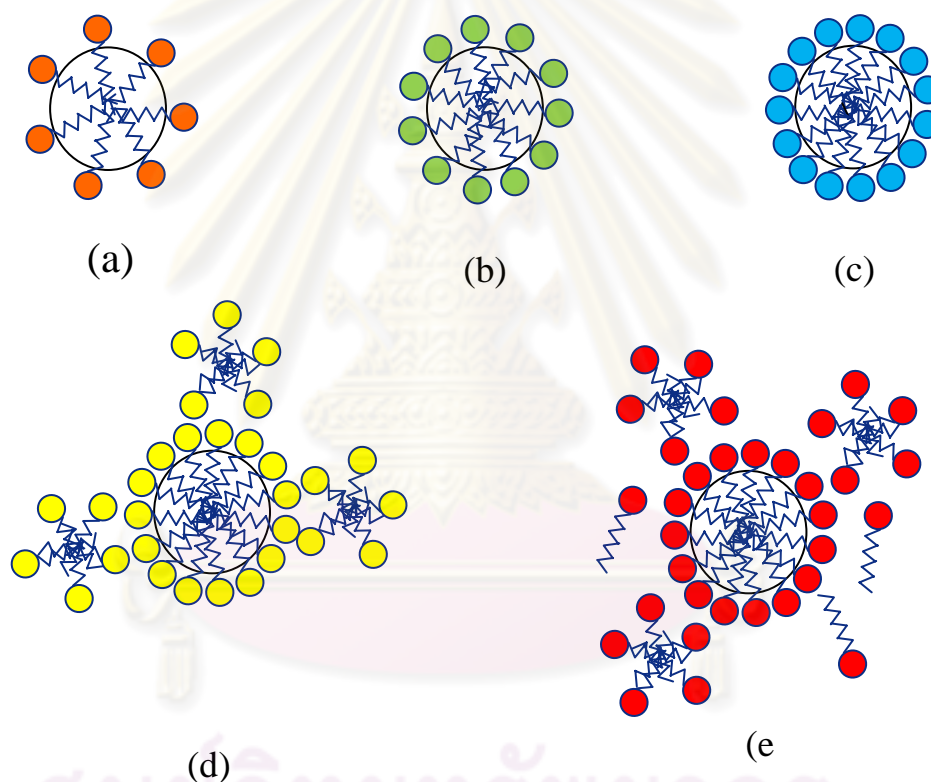
Figure 4.20 The absorption of surfactant molecules on bubble surface at (a) 0.1 CMC, (b) 0.5 CMC, (c) 1 CMC, (d) 3 CMC, and (e) 5 CMC

In next part, the $K_L a$ coefficient was analyzed in order to understand the VOCs removal efficiency obtained in bubble column. Note that, the C_L^S and C_L values from previous study were applied for calculating the $K_L a$ coefficient. Moreover, this global value was separately dissociated in terms of interfacial area (a) and liquid-side mass transfer coefficient (K_L).

4.3.4 Overall mass transfer coefficient in liquid phase ($K_L a$)

Figure 4.21 shows the overall mass transfer coefficient ($K_L a$) obtained in different liquid phases (tap water and aqueous solutions of surfactant with 0.1, 0.5, 1, 3, and 5 CMC). The gas flow rates vary between 0.5 – 3.0 ml/s. Note that, the overall mass transfer coefficient in liquid phase was given by using equation (4.13) as previously presented.
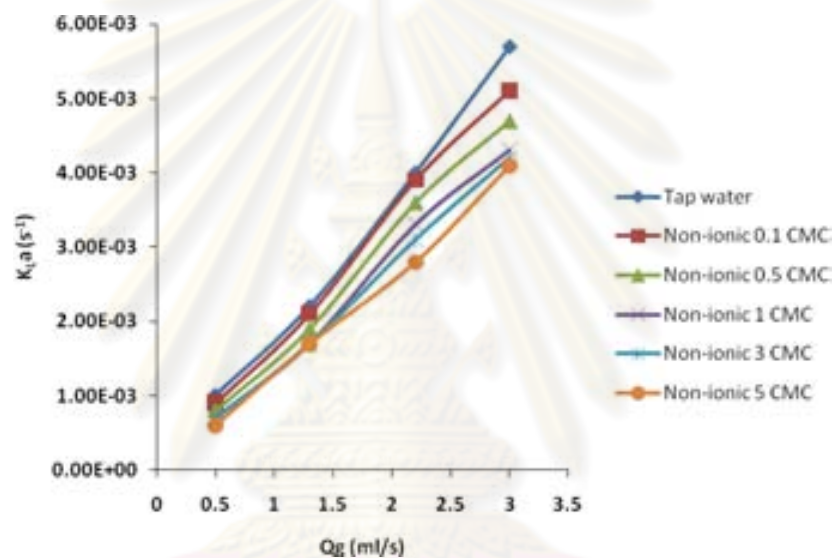
Figure 4.21 Overall mass transfer coefficient based on liquid phase versus gas flow rate of tap water and aqueous solution of surfactant concentrations

Concerning to Figure 4.21, the $K_L a$ coefficients increase with the gas flow rates due to the difference of mass transfer capability from inlet VOCs loading to bubble column. So, it can be expressed that the increased $K_L a$ coefficients was based on the concentration gradient related to gas flow rate. These values vary between 0.0006 and 0.0051 s^{-1}for gas flow rates varying between 0.5 and 3.0 ml/s. Although, the $K_L a$ coefficients were higher at high gas flow rate, but the associated turbulent condition can also cause the desorption or stripping phenomena and thus reduce the VOCs removal efficiency as presented in Figure 4.20. From Treybal (1980), the mass transfer mechanism was related to the applied gas flow rate and also the fluid flow regime in bubble column that can be divided into 2 types:

1. Ordinary flow was obtained with low gas flow rate ($Re_0 < 2100$). The generated bubbles was smoothly flow along the column and thus the mass transfer mechanism from bubble to absorbent was fine with small desorption problem as shown in Figure 4.22.

2. Eddy diffusion corresponds to the turbulent flow of generated bubbles in bubble column ($Re_0 = 10,000$ to $50,000$) as shown in Figure 4.23. Due to the turbulent condition, the bubbles can be provided the mixing condition occurred in absorbent. Thus, hydrophobic VOCs can be easily desorbed from the bubble column, and thus the concentrations in gas phase at high gas flow rate were increased.
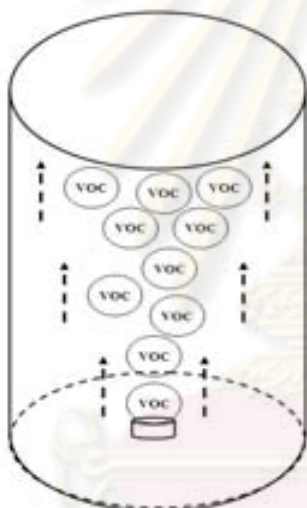
Figure 4.22 Ordinary flow at low
gas flow rate in bubble column
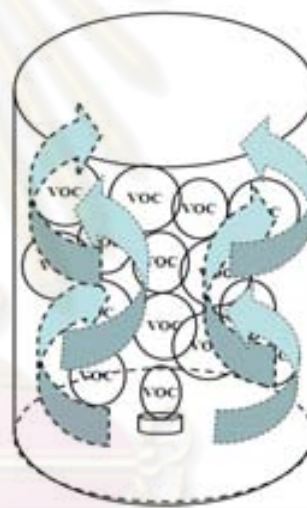
Figure 4.23 Eddy flow at high gas
flow rate in bubble column

Therefore, similar to that discussed for tap water used as absorbent, the optimal K_La values and turbulent condition should be chosen in order to obtain the high VOCs absorption performance in surfactant solution. Moreover, by considering the different surfactant solutions, it can be noted that the K_La coefficients were lower than those obtained with tap water. Moreover, the different of surfactant concentrations were effected to the K_La values. The values of K_La were related to surface tension (independence with concentrations of surfactant). Nonetheless, the K_La values of 1, 3, and 5 CMC were less pronounced. To provided understand this phenomenon, it essential to separately consider between the interfacial area (a) was

deduced to hydrodynamic conditions and also the K_L coefficient was deduced to the liquid film mass transfer. Overall, the following trend of K_La was found:

$$K_La_{\text{Tap water}} > K_La_{0.1 \text{ CMC}} > K_La_{0.5 \text{ CMC}} > K_La_{1 \text{ CMC}} \approx K_La_{3 \text{ CMC}} \approx K_La_{5 \text{ CMC}}$$

4.3.5 Hydrodynamic parameters

Bubble diameter (D_B)

Figure 4.24 demonstrates the variation of the generated bubble diameter (D_B) with gas flow rate. These experimental results can be obtained from the Image analyzing Techniques by using high speed camera (100 image/s) and Image Treatment program.
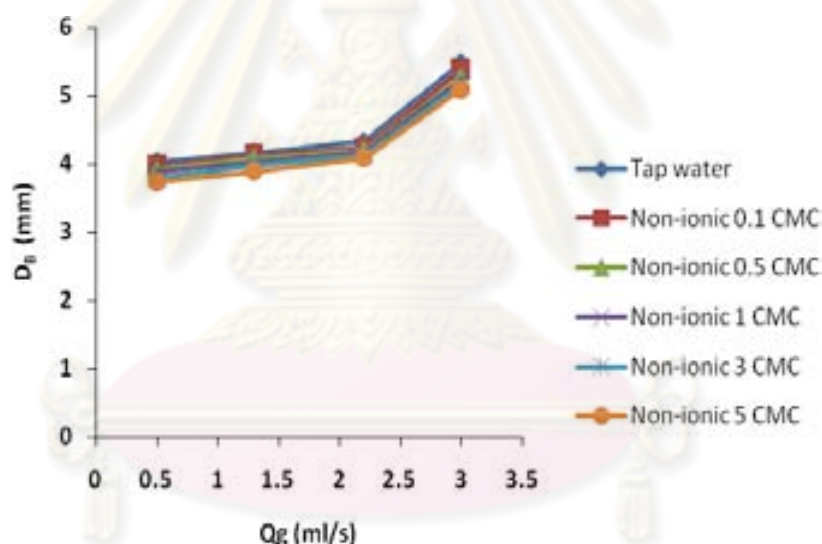
Figure 4.24 Bubble diameter versus gas flow rate of tap water and aqueous solution of surfactant concentrations

According to Figure 4.24, the bubble diameters obtained experimentally vary between 3.74 -5.39 mm, while gas flow rates can change between 0.5 - 3.0 ml/s. The bubble diameter increases with gas flow rate. Moreover, the results shown that at low gas flow rate 0.5 – 2.2 ml/s the bubble diameters were mainly constant and then increase at high gas flow rate (>2.0 ml/s): the coalescence and rupture phenomena was responsible for these results. Same as previously discussed, the large bubble size

generation at high Q_G values correspond to the high power consumption, turbulent condition, and also desorption process.

Moreover, the bubble diameter was related to surface tension. If the liquid phases contain the surfactant molecules, the surface tension and bubble size can be reduced due to the Laplace's equation (Painmanakul *et al.,* 2005). Therefore, the highest and smallest D_B values can be observed at the liquid phases with tap water and surfactant concentration with 5 CMC, respectively.

Bubble formation frequency (f_B)

Figure 4.25 demonstrate the variation of the bubble formation frequency (f_B) with gas flow rate.
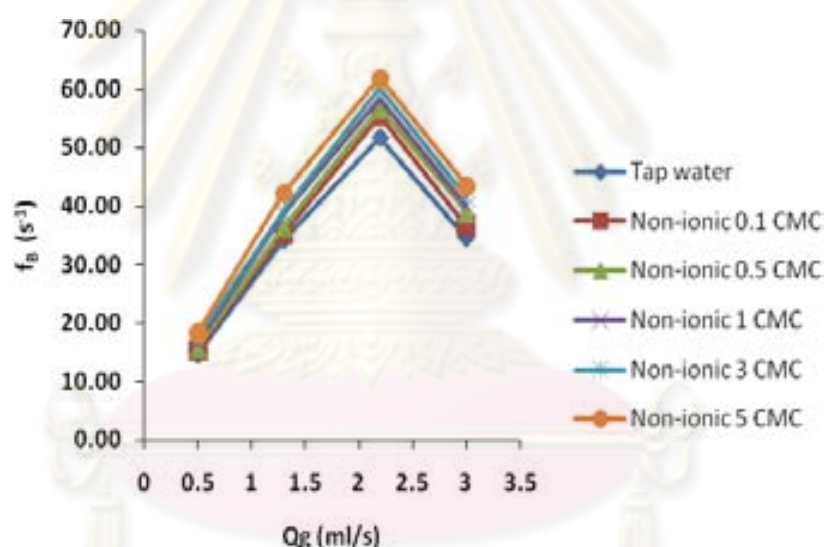
Figure 4.25 Relation between the variations of bubble formation frequency and gas
flow rate of tap water and aqueous solution of surfactant concentrations

Concerning to Figure 4.25, the bubble formation frequency obtained experimentally vary between 15.26 -61.84 s^{-1} while gas flow rates can change between 0.5 - 3.0 ml/s. For gas flow rate between 0.5 and 2.2 ml/s, the f_B values were obviously increased until the gas flow rate equal to 3.0 ml/s and then start decreasing for any liquid phases used as absorbent. Note that, the small f_B values obtained with 3.0 ml/s gas flow rate corresponds to the highest bubble size obtained as in Figure 4.24. Moreover, the f_B values obtained with surfactant solution were higher than those

obtained with tap water: this relates to the small bubble diameter generated in bubble column. It can be expressed that the high f_B values (high number of bubble generated per second in bubble column) was the foremost reason for the sharp reduction of %Eff values in the case of surfactants compared with tap water as shown in Figure 4.19. Thus, the control of turbulent condition from bubble hydrodynamic condition was the very important factors in this case.

Bubble rising velocity (U_B)

Figure 4.26 shows the relation between the bubble rising velocity (U_B) with the generated bubble diameter.
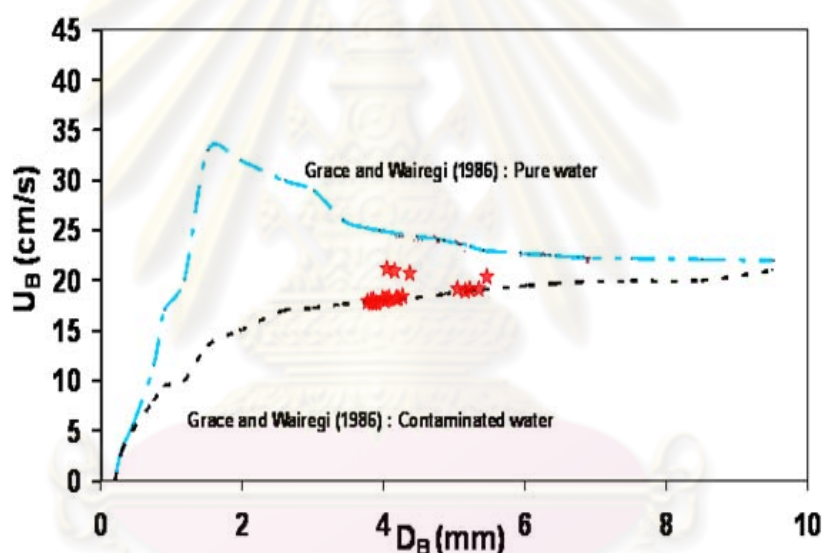
Figure 4.26 Comparison of experimental and theoretical bubble rising velocity for different bubble diameter of tap water and aqueous solution of surfactant concentrations

According to Figure 4.26, over the whole bubble diameter range (3.61 -5.03 mm), the U_B values were nearly constant which vary between 18 – 19 cm.s^{-1}. These correspond with the experimental values obtained by Grace and Wairegi, (1986) in the average value between pure and contaminated water. In this study, the addition of gas flow rates and also of surfactant concentrations were less pronounced to the bubble rising velocity and the retention time of bubble in column. Therefore, the bubble

rising velocity has the small effect on the calculated interfacial area and thus mass transfer mechanism in this study.

Specific interfacial area (a)

Figure 4.27 presents the variation of the interfacial area (a) with the gas flow rate. Note that the interfacial area (a) was deduced from the bubble diameter (D_B), the bubble frequency (f_B) and the terminal bubble rising velocity (U_B) obtained experimentally in this work.
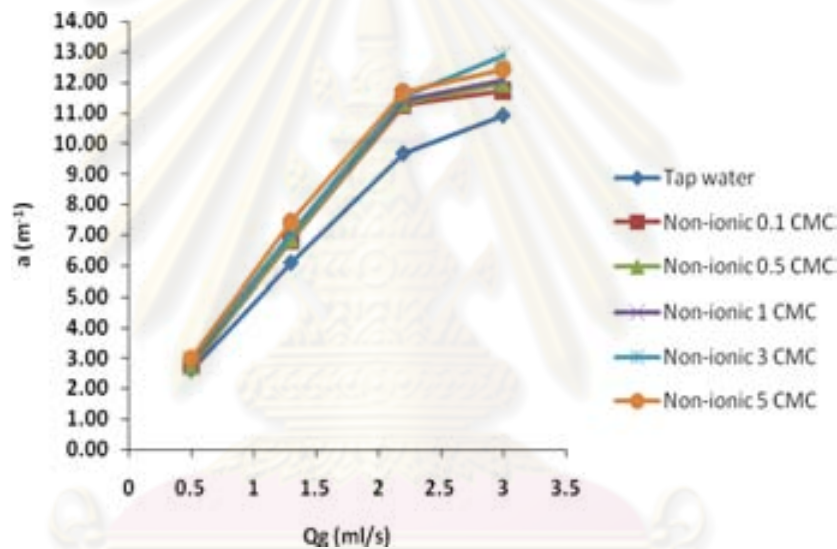
Figure 4.27 Interfacial area versus gas flow rate of tap water and aqueous solution of surfactant concentrations

From the results in Figure 4.27, whatever the liquid phases applied in this work, the values of a increase linearly with the gas flow rates and then become slowly increasing. Moreover, the a values vary between 2.72 – 12.41 m^{-1} for gas flow rates varying between 0.5 - 3.0 ml/s. For a given gas flow rate, the interfacial areas obtained with non-ionic surfactant were greater than those obtained with tap water. The difference was more pronounced at high Q_G values: the associated D_B and f_B values, as presented in Figure 4.24 and 4.25 respectively, were responsible for these results. Furthermore, the highest values of a were found at the smallest bubble sizes

due to the lowest surface tension from increased surfactant concentration. In this study, the following overall trend was found:

$$a_{5CMC} > a_{3CMC} > a_{1CMC} > a_{0.5\ CMC} > a_{0.1\ CMC} > a_{Tap\ water}$$

Concerning to the augmentation of interfacial are (a) by adding the surfactants in liquid phase, higher VOCs removal efficiency can be obtained; however, the K_La coefficient was decreased. Therefore, higher VOCs saturated concentration in liquid phase (C_L^S) or concentration gradient (ΔC) was responsible for increasing the mass transfer rate (dC/dt) in liquid phase containing with non-ionic surfactants as previously presented in equation 4.13, but the decrease of K_La coefficient can also be found. In this case, it can be stated that the positive effect on ΔC values were more pronounced than the negative effect obtained with the decreased K_La coefficient. Next, the liquid – film mass transfer coefficient (K_L) was determined in order to provide a better understanding on effect of non-ionic surfactant presence in liquid phase.

4.3.6 Liquid – film mass transfer coefficient (K_L)

Figure 4.28 shows the liquid-film mass transfer coefficient (K_L) obtained in different liquid phases (tap water and aqueous solutions of surfactant with 0.1, 0.5, 1, 3, and 5 CMC). The gas flow rates vary between 0.5 – 3.0 ml/s. Note that, the overall mass transfer coefficient in liquid phase was given by using equation (4.17) as previously presented.

From Figure 4.28, it can be expressed that the values of K_L obtained vary between 0.00020 and 0.00044 m.s^{-1} for gas flow rates varying between 0.5 – 3.0 ml/s. At low the gas flow rates ($Q_G < 2.5$ ml/s), the K_L values remain roughly constant for each liquid phase. Then increase with the Q_G values: the additional energy due to the mixing and turbulent condition was responsible for these results. Moreover, the K_L coefficients obtained with the surfactant solutions were smaller than those obtained with tap water: these results clearly indicate that the presence of surfactants at the bubble interface disturbs the mass transfer, certainly by modifying the composition or the thickness of liquid film around the air bubbles (Painmanakul *et al.,* 2005). For a given gas flow rate, it can be observed that the K_L coefficients obtained with the

higher surfactant concentrations were lower than those obtained with the lower ones. In this study, the following overall trend was found:

$$K_{L \text{ Tap water}} > K_{L \text{ 0.1 CMC}} > K_{L \text{ 0.5 CMC}} > K_{L \text{ 1CMC}} \approx K_{L \text{ 3CMC}} \approx K_{L \text{ 5CMC}}$$
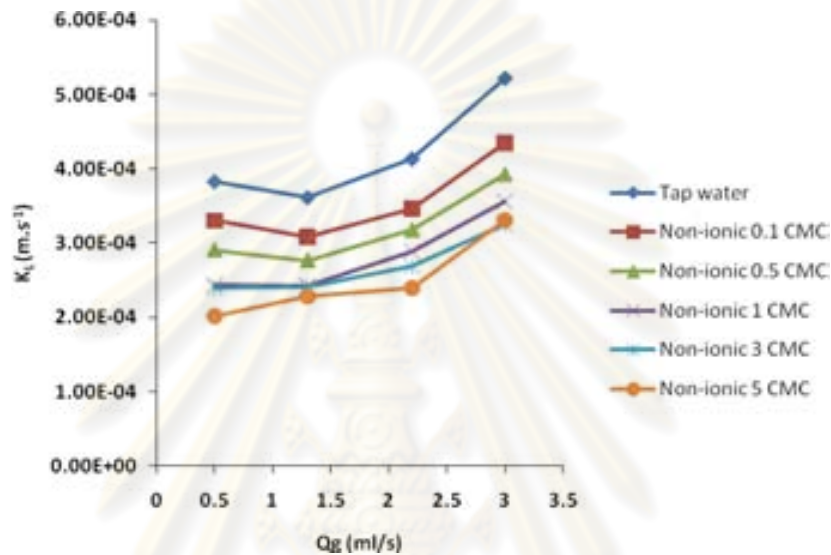
Figure 4.28 Liquid-film mass transfer coefficient versus gas flow rate obtained with tap water and aqueous solutions of surfactant with different concentrations

Moreover, the K_L values related to high surfactant concentrations (i.e., at 1, 3, 5 CMC) were quite similar, whereas significant differences can be found in the case of low surfactant concentrations (0.1, and 0.5 CMC). Therefore, it can be concluded that the micelle formed in liquid phase at higher surfactant concentration provide the insignificant negative effect on the reduction of K_L coefficients compared with that obtained with the presence of surfactant molecules at the bubble interface.

At this stage, it can be assumed that the increase in the surfactant concentrations can possibly decrease the gas diffusivity due to the Higbie's equation and thus modify the resistance of the gas–liquid interface. As a result, the decreasing mass transfer coefficients *(*K_La and K_L*)* in the presence of surfactants would be the consequence of a modification of the gas–liquid interface nature coupled with local hydrodynamic changes (Dumont and Delmas, 2003). In conclusion, the experimental results obtained in this part can be summarized as in Table 4.8.

Table 4.8 Summary of different parameters (VOCs removal efficiency, mass transfer and bubble hydrodynamic parameters) on VOCs absorption process

Liquid phase	Q_g (ml/s)	%Eff at 185 minutes	K_La (s^{-1})	D_B (mm)	f_B (s^{-1})	U_B (cm/s)	a (m^{-1})	K_L (m/s)
Tap water	0.5	8.97	0.0010	4.03	14.58	19	2.61	0.00038
	1.3	6.68	0.0022	4.17	34.23	20.5	6.08	0.00036
	2.2	6.09	0.0040	4.33	51.74	21	9.68	0.00037
	3.0	5.83	0.0057	5.49	34.61	20	10.93	0.00052
Non-ionic 0.1 CMC	0.5	16.24	0.0009	3.97	15.26	18.5	2.72	0.00033
	1.3	6.99	0.0021	4.13	35.23	18.5	6.81	0.00031
	2.2	6.43	0.0039	4.23	55.49	18.5	11.25	0.00035
	3.0	6.27	0.0051	5.39	36.57	19	11.72	0.00044
Non-ionic 0.5 CMC	0.5	16.74	0.0008	3.93	15.73	18.5	2.75	0.00029
	1.3	9.53	0.0019	4.09	36.27	18.5	6.87	0.00028
	2.2	7.07	0.0036	4.20	56.69	18.5	11.33	0.00032
	3.0	6.58	0.0047	5.28	38.91	19	11.96	0.00039
Non-ionic 1 CMC	0.5	18.08	0.0007	3.88	16.34	18	2.86	0.00024
	1.3	10.05	0.0016	4.01	38.49	18.5	7.01	0.00023
	2.2	8.03	0.0033	4.16	58.34	18.5	11.43	0.00029
	3.0	7.97	0.0044	5.23	40.04	19	12.08	0.00036
Non-ionic 3 CMC	0.5	24.46	0.0007	3.80	17.40	18	2.92	0.00024
	1.3	18.46	0.0017	3.99	39.07	18.5	7.04	0.00024
	2.2	15.42	0.0031	4.12	60.06	18.5	11.55	0.00027
	3.0	13.85	0.0042	5.17	41.45	18	12.89	0.00033
Non-ionic 5 CMC	0.5	27.56	0.0006	3.74	18.25	18	2.97	0.00020
	1.3	24.88	0.0017	3.89	42.16	18	7.43	0.00023
	2.2	24.01	0.0028	4.08	61.84	18.5	11.66	0.00024
	3.0	21.38	0.0041	5.09	43.43	19	12.41	0.00033

From Table 4.8, it can be concluded that:

- At the higher gas flow rate, low VOCs removal efficiency can be obtained due to the turbulent condition in bubble column. High energy consumption for generating the numerous bubble presences in bubble column was required. Whatever gas flow rates, the VOCs removal efficiencies in aqueous solution of surfactant were higher than tap water;

- The saturated concentration of hydrophobic VOCs (benzene) in surfactant solution (C_L^S) was greater than those obtained in tap water. The C_L^S values relate with the surfactant concentration and thus

associated surface tension of liquid phase. Therefore, the augmentation of hydrophobic part due to the surfactant molecules added in liquid phase was possibly responsible for these results;

- Concerning to the C_L and $C_L{}^S$, the K_La coefficient can be deduced. The values of K_La coefficient were increasing with gas flow rate. The K_La values obtained with surfactant solution were smaller than those obtained with tap water. These results indicate that the surfactant presence in liquid phase can affect the mass transfer mechanism of benzene gas in bubble to liquid phase;

- Due to the local analyzing method of bubble hydrodynamic parameters, the interfacial area (a) can be deduced. The values of a increase linearly with the gas flow rates and then become slowly increasing. Moreover, the values of a obtained with aqueous solution of surfactants were greater than those obtained with tap water whatever gas flow rates. These results were directly correlated with the experimental results of D_B, f_B and U_B;

- According to the values of K_La and a obtained experimentally in this work, the K_L coefficient can be then determined and affect certainly the liquid-film mass transfer resistance by increasing the composition or the thickness of liquid film around the air bubbles, and thus decreasing the K_L coefficient.

- The interfacial area and the K_L coefficient were found to be compensated with each other in the liquid phase containing with surfactant. Moreover, the K_L values related to high surfactant concentrations were quite similar, whereas significant differences appear at low surfactant concentrations. Therefore, it was not necessary to generate too fine bubbles to increase the a values because not only, high power consumption and clogging problem due to small orifice applied, but also the K_L coefficients reduction can be obtained;

- Appropriate amount of surfactants and bubble hydrodynamic condition were necessary in order to obtain the fine absorption performance of hydrophobic VOCs in bubble column.

The next part was discussed the effect of oil-in-water emulsion on the VOCs removal efficiency, mass transfer and bubble hydrodynamic parameters. Note that, the non-ionic surfactant (Tween 80) used in this part was applied for preparing the stabilized oil-in-water emulsion and thus enhancing the hydrophobic VOC treatment by absorption process.

4.4 The effect of oil-in-water emulsion on hydrophobic VOCs absorption process

The objective of this part was to study the effect of oil-in-water emulsion (Lubricant oil) containing with different oil concentrations (50 and 300 mg/L) at surfactant concentration equal to 1 CMC used as absorbents. Moreover, these results were compared with those obtained with tap water and surfactant solutions as previously presented in former part.

4.4.1 Outlet VOCs concentration in gas phase

Figure 4.29 presents the variation of the outlet VOCs concentration in gas phase (C_G) with times. The gas flow rates, used in this study, range between 0.5-3.0 ml/s.

From Figure 4.29, the outlet gas concentrations increase with time due to the inlet concentration and loading as shown in Table 4.1. The variation of outlet concentrations vary between 0.0005 – 0.0045 mol/L. The outlet concentrations obtained with 50 mg/L lubricant oil were higher than those obtained with 300 mg/L: these were the smallest values compared with different liquid phases. The increase of non-polar or hydrophobic part was responsible for these results. Moreover, the significant influence of lubricant oil at different concentrations (50 and 300 mg/L) can be observed in this study. Note that, the C_G values obtained in this study were increased continuously until they were equal to the inlet concentrations (saturation

stage) as discussed previously. It can be noted that the longest time for reaching saturation or equilibrium stage seem to be obtained with the stabilized oil-in-water emulsion in this part.

(a)   (b)

(c)   (d)
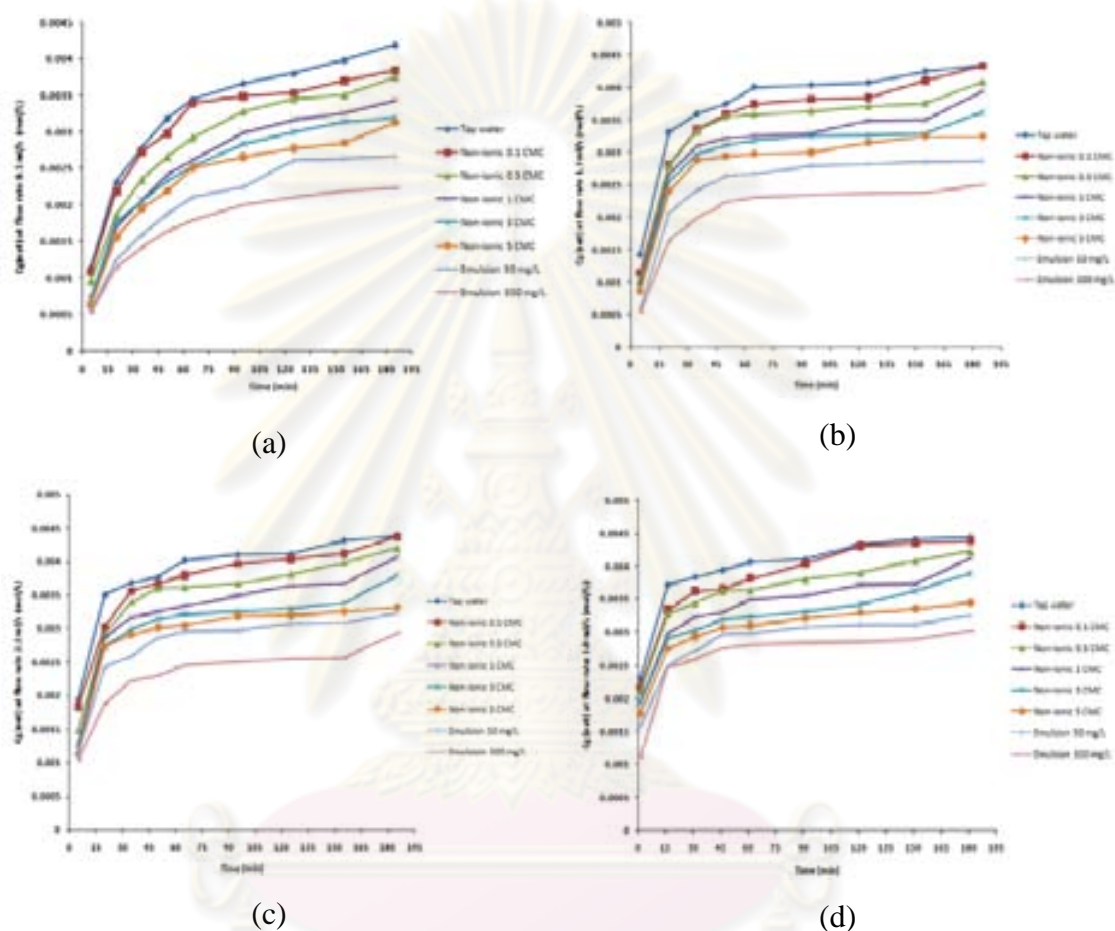
Figure 4.29 Outlet VOCs concentration in gas phase versus time: (a) gas flow rate 0.5, (b) gas flow rate 1.3 ml/s, (c) gas flow rate 2.2 ml/s, (d) gas flow rate 3.0 ml/s for 3 types of absorbent

4.4.2 VOCs concentration in liquid phase

Figure 4.30 presents the variation of VOCs concentrations in liquid phase (C_L) with times. The gas flow rates used in this study ranges between 0.5-3.0 ml/s and the stabilized oil-in-water emulsions at 50 and 300 mg/L were used as absorbent. Note that, the calculation of the concentration of VOCs in emulsion concentrations (50 and 300 mg/L) was done by using the mass balance equation as shown in equation (4.5).

(a)

(b)

(c)

(d)
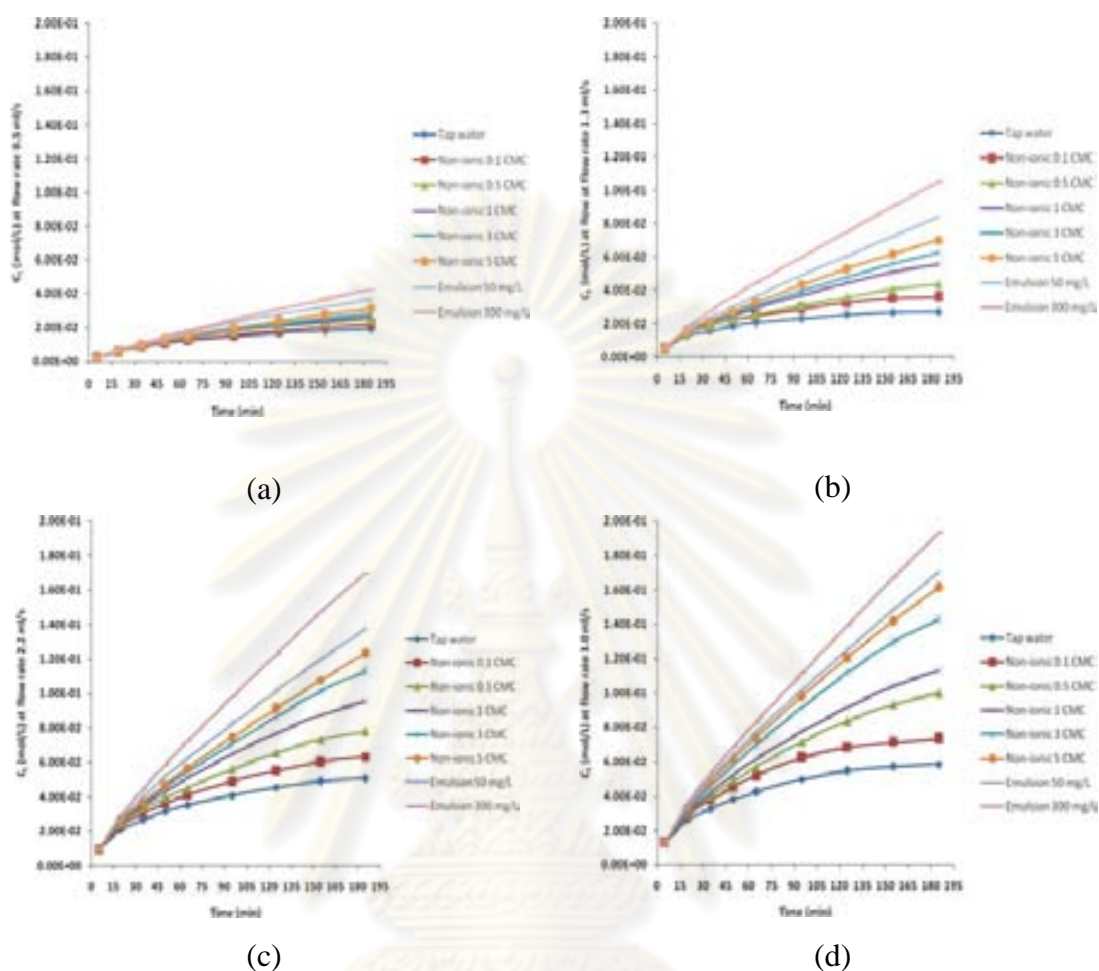
Figure 4.30 VOCs concentration in liquid phase versus time: (a) gas flow rate 0.5, (b) gas flow rate 1.3 ml/s, (c) gas flow rate 2.2 ml/s, (d) gas flow rate 3.0 ml/s for 3 types of absorbent

According to Figure 4.30, the values of C_L increase linearly with time, especially in case of oil-in-water emulsion. These results confirm that benzene molecules dissolve preferably in these applied absorbents. However, due to their low solubility values, it can be noted that the mass transfer was again controlled by liquid phase. This phenomenon was confirmed by Franck L. *et al.,* (2008) (Figure 4.5). Similarly, in order to obtain the saturated VOCs concentration (C_L^S) and also the saturation time (T_{SAT}), the experimental method as previously described was used. The results obtained can be summarized in Table 4.9.

Table 4.9 Saturated concentrations of VOCs in liquid phase and the saturated time at different gas flow rates for 50 and 300 mg/L of stabilized oil-in-water emulsions

Liquid phase	Qg (ml/s)	Saturated concentration in liquid phase (C_L^S) (mol/L)	Saturated time in liquid phase (T_{sat}) (minute)
Tap water	0.5	0.0695	635
	1.3	0.0680	290
	2.2	0.0708	190
	3.0	0.0697	140
Oil-in-water emulsion 50 mg/L	0.5	0.3624	1410
	1.3	0.3599	580
	2.2	0.3540	400
	3.0	0.3521	295
Oil-in-water emulsion 300 mg/L	0.5	0.4130	1430
	1.3	0.4130	590
	2.2	0.4152	410
	3.0	0.4139	300

Concerning to Table 4.9, the average VOCs concentration at saturation stage were about 0.36 and 0.42 mg/L for 50 and 300 mg/L oil-in-water emulsions, respectively. It can be noted that the T_{SAT} values obtained relate to those presented in the experimental results with the highest Q_G (3 ml/s) as shown in Figure 4.29 (d). Moreover, the values of T_{SAT} increase sharply with the reduction of gas flow rates. This corresponds with VOCs loading entered into the bubble column. Note that, the concentration of VOCs in liquid phase and the saturated concentration of VOCs in liquid phase were important key parameters for calculating the overall mass transfer coefficient. By considering the experimental results in Table 4.9, it can be expressed that the C_L^S values of oil-in-water emulsion were greater than those obtained with others absorbents. It was related to the additional of hydrophobic part in liquid phase. Moreover, the values of T_{SAT} from oil-in-water emulsion were higher than tap water at 5 times, it can be stated that the application of oil-in-water emulsion as absorbent used in many times and also the little maintenance (change or absorbent cleaning).

Furthermore, it was interested aspect to apply these absorbent used in absorption in form of bubble.

4.4.3 VOCs removal efficiency

Figure 4.31 presents the relation between the VOCs removal efficiency and gas flow rate for 50 and 300 mg/L of stabilized oil-in-water emulsion. The results were compared with those obtained with different liquid phases (tap water and aqueous solution with non-ionic surfactants at 0.1, 0.5, 1, 3, and 5 CMC). The gas flow rate used in this study ranges between 0.5-3.0 ml/s. the VOCs removal efficiency (%Eff) was calculated at 185 minutes by using the equation (4.12).

Figure 4.31 VOCs removal efficiency versus gas flow rate for 3 types of absorbents used in this study (tap water, surfactant solutions and stabilized oil-in-water emulsion)

As shown in Figure 4.31, the values of %Eff vary between 5.83% - 47.67%. The highest %Eff values were observed at gas flow rate 0.5 ml/s and then tend to decrease when gas flow rate increases: the negative effect due to the turbulent condition can be over again observed. These results confirm that low values of Q_G were necessary to acquire the optimal absorption performance. Moreover, the values of %Eff obtained with oil-in-water emulsion were greater than those obtained with others absorbent, especially higher than tap water 5 times, so these results were related to the higher solubility of benzene since the non polar proportions in liquid

phase were higher. However, it can be stated that the effect of turbulent occurred in reactor also caused the desorption of emulsion higher than those absorbents. Thus, this phenomenon was related to the solubility of benzene in liquid phase. Therefore, the turbulent condition due to high gas flow rates, effected to the desorption of benzene gas at different concentrations between soluble in liquid phase part and in gas phase (Concentration gradient, $\Delta C = C_{AL}-C_{AG}$). Due to the higher fluxes of mass transfer, the higher concentrations of surfactant in absorbent, and hence the aggregations of micelles were higher, it was important factors of the sorption or desorption of benzene gas effectively. Furthermore, the %Eff at gas flow rate 3.0 ml/s of aqueous solution of surfactant at 5 CMC were closed to emulsion 50 mg/L for the different C_L^S values (30%). In practice, it should be applied the solution of surfactant at 5 CMC because higher efficiency, easy to prepared the absorbent, small amount of desorption and also easy to treated waste from bubble column.

4.4.4 Overall mass transfer coefficient in liquid phase (K_La)
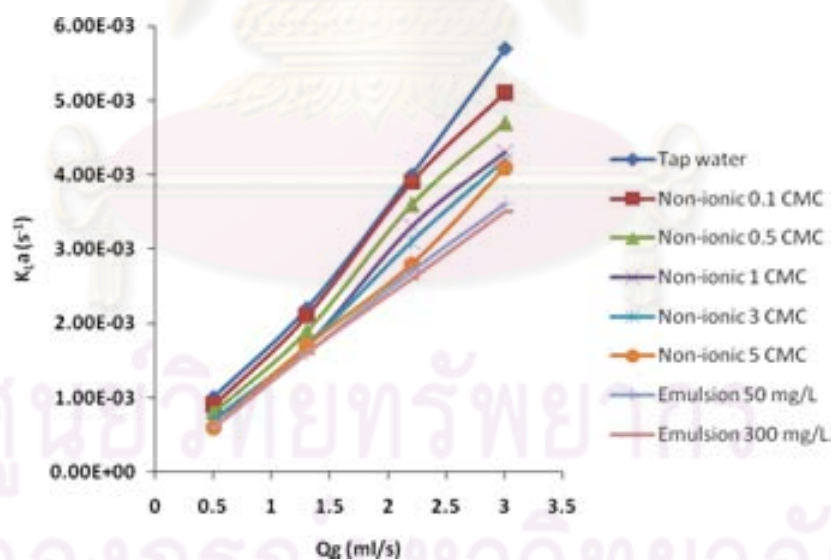
Figure 4.32 Overall mass transfer coefficient versus gas flow rate for 3 types of absorbents used in this study (tap water, surfactant solutions and stabilized oil-in-water emulsion)

Figure 4.32 presents the relation between the K_La coefficients and gas flow rate for 50 and 300 mg/L of stabilized oil-in-water emulsion. The results were compared with those obtained with different liquid phases (tap water and aqueous solution with non-ionic surfactants at 0.1, 0.5, 1, 3, and 5 CMC).

Concerning to Figure 4.32, the K_La coefficients increase with the gas flow rates. These values vary between 0.001 and 0.0044 s^{-1} for gas flow rates varying between 0.5 and 3.0 ml/s: K_La coefficients obtained with high gas flow rate was greater than low gas flow rate. Although, the K_La coefficients were higher at high gas flow rate, but the desorption or stripping phenomena due to the turbulent condition should be taken into account as previously described. Moreover, the K_La values of oil-in-water emulsion were lower than those obtained with other absorbent. Due to the oil particles were reduce mass transfer from benzene to liquid phase and the different concentrations of lubricant oil also little affected to the K_La values. When comparison to the K_La values of solution of surfactant, it was founded that it really closed to the results at higher concentration 5 CMC and lower than tap water. Overall, the following trend of K_La was found:

$$K_La \text{ }_{Tap \text{ } water} > K_La \text{ }_{non-ionic \text{ } surfactant} \approx K_La \text{ }_{oil-in-water \text{ } emulsion}$$

Therefore, the higher VOCs removal efficiencies due to the better results from the additional of ΔC in higher proportion of the decrease of K_La values and influence to the increasing of mass transfer rate $dC/dt = k_La.(C_L^S - C_L)$ as shown in Eq.4.13. The next part was study the effect of hydrodynamic parameters and also the application to calculate the K_L coefficient.

4.4.5 Hydrodynamic parameters

Bubble diameter (D_B)

Figure 4.33 demonstrates the variation of the generated bubble diameter (D_B) with gas flow rate. These results can be got from Image Treatment Techniques by high speed camera (100 image/s).

According to Figure 4.33, the bubble diameters obtained experimentally vary between 3.60 -5.00 mm while gas flow rates can change between 0.5 - 3.0 ml/s. The bubble diameter was increased with gas flow rate. At low gas flow rate 0.5 – 2.2 ml/s

the bubble diameters were mainly constant and start increasing at high gas flow rate (>2.0 ml/s). It can be noted that same trend line as obtained with previous experiments can be observed. Moreover, due to Laplace 's equation (Painmanakul *et al.,* 2005), the bubble diameter, especially at low Q_G values, was related to surface tension as presented in Table 4.2 and 4.3. The lowest and biggest bubble diameter can be thus obtained with 300 mg/L of oil-in-water emulsion and tap water, respectively. However, the difference in values was reduced at higher gas flow rate: the power dissipated in the liquid, conditioning the bubble break up and coalescence phenomena was answerable for these results.
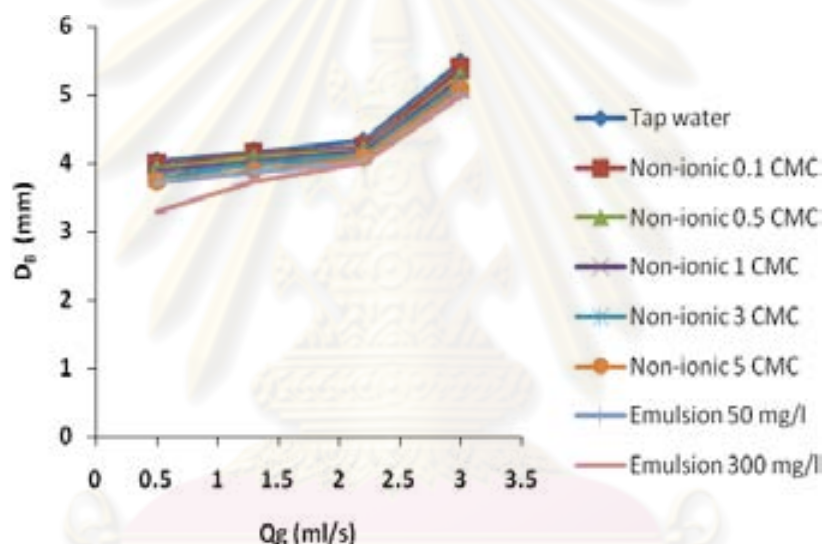
Figure 4.33 Bubble diameter versus gas flow rate for 3 types of absorbents used in this study (tap water, surfactant solutions and stabilized oil-in-water emulsion)

Bubble formation frequency (f_B)

Figure 4.34 demonstrate the variation of the bubble formation frequency (f_B) with gas flow rate.

Concerning to Figure 4.34, the f_B values obtained experimentally vary between 20.46 - 65.14 s^{-1} while gas flow rates range between 0.5 - 3.0 ml/s. For gas flow rate between 0.5 and 2.2 ml/s, the bubble formation frequency was obviously increased until the gas flow rate 3.0 ml/s: the bubble formation frequency starts decreasing. Moreover, it was founded that the f_B values obtained with oil-in-water

emulsion were greater than those obtained with others absorbents: these relate to the bubble diameter as presented in Figure 4.33.
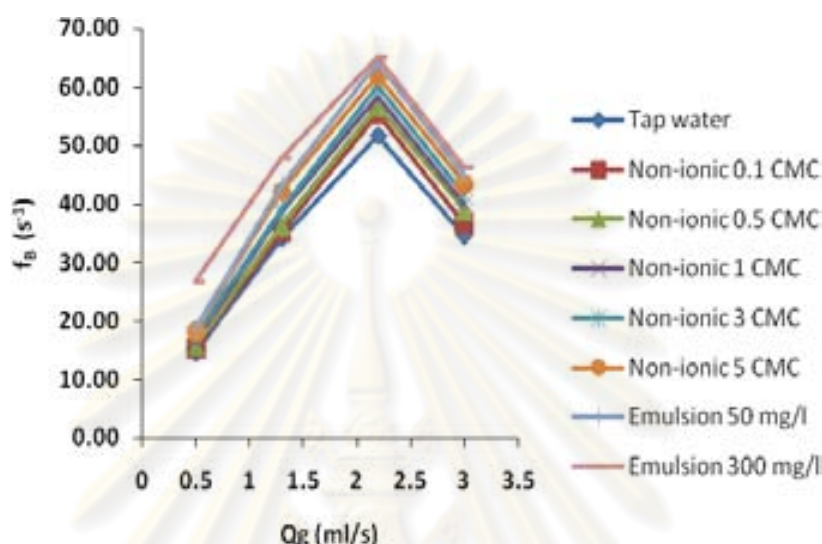
Figure 4.34 Bubble formation frequency versus gas flow rate for 3 types of absorbents used in this study (tap water, surfactant solutions and stabilized oil-in-water emulsion)

Bubble rising velocity (U_B)

Figure 4.35 shows the relation between the bubble rising velocity (U_B) with the generated bubble diameter.

According to Figure 4.35, over the whole bubble diameter range (3.60 -5.00 mm), the U_B values were nearly constant which vary between $17 - 19$ cm.s^{-1}: this corresponds with those presented by Grace and Wairegi (1986). Moreover, it can be noted that the U_B values were nearly constant at different liquid phases and gas flow rates. Therefore, it can be conclude that the bubble rising velocity provide small effect on bubble hydrodynamic parameters, interfacial area, and thus VOCs removal efficiency in this study.
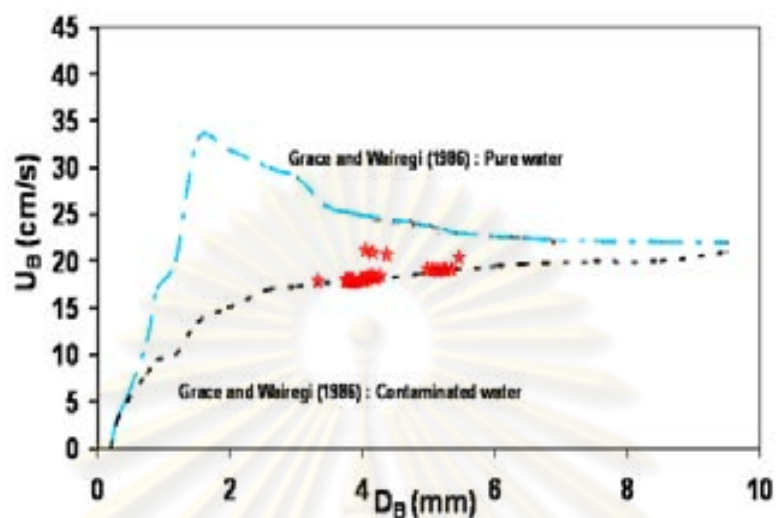
Figure 4.35 Comparison of experimental and theoretical bubble rising velocity for different bubble diameter for 3 types of absorbents used in this study (tap water, surfactant solutions and stabilized oil-in-water emulsion)
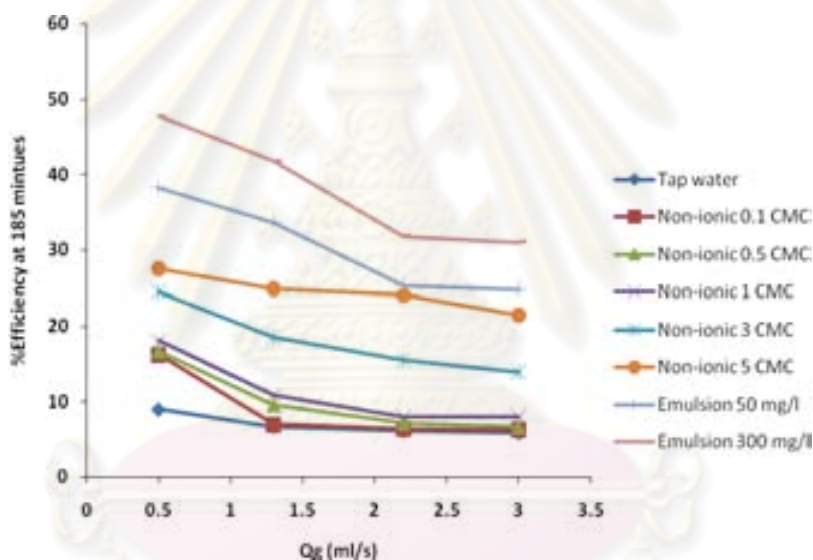
Specific interfacial area (a)
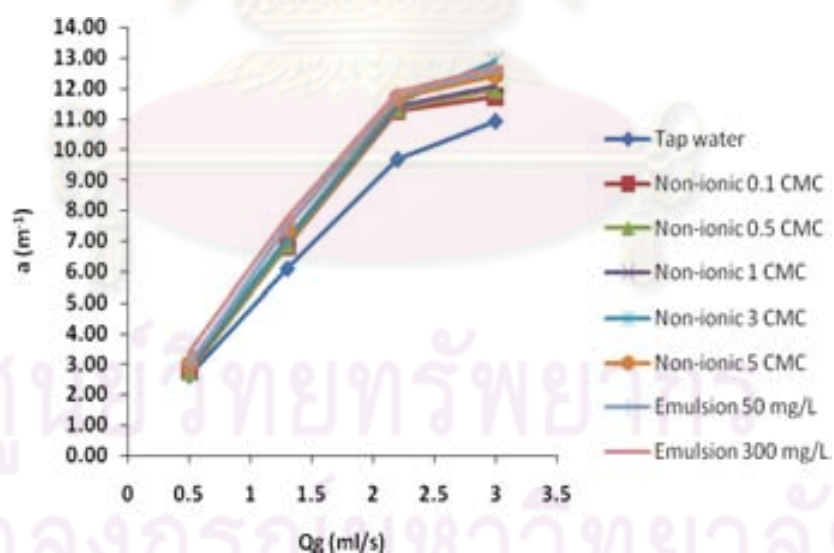
Figure 4.36 Interfacial area versus gas flow rate for 3 types of absorbents used in this study (tap water, surfactant solutions and stabilized oil-in-water emulsion)

Figure 4.36 presents the variation of the interfacial area (a) with the gas flow rate. Note that the interfacial area (a) was deduced from the bubble diameter (D_B), the

bubble frequency (f_B) and the terminal bubble rising velocity (U_B) obtained experimentally in this work.

Concerning to Figure 4.36, it can be found that, whatever the liquid phases, the values of a increase linearly with the gas flow rates and then become slowly increase. The values of a vary between $3.27 – 14.41$ m^{-1} for gas flow rates varying between $0.5 - 3.0$ ml/s. Moreover, for a given gas flow rate, the interfacial areas obtained with emulsion at 300 mg/L were greater than those obtained with another: these results were directly correlated with the experimental results of D_B, f_B and U_B as presented in Figure $4.33 – 4.35$. Therefore, the experimental results of K_La and a were then used in order to calculate the liquid–film mass transfer coefficient (K_L). Note that, this parameter can be applied for providing a better understanding on the effect of different contaminants covered the generated bubbles.

4.4.6 Liquid – film mass transfer coefficient (K_L)

Figure 4.37 presents the relation between the K_L coefficients and gas flow rate for 50 and 300 mg/L of stabilized oil-in-water emulsion. The results were compared with those obtained with different liquid phases (tap water and aqueous solution with non-ionic surfactants at 0.1, 0.5, 1, 3, and 5 CMC).
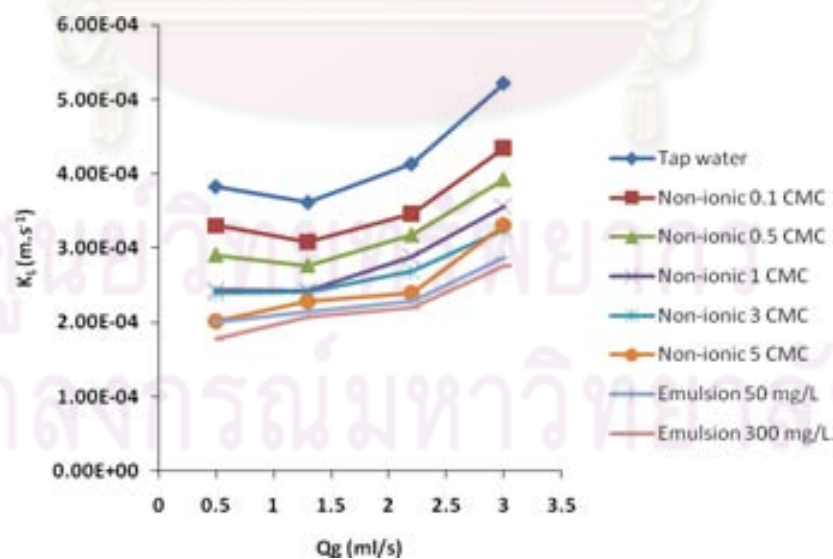
Figure 4.37 Liquid-film mass transfer coefficient versus gas flow rate for 3 types of absorbent

According to Figure 4.37, it can be expressed that the values of K_L obtained vary between 0.00025 and 0.00042 m.s^{-1}for gas flow rates varying between 0.5 – 3.0 ml/s. At low the gas flow rates ($Q_G < 2.5$ ml/s), the K_L values remain roughly constant for each liquid phase. Then increase with the Q_G values: the additional energy due to the mixing and turbulent condition was responsible for these results. The K_L values obtained with oil-in-water emulsion and surfactant solutions were significantly smaller than those obtained with tap water: these results clearly indicate that the presence of oil droplets and surfactant molecules at the bubble interface can disturb the mass transfer mechanism, certainly by modifying the composition or the thickness of liquid film around the benzene bubbles.

Note that, different oil concentrations (50 and 300 mg/L) were proven to have similar effect on the variation of K_L coefficients and thus associated liquid film. Moreover, the K_L values related to high surfactant concentrations (1, 3 and 5 CMC) and oil-in-water emulsion were quite similar, whereas significant differences appear in the case of low surfactant concentrations (0.1, and 0.5 CMC). Thus, it can be concluded that the formation of micelle at higher surfactant concentration and also augmentation of oil droplets or concentrations provide the small effect on the reduction of K_L coefficients: the presence of contaminant molecules at the bubble interface was the most important factor obtained in this study. However, at higher Q_g values, the remarkable difference ($K_{L\ Surfactant} > K_{L\ Oil\text{-}in\text{-}water\ emulsion}$) can be observed: the separation of surfactant micelles due to the attachment between micelles and bubble as flotation process and thus generation of foam at the column surface was possibly responsible for these results.

Table 4.10 Summary of the different parameters obtained in this study including VOCs removal efficiency, mass transfer and bubble hydrodynamic parameters.

Liquid phase	Qg (ml/s)	%Eff at 185 minutes	K_La (s⁻¹)	D_B (mm)	f_B (s⁻¹)	U_B (cm/s)	a (m⁻¹)	K_L (m/s)
Tap water	0.5	8.97	0.0010	4.03	14.58	19	2.61	0.00038
	1.3	6.68	0.0022	4.17	34.23	20.5	6.08	0.00036
	2.2	6.09	0.0040	4.33	51.74	21	9.68	0.00037
	3.0	5.83	0.0057	5.49	34.61	20	10.93	0.00052
Non-ionic 0.1 CMC	0.5	16.24	0.0009	3.97	15.26	18.5	2.72	0.00033
	1.3	6.99	0.0021	4.13	35.23	18.5	6.81	0.00031
	2.2	6.43	0.0039	4.23	55.49	18.5	11.25	0.00035
	3.0	6.27	0.0051	5.39	36.57	19	11.72	0.00044
Non-ionic 0.5 CMC	0.5	16.74	0.0008	3.93	15.73	18.5	2.75	0.00029
	1.3	9.53	0.0019	4.09	36.27	18.5	6.87	0.00028
	2.2	7.07	0.0036	4.20	56.69	18.5	11.33	0.00032
	3.0	6.58	0.0047	5.28	38.91	19	11.96	0.00039
Non-ionic 1 CMC	0.5	18.08	0.0007	3.88	16.34	18	2.86	0.00024
	1.3	10.05	0.0016	4.01	38.49	18.5	7.01	0.00023
	2.2	8.03	0.0033	4.16	58.34	18.5	11.43	0.00029
	3.0	7.97	0.0044	5.23	40.04	19	12.08	0.00036
Non-ionic 3 CMC	0.5	24.46	0.0007	3.80	17.40	18	2.92	0.00024
	1.3	18.46	0.0017	3.99	39.07	18.5	7.04	0.00024
	2.2	15.42	0.0031	4.12	60.06	18.5	11.55	0.00027
	3.0	13.85	0.0042	5.17	41.45	18	12.89	0.00033
Non-ionic 5 CMC	0.5	27.56	0.0006	3.74	18.25	18	2.97	0.00020
	1.3	24.88	0.0017	3.89	42.16	18	7.43	0.00023
	2.2	24.01	0.0028	4.08	61.84	18.5	11.66	0.00024
	3.0	21.38	0.0041	5.09	43.43	19	12.41	0.00033
Oil-in-water emulsion 50 mg/L	0.5	38.24	0.0006	3.71	18.69	18	2.99	0.00020
	1.3	33.61	0.0016	3.86	43.15	18	7.48	0.00021
	2.2	25.34	0.0027	4.03	64.17	18.5	11.80	0.00023
	3.0	24.75	0.0036	5.03	45.00	19	12.56	0.00029
Oil-in-water emulsion 300 mg/L	0.5	47.67	0.0006	3.29	26.80	18	3.38	0.00018
	1.3	41.78	0.0016	3.73	47.82	18	7.75	0.00021
	2.2	31.79	0.0026	4.01	65.14	18.5	11.86	0.00022
	3.0	31.01	0.0035	4.98	46.37	19	12.68	0.00028

In conclusion, it can be expressed that the increase in the surfactant and emulsion concentrations should decrease the gas diffusivity and thus modify the resistance of the gas–liquid interface. As a result, the decreasing mass transfer coefficients $(K_La$ and $K_L)$ in the presence of surfactants and oil-in-water emulsion would be the consequence of a modification of the gas–liquid interface nature coupled with local hydrodynamic changes (Dumont and Delmas, 2003).

From table 4.10, it can be concluded that:

- For a given gas flow rate, the VOCs removal efficiencies in emulsion solution were greater than tap water and aqueous solution of surfactant due to the increase of benzene solubility in oil-in-water emulsion;

- At the higher gas flow rate, it can cause the lower VOCs removal efficiency due to the turbulent condition in bubble column and also more energy consumption for generating the numerous bubble presences in bubble column;

- Concerning to the C_L and C_L^S, the K_La coefficient were increasing with gas flow rate. These K_La values obtained with oil-in-water emulsion and surfactant solution were smaller than those obtained with tap water. These results indicate that the oil droplets and surfactant concentrations can affect the mass transfer of benzene gas to liquid phase;

- Due to the local analyzing method of bubble hydrodynamic parameters, the calculated interfacial area (a) obtained with oil-in-water emulsion were higher than those obtained with tap water and surfactant solutions whatever gas flow rates. these results were directly correlated with the experimental results of D_B, f_B and U_B;

- According to the values of K_La and a obtained experimentally in this work, the K_L coefficient can be then determined and affect certainly the liquid-film mass transfer resistance by increasing the composition or the thickness of liquid film around the air bubbles, and thus decreasing the K_L coefficient.

- The interfacial area and the K_L coefficient were found to be compensated with each other in the mass transfer process. Moreover, the K_L values related to the oil-in-water emulsion (50 and 300 mg/L) and the surfactant solution with high concentrations were quite similar, however, at higher Q_g values, the remarkable difference ($K_{L\ Surfactant} > K_{L\ Oil-in-water\ emulsion}$) can be observed;

- In practice, the application of oil-in-water emulsion was interesting issues because the higher benzene solubility can be obtained with added oily concentration and also small effect on K_La coefficients have been proven, however, the issues about absorbent preparation, wastewater treatment and also desorption phenomena should be taken into account.

CHAPTER V

CONCLUSIONS AND RECOMMENDATIONS

5.1 Conclusions

Volatile Organic Compounds (VOCs) were widely used in the industrialized countries as solvents. A large amount of the industrially used VOCs was emitted via gas exhaust and contaminated wastewater streams, and represents a severe environmental hazard. Therefore, the objectives of this work were to study the effect of gas flow rates, aqueous solution of non-ionic surfactant and stabilized oil-in-water emulsion containing with non-ionic surfactant presence in liquid phase (absorbent) on hydrophobic VOCs absorption mechanism in terms of removal efficiency, bubble hydrodynamic and mass transfer parameters.

In this work, the experiments were carried out in a small bubble column (4.4 cm in diameter and 30 cm in height) and measured the inlet and outlet VOCs concentrations in gas phase by using the GC-FID equipment. Due to the dynamic method, the overall mass transfer coefficients (K_La) were then analyzed by using the VOCs concentration in liquid phase based on the mass balance equation. Moreover, the bubble diameter (D_B), bubble rising velocity (U_B), bubble formation frequency (f_B) and interfacial area (a) were determined by using the image analyzing technique as the bubble hydrodynamic parameters. Then, the liquid-film mass transfer coefficient (K_L) can be calculated as the ratio between the K_La and the a values obtained experimentally. In this study, benzene was chosen as hydrophobic VOCs. Tap water, aqueous solution with non-ionic surfactant (Tween80) at different concentrations (0.1, 0.5, 1, 3, and 5 CMC) and 50 and 300 mg/L of stabilized oil-in-water emulsion containing non-ionic surfactant at 1 CMC were applied as the liquid phase (absorbent). The operating conditions were as follows: liquid height H_L = 20 cm, room temperature and gas flow rate of 0.5, 1.3, 2.2, and 3.0 ml/s.

In this study, the following results have been obtained;

- VOCs removal efficiencies obtained with stabilized oil-in-water emulsion were greater than those obtained with other liquid phases. The trend obtained was summed up as: $\%\text{Eff}_{\text{tap water}} < \%\text{Eff}_{\text{non-ionic surfactant}} < \%\text{Eff}_{\text{oil-in-water emulsion}}$;

- In presence of surfactants and oil-in-water emulsion at different concentrations, the saturated VOCs concentration in different liquid phases (C_L^S) obtained in this study can be increased. The high C_L^S values related to the increase of surfactant and oil concentrations can be thus enhance the VOCs removal efficiencies;

- At high gas flow rate, the reduction of VOCs removal efficiencies can be observed for a given liquid phase: the mixing or turbulent condition was possibly responsible for these results. In the case of oil-in-water emulsion, this phenomenon was more remarkable;

- The overall mass transfer coefficient ($K_L a$) increase with the gas flow rates whatever the liquid phases. The $K_L a$ values for both oil-in-water emulsion and surfactants were significantly smaller than those of water. The trend obtained was summed up as: $K_L a_{\text{oil-in-water emulsion}} < K_L a_{\text{non-ionic surfactant}} < K_L a_{\text{tap water}}$;

- Concerning to the experimental results of D_B, f_B and U_B values, the interfacial area (a) can be deduced. The values of a increases with the gas flow rates whatever the liquid phases and the interfacial area values for both oil-in-water emulsion and surfactants were significantly greater than those of water. The trend obtained can be concluded as: $a_{\text{tap water}} < a_{\text{non-ionic surfactant}} < a_{\text{oil-in-water emulsion}}$;

- At low gas flow rates, the liquid-film mass transfer coefficient (K_L) remains roughly constant for a given liquid phase. Then, the augmentation can be observed at higher Q_G values due to the additional energy from mixing and turbulent condition;

- The K_L coefficients obtained with the oil-in-water emulsion and surfactants were significantly smaller than those obtained with tap water. The following overall trend was found: $K_{L\text{oil-in-water emulsion}} < K_{L\text{non-ionic surfactant}} < K_{L\text{tap water}}$. These results clearly indicate that the presence of oil droplets in liquid phase

and surfactant molecules at the bubble interface can be disturbed the mass transfer mechanism, certainly by modifying the composition or the thickness of liquid film around the benzene bubbles;

- Different oil concentrations (50 and 300 mg/L) were proven to have similar effect on the variation of K_L coefficients and thus associated liquid film. Moreover, the K_L values related to high surfactant concentrations (1, 3 and 5 CMC) and oil-in-water emulsion were quite comparable, whereas significant differences appear in the case of low surfactant concentrations (0.1, and 0.5 CMC);

- The formation of micelle at higher surfactant concentrations and also augmentation of oil droplets provided the small effect on the reduction of K_L coefficients which relate with the modification of the composition or the thickness of liquid film around the benzene bubbles;

- The effect of various surfactants and lubricant oil concentrations on the $K_L a$, a and K_L values were less pronounced than that on the C_L^S values. Thus, in order to increase the VOCs absorption or mass transfer rate $dC/dt = K_L a.(C_L^S - C_L)$, the optimal concentrations of surfactant and lubricant oil should be applied with the suitable Q_G values (small desorption phenomena).

In conclusion, in order to obtain the high VOCs removal efficiency without the problems about the desorption / stripping phenomena, oily wastewater and operation cost, the aqueous solution with 5 CMC were suggested in this study. The overall results obtained in this study can be summarized as in Table 5.1.

From table 5.1, it can be concluded that tap water should not be used as absorbent for the hydrophobic VOCs absorption process. Moreover, it not necessary to generated the numerous small bubble sizes because of high energy consumption required and also the desorption or stripping phenomena occurred. The additional of surfactants at suitable concentration can be provided the high VOCs removal efficiency due to the increase of VOCs solubility in liquid phase and also the modification of bubble hydrodynamic parameters. However, the decreasing of $K_L a$ and K_L coefficients due to the increasing of composition or the thickness of liquid film around the air bubbles

should be considered as the drawback of the surfactant molecules presence in liquid phase. Concerning to the stabilized oil-in-water emulsion used in this study, this can be provided the similar results as in the case of surfactant: desorption or stripping phenomena, treatment of oily wastewater (absorbent) and absorbent preparation and also operation cost have to be well considered.

5.2 Recommendations for future work

In the future, the different types of VOCs gas and gas diffusers (flexible gas diffuser) should be studied in order to provide a better understanding of the VOCs absorption process in bubble column. Moreover, it was evident that the results observed in the small bubble column have to be validated into a tall bubble column and at higher superficial velocities. Finally, the theoretical models or correlations should be considered to compare the experimental results of bubble hydrodynamic and mass transfer parameters and also predict the absorption efficiency obtained in bubble column.

Table 5.1 The overall results obtained in this study

Absorbents	%Eff	C_L (mol/L)	C_L^S (mol/L)	K_La (s^{-1})	a (m^{-1})	K_L (m/s^{-1})	Remark
Tap water (Q_G 0.5 ml/s)	8.97	0.020	0.0690	0.0010	2.61	0.00038	Low removal efficiency
Effect of the increasing Q_G	↓	↑	≈	↑	↑	≈ at Q_G↓ ↑ at Q_G↑	• It was not necessary to operate at high Q_G due to desorption or stripping phenomena
Effect of surfactant (0.1 CMC)	↑	↑	↑	↓	↑	↓	• Surfactant molecules can increase the C_L^S values and modify the bubble hydrodynamic parameters and interfacial area (a). • K_La and K_L coefficients decrease due to the modification of liquid film around bubble.
Increasing of surfactant concentratios	↑	↑	↑	↓	↑	↓	
Effect of oil-in-water emulsion	↑	↑	↑	↓	↑	↓	• Significant augmentation of C_L^S values was obtained in this case. • Reduction of K_La and K_L values can be obtained, but, uncertain condition occurred when oil concentration increases. • Desorption phenomena is more pronounced in this study compared with other liquid phases.
Increasing of oil-in-water emulsion concentrations	↑	↑	↑	≈	≈	≈	

REFERENCES

Akosman, C., Orhan, R., Dursun, G., 2004. Effects of liquid property on gas holdup and mass transfer in co-current downflow contacting column. Chemical Engineering and Processing. 43: 503–509.

Benitex, J., 2002. Principles and Modern Applications of Mass Transfer Operations. New York: Wiley-Interscience.

Bethea, R.M., 1978. Air pollution control technology: an engineering analysis point of view. New York: Van Nostrand Reinhold.

Bouaifi M., Hébrard G., BastouD. l, Roustan M., 2001. A comparative study of gas hold-up, bubble size, interfacial area and mass transfer coefficients in stirred gas–liquid reactors and bubble columns. Chem. Eng. Proc. 40: 97–111.

Calderbank, P.H., Moo-Young, M.B., 1961. The continuous phase heat and mass-transfer properties of dispersions. Chemical Engineering Science. 16: 39–54.

Cents, A.H.G., Brilman, D.W.F., Versteeg, G.F., 2001. Gas absorption in an agitated gas–liquid–liquid system. Chemical Engineering Science. 56: 1075–1083.

Cotte, F., Fanlo, J.L., Le Cloirec, P., Escobar, P., 1995. Absorption of odorous molecules in aqueous solutions of polyethylene glycol. Environ. Technol. 16: 127–136.

Couvert, A., Roustan, M., Chatellier, P., 1999. Two-phase hydrodynamic study for a rectangular air-lift loop reactor with an internal baffle. Chemical Engineering Science. 54 (21): 5245–5252

Daubert-Deleris I., Hoffmann P.A., Fonade C. and Maranges C. 2006. Hydrodynamic and mass transfer performance of a new aero-ejector with its application toVOC abatement. Chemical Engineering Science. 61: 4982–4993.

De Billerbeck G., Condoret J.S., Fonade C. 1999. Study of mass transfer in a novel gas–liquid contactor: the aero-ejector. Chemical Engineering Journal. 72: 185–193.

Deckwer, W.D., Trad, D.E., Cottrell, V., 1992. Bubble Column Reactors. Wiley, Chichester, pp. 239–254.

De Nevers, N., 2000. Air pollution control engineering. 2 nd ed. Boston: McGraw-Hill.

Dumont, E., Andrs, Y. and Cloirec, P., 2002. Mass transfer coefficients of styrene and oxygen into silicone oil emulsions in a bubble reactor. Chemical Engineering Science. 61: 5612-5619.

Dumont, E., Delmas, H., 2003. Mass transfer enhancement of gas absorption in oil-in-water systems: a review. Chemical Engineering and Processing. 42: 419-438.

Franck, L., Luc, M., Jean-Claude, R. and Jean-Louis, F., 2008. Absorption of a mixture of Volatile organic compounds (VOCs) in aqueous solutions of soluble cutting oil. Bioresource Technology. 99: 1699-1707.

Geankoplis, C.J., 1993. Transport processes and Unit operations. 3 rd ed. Engelwood Cliffs, N. J.: PTR Prentice Hall.

Grace J.R. and Wairegi T. 1986. Properties and Characteristics of drops and bubbles. Encyclopedia of Fluid Mechanics, Cheremisinoff. gulf Publishing Corporation, Huston, TX., 43-57. (Chap 3)

Hbrard, G., Bastoul, D., Roustan, M., 1996. Influence of the gas spargers on the hydrodynamic behaviour of bubble columns. Transaction of the Institution of Chemical Engineers. 74 (A): 406–414.

Hesketh, H.E., 1979. Air pollution control. Ann Arbor, Mich: Ann Arbor Science.

Heymes, F., Manno-Demoustier, P., Charbit, F., Fanlo, J.L. and Moulin, P., 2006. A new efficient absorption liquid to treat exhaust air loaded with toluene. Chemical Engineering Journal. 115: 225-231.

Heymes, F., Manno-Demoustier, P., Charbit, F., Fanlo, J.L. and Moulin, P., 2006. Hydrodynamics and mass transfer in a packed column: Case of toluene absorption with a viscous absorbent. Chemical Engineering Science. 61: 5094-5106.

Kaiser R., 1968. Reappraisal of the Discovery of Benzene in 1825 with the Analytical Methods of 1968. Angewandte Chemie International Edition in English, **7**(5): 345–350. [online] 2008. Available from: http://en.wikipedia.org/wiki/Benzene.

Loubière, K., Hébrard, G., 2003. Bubble formation from a flexible hole submerged in an inviscid liquid. Chemical Engineering Science. 58: 135-148.

Loubière, K., Hébrard, G., 2004. Influence of liquid surface tension (surfactants) on bubble formation at rigid and flexible orifices. Chemical Engineering and Processing. 43: 1361–1369.

Mycock, J.C., McKenna, J.D., 1995. Handbook of air pollution control engineering and technology. Boca Raton, Fla: Lewis.

Noble, R.D., Terry, P.A., 2004. Principle of chemical separations with environmental application. Cambridge, UK; New York: Cambridge University Press.

Painmanakul, P., Loubière, K., Hébrard, G. and Buffire, P., 2004. Study of different membrane spargers used in waste water treatment: characterization and performance. Chemical Engineering and Processing. 7: 1347-1359.

Painmanakul, P., Loubière, K., Hébrard, G. and Mietoon-Peuchot, M., 2005. Effects of surfactants on liquid-side mass transfer coefficients. Chemical Engineering Science. 60: 6480-6491.

Panpanit, S., and Visvanathan, C. 2001. The role of bentonite addition in UF flux enhancement mechanisms for oil/water emulsion. Journal of Membrane Science. 184: 59-68.

Peeva, L., Ben-zvi, S.Y. and Merchuk, J.C., 2001. Mass transfer coefficients of decane to emulsions in a bubble column reactor. Chemical Engineering Science. 56: 5201-5206.

Poddar T. K., Majumdar S. and Sirkar K. K., 1999. Removal of VOCs from air by membrane-based absorption and stripping. Journal of Membrane Science. 120: 221-237.

Rafson, H.J., 1998. Odor and VOC control handbook. New York: McGraw-Hill.

Rao, M.N., Rao, H.V.N., 1989. Air pollution. New Delhi: Tata McGraw-Hill.

Rice, R.G., Tupperainen, J.M.I., Hedge, R., 1981. Dispersion and hold up in bubble columns. Comparison of rigid and flexible sparger. Canadian Journal of Chemical Engineering. 59: 677–687.

Rice, R.G., & Lakhani N.B., 1983. Bubble Formation at a puncture in a submerged rubber membrane. Chem. Eng. Commun. 24: 215–234.

Rosen, M., 2004. Surfactants and interfacial phenomena. 3 rd ed. New Jersey: Wiley-Interscience.

Sardeing R., Painmanakul P. and Hébrard G, 2006. Effect of surfactants on liquid-side mass transfer coefficients in gas-liquid systems: A first step to modeling. Chemical Engineering Science. 61: 6249-6260.

Schramm, L.L., 2005. Emulsions, foams, and suspensions: fundamentals and applications. Weinheim, [Great Britain]: Wiley-VCH.

Seader, J.D., and Henley, E.J., 2006. Separation process principles. 2 nd ed. New Jersey: Hoboken.

Tom R., 2009. Perma Pure LLC [online]. NJ 08754. Available from: http://www.permapure.com/Products/ZAG/ZAG.htm

Treybal, R.E., 1980. Mass-transfer operations. 3 rd ed. Auckland: McGraw-Hill.

Vane, L.M. and Giroux, E.L., 2000. Henry's Law Constants and Micellar Partitioning of Volatile Organic compounds in Surfactant Solution. J. Chem.Eng.Data. 45: 28-47.

Vasconcelos, J.M.T., Rodrigues, J.M.L., Orvalho, S.C.P., Alves, S.S., Mendes, R.L., Reis, A., 2003. Effect of contaminants on mass transfer coefficients in bubble column and airlift contactors. Chemical Engineering Science. 58: 1431–1440.

Vazquez, G., Cancela, M.A., Varela, R., Alvarez, E., Navaza, J.M., 1997. Influence of surfactants on absorption of CO2 in a stirred tank with and without bubbling. Chemical Engineering Journal. 67: 131–137.

Vazquez, G., Cancela, M.A., Riverol, C., Alvarez, E., Navaza, J.M., 2000. Application of the Danckwerts method in a bubble column: effects of surfactants on mass transfer coefficient and interfacial area. Chemical Engineering Journal. 78: 13–19.

Welty, J.R., Wicks, C.E., and Wilson, R.E., 1984. 3 rd ed. Fundamentals of Momentum, Heat, and Mass Transfer. New York: Wiley.

Zhao, B., Wang, J., Yang, W., Jin, Y., 2003a. Gas–liquid mass transfer in slurry bubble systems: I. Mathematical modeling based on a single bubble mechanism. Chemical Engineering Journal. 96: 23–27.

Zhao, B., Wang, J., Yang, W., Jin, Y., 2003b. Gas–liquid mass transfer in slurry bubble systems: II. Mathematical modeling based on a single bubble mechanism. Chemical Engineering Journal. 96: 29–35.

APPENDIX

APPENDIX

1. The calibration curve for determination the concentration of benzene gas
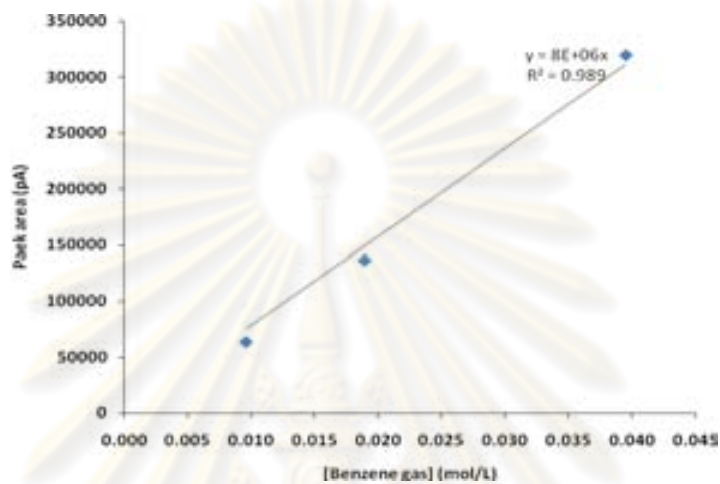
2. Synthetic oil-in-water emulsion

Table 2-1 Surface Tension Value of oil-in-water emulsion at 50 mg/L with tween80

Concentration of surfactant ($\times 10^{-2}$ mol/l)	Surface Tension, SFT (mN/m)
0.00001	52.946
0.0001	47.425
0.001	46.252
0.005	44.241
0.01	41.796
0.02	40.399
0.03	40.111
0.04	39.948
0.05	39.843
0.06	39.721
0.1	38.368
1	37.879
5	37.852

Table 2-2 Surface Tension Value of oil-in-water emulsion at 300 mg/L with tween80

Concentration of surfactant ($\times 10^{-2}$ mol/l)	Surface Tension, SFT (mN/m)
0.0001	48.873
0.0005	46.147
0.001	44.810
0.005	43.375
0.01	42.442
0.02	40.448
0.03	40.156
0.04	39.713
0.05	39.548
0.06	39.020
0.1	38.008
0.5	37.587
1	37.100

3. The saturated time for different liquid phases at gas flow rate 3.0 ml/s
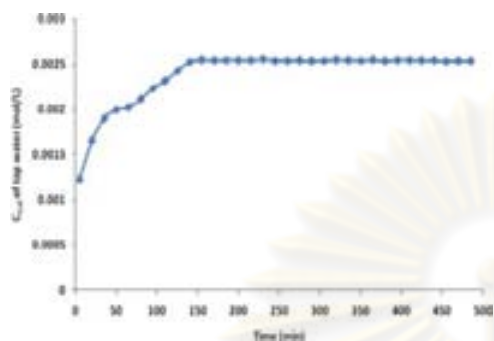
Tap water
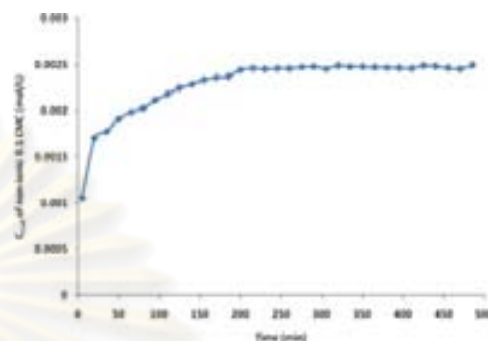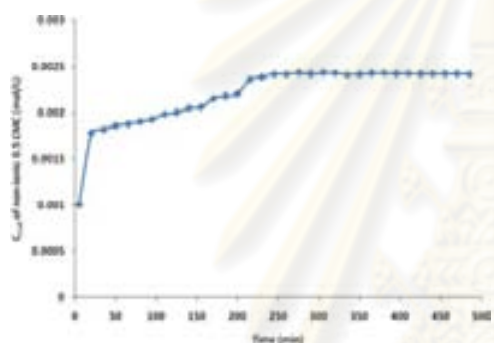
Non-ionic 0.1 CMC

Non-ionic 0.5 CMC

Non-ionic 1 CMC

Non-ionic 3 CMC
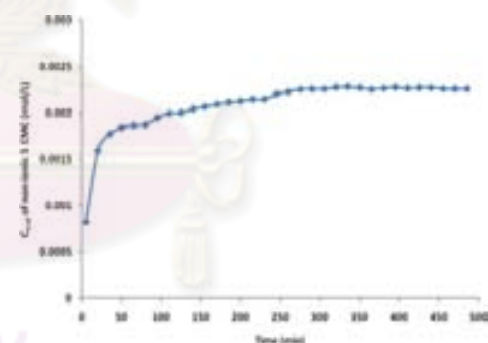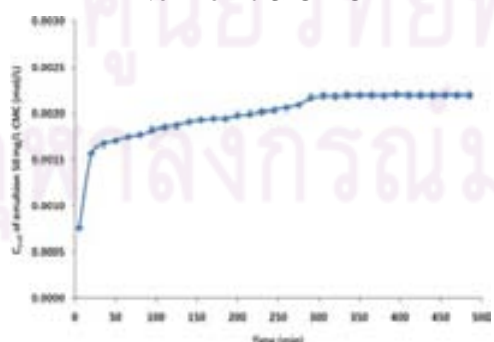
Non-ionic 5 CMC

Emulsion 50 mg/L

Emulsion 300 mg/L

4. Outlet VOCs concentration in gas phase: $C_{g\,out}$ (mol/L)

Table 4-1 Outlet VOCs concentration in gas phase at gas flow rate 0.5 ml/s with time

Time	Tap water	Non-ionic 0.1 CMC	Non-ionic 0.5 CMC	Non-ionic 1 CMC	Non-ionic 3 CMC	Non-ionic 5 CMC	Emulsion 50 mg/L	Emulsion 300 mg/L
5	0.001139	0.001089	0.000961	0.000720	0.000716	0.000630	0.000551	0.000525
20	0.002316	0.002184	0.001857	0.001697	0.001767	0.001561	0.001249	0.001134
35	0.002780	0.002728	0.002349	0.002059	0.002048	0.001953	0.001594	0.001421
50	0.003183	0.002988	0.002654	0.002414	0.002329	0.002192	0.001872	0.001649
65	0.003443	0.003394	0.002921	0.002610	0.002531	0.002505	0.002105	0.001785
95	0.003668	0.003491	0.003277	0.002988	0.002835	0.002657	0.002245	0.002008
125	0.003801	0.003542	0.003456	0.003164	0.002996	0.002773	0.002605	0.002107
155	0.003981	0.003701	0.003503	0.003263	0.003141	0.002847	0.002629	0.002196
185	0.004193	0.003843	0.003751	0.003435	0.003187	0.003131	0.002667	0.002239

Table 4-2 Outlet VOCs concentration in gas phase at gas flow rate 1.3 ml/s with time

Time	Tap water	Non-ionic 0.1 CMC	Non-ionic 0.5 CMC	Non-ionic 1 CMC	Non-ionic 3 CMC	Non-ionic 5 CMC	Emulsion 50 mg/L	Emulsion 300 mg/L
5	0.001422	0.001142	0.001037	0.000968	0.000908	0.000860	0.000578	0.000526
20	0.003313	0.002814	0.002794	0.002664	0.002547	0.002397	0.002079	0.001650
35	0.003606	0.003359	0.003335	0.003100	0.002973	0.002886	0.002414	0.001996
50	0.003749	0.003597	0.003559	0.003223	0.003116	0.002945	0.002643	0.002230
65	0.004012	0.003746	0.003595	0.003262	0.003178	0.002989	0.002681	0.002304
95	0.004041	0.003824	0.003645	0.003295	0.003251	0.003004	0.002793	0.002349
125	0.004076	0.003843	0.003717	0.003497	0.003266	0.003154	0.002816	0.002371
155	0.004252	0.004114	0.003764	0.003509	0.003292	0.003252	0.002852	0.002382
185	0.004348	0.004336	0.004091	0.003942	0.003622	0.003252	0.002870	0.002503

ศูนย์วิทยทรัพยากร
จุฬาลงกรณ์มหาวิทยาลัย

Table 4-3 Outlet VOCs concentration in gas phase at gas flow rate 2.2 ml/s with time

Time	Tap water	Non-ionic 0.1 CMC	Non-ionic 0.5 CMC	Non-ionic 1 CMC	Non-ionic 3 CMC	Non-ionic 5 CMC	Emulsion 50 mg/L	Emulsion 300 mg/L
5	0.001947	0.001835	0.001481	0.001265	0.001213	0.001129	0.001115	0.001032
20	0.003501	0.003012	0.002909	0.002871	0.002736	0.002728	0.002422	0.001879
35	0.003682	0.003555	0.003398	0.003167	0.002982	0.002913	0.002584	0.002226
50	0.003760	0.003669	0.003601	0.003245	0.003144	0.003013	0.002862	0.002301
65	0.004016	0.003792	0.003617	0.003339	0.003213	0.003042	0.002949	0.002461
95	0.004097	0.003967	0.003668	0.003495	0.003251	0.003185	0.002960	0.002505
125	0.004109	0.004040	0.003808	0.003631	0.003292	0.003200	0.003057	0.002555
155	0.004308	0.004118	0.003988	0.003675	0.003384	0.003255	0.003073	0.002569
185	0.004380	0.004365	0.004204	0.004068	0.003789	0.003311	0.003230	0.002939

ศูนย์วิทยทรัพยากร
จุฬาลงกรณ์มหาวิทยาลัย

Table 4-4 Outlet VOCs concentration in gas phase at gas flow rate 3.0 ml/s with time

Time	Tap water	Non-ionic 0.1 CMC	Non-ionic 0.5 CMC	Non-ionic 1 CMC	Non-ionic 3 CMC	Non-ionic 5 CMC	Emulsion 50 mg/L	Emulsion 300 mg/L
5	0.002304	0.002168	0.002094	0.001941	0.001932	0.001775	0.001570	0.001111
20	0.003721	0.003343	0.003282	0.002988	0.002910	0.002763	0.002499	0.002480
35	0.003845	0.003633	0.003442	0.003232	0.003027	0.002930	0.002719	0.002694
50	0.003948	0.003669	0.003633	0.003314	0.003191	0.003073	0.002967	0.002767
65	0.004072	0.003822	0.003647	0.003498	0.003236	0.003107	0.002979	0.002817
95	0.004112	0.004040	0.003803	0.003556	0.003318	0.003214	0.003077	0.002839
125	0.004337	0.004315	0.003904	0.003722	0.003421	0.003297	0.003116	0.002853
155	0.004413	0.004357	0.004090	0.003732	0.003633	0.003363	0.003117	0.002887
185	0.004444	0.004382	0.004234	0.004124	0.003893	0.003449	0.003253	0.003014

ศูนย์วิทยทรัพยากร

จุฬาลงกรณ์มหาวิทยาลัย

5. VOCs concentration in liquid phase: C_L (mol/L)

Table 5-1 VOCs concentration in liquid phase at gas flow rate 0.5 ml/s

Time	Tap water	Non-ionic 0.1 CMC	Non-ionic 0.5 CMC	Non-ionic 1 CMC	Non-ionic 3 CMC	Non-ionic 5 CMC	Emulsion 50 mg/L	Emulsion 300 mg/L
5	0.00190	0.00191	0.00190	0.00186	0.00186	0.00189	0.00191	0.00191
20	0.00588	0.00599	0.00622	0.00618	0.00613	0.00637	0.00668	0.00680
35	0.00863	0.00884	0.00949	0.00949	0.00940	0.00986	0.01068	0.01101
50	0.01072	0.01109	0.01217	0.01227	0.01225	0.01288	0.01421	0.01484
65	0.01232	0.01284	0.01442	0.01463	0.01473	0.01549	0.01736	0.01839
95	0.01479	0.01558	0.01798	0.01849	0.01894	0.02001	0.02309	0.02496
125	0.01672	0.01810	0.02074	0.02152	0.02245	0.02412	0.02807	0.03104
155	0.01819	0.02031	0.02316	0.02414	0.02550	0.02795	0.03248	0.03685
185	0.01906	0.02206	0.02513	0.02635	0.02827	0.03124	0.03680	0.04245

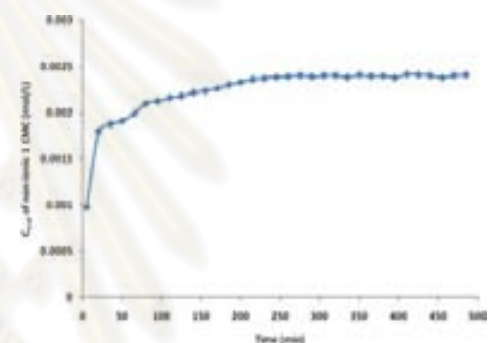**Table 5-2** VOCs concentration in liquid phase at gas flow rate 1.3 ml/s
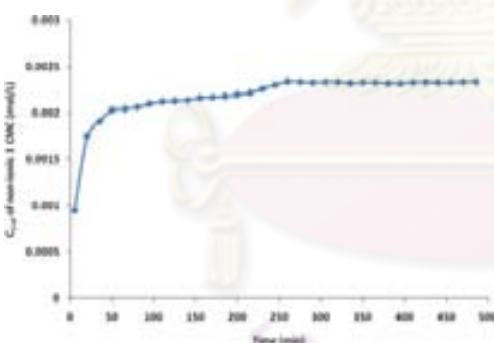
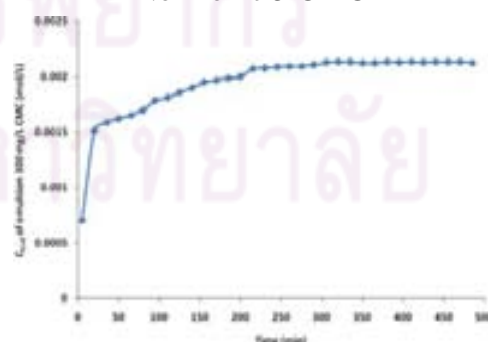| Time	Tap water	Non-ionic 0.1 CMC	Non-ionic 0.5 CMC	Non-ionic 1 CMC	Non-ionic 3 CMC	Non-ionic 5 CMC	Emulsion 50 mg/L	Emulsion 300 mg/L
5	0.00474	0.00488	0.00495	0.00499	0.00503	0.00506	0.00524	0.00528
20	0.01248	0.01402	0.01434	0.01477	0.01515	0.01557	0.01692	0.01789
35	0.01598	0.01885	0.01924	0.02039	0.02125	0.02213	0.02405	0.02764
50	0.01862	0.02214	0.02266	0.02492	0.02623	0.02762	0.03007	0.03626
65	0.02047	0.02468	0.02557	0.02913	0.03082	0.03290	0.03655	0.04428
95	0.02302	0.02888	0.03105	0.03728	0.03947	0.04325	0.04892	0.05985
125	0.02533	0.03270	0.03606	0.04451	0.04777	0.05295	0.06076	0.07517
155	0.02681	0.03538	0.04060	0.05091	0.05591	0.06169	0.07238	0.09035
185	0.02723	0.03615	0.04369	0.05557	0.06267	0.07004	0.08378	0.10502

ศูนย์วิทยทรัพยากร
จุฬาลงกรณ์มหาวิทยาลัย

Table 5-3 VOCs concentration in liquid phase at gas flow rate 2.2 ml/s

Time	Tap water	Non-ionic 0.1 CMC	Non-ionic 0.5 CMC	Non-ionic 1 CMC	Non-ionic 3 CMC	Non-ionic 5 CMC	Emulsion 50 mg/L	Emulsion 300 mg/L
5	0.00940	0.00943	0.00950	0.00955	0.00956	0.00958	0.00958	0.00950
20	0.02091	0.02292	0.02451	0.02539	0.02602	0.02634	0.02740	0.02906
35	0.02670	0.03074	0.03318	0.03495	0.03664	0.03722	0.04037	0.04469
50	0.03163	0.03639	0.03957	0.04328	0.04591	0.04715	0.05189	0.05892
65	0.03545	0.04125	0.04524	0.05105	0.05442	0.05666	0.06220	0.07238
95	0.04089	0.04902	0.05614	0.06492	0.07074	0.07454	0.08218	0.09795
125	0.04570	0.05515	0.06578	0.07686	0.08653	0.09137	0.10144	0.12289
155	0.04913	0.06029	0.07330	0.08762	0.10145	0.10775	0.11996	0.14742
185	0.05077	0.06328	0.07821	0.09550	0.11308	0.12339	0.13734	0.16941

ศูนย์วิทยทรัพยากร
จุฬาลงกรณ์มหาวิทยาลัย

Table 5-4 VOCs concentration in liquid phase at gas flow rate 3.0 ml/s

Time	Tap water	Non-ionic 0.1 CMC	Non-ionic 0.5 CMC	Non-ionic 1 CMC	Non-ionic 3 CMC	Non-ionic 5 CMC	Emulsion 50 mg/L	Emulsion 300 mg/L
5	0.01281	0.01285	0.01296	0.01268	0.01292	0.01297	0.01273	0.01287
20	0.02621	0.02856	0.02954	0.03028	0.03164	0.03306	0.03403	0.03632
35	0.03267	0.03768	0.04005	0.04207	0.04544	0.04795	0.05016	0.05314
50	0.03811	0.04533	0.04898	0.05239	0.05796	0.06144	0.06418	0.06867
65	0.04253	0.05213	0.05699	0.06152	0.06955	0.07414	0.07703	0.08315
95	0.04989	0.06239	0.07148	0.07759	0.09158	0.09827	0.10175	0.11146
125	0.05487	0.06821	0.08366	0.09165	0.11195	0.12069	0.12523	0.13945
155	0.05714	0.07118	0.09326	0.10412	0.12948	0.14177	0.14835	0.16701
185	0.05844	0.07355	0.09988	0.11298	0.14277	0.16148	0.17024	0.19312

ศูนย์วิทยทรัพยากร
จุฬาลงกรณ์มหาวิทยาลัย

6. Bubble diameter of different types of absorbent

Table 6-1 Bubble diameter of different types of absorbent at flow rate 0.5 ml/s

Tap water		Non-ionic 0.1 CMC		Non-ionic 0.5 CMC		Non-ionic 1 CMC		Non-ionic 3 CMC		Non-ionic 5 CMC		Emulsion 50 mg/L		Emulsion 300 mg/L	
3.82	4.05	3.78	4.01	3.84	3.94	4.05	3.61	3.59	3.98	3.92	3.76	3.69	3.64	3.36	3.16
3.82	4.07	3.81	4.02	3.85	3.94	4.06	3.61	3.60	4.09	3.93	3.76	3.69	3.79	3.36	3.18
3.84	4.07	3.81	4.02	3.85	3.94	4.07	3.68	3.61	4.11	3.93	3.78	3.72	3.72	3.37	3.19
3.85	4.08	3.81	4.03	3.86	3.94	4.07	3.73	3.61	4.15	3.95	3.80	3.72	3.73	3.39	3.20
3.86	4.08	3.83	4.03	3.86	3.95	4.07	3.77	3.51	4.15	3.96	3.84	3.71	3.74	3.39	3.21
3.86	4.08	3.84	4.03	3.87	3.96	4.08	3.79	3.52	4.16	3.97	3.84	3.70	3.75	3.40	3.23
3.88	4.09	3.85	4.03	3.87	3.96	4.08	3.82	3.53	4.16	3.99	3.85	3.70	3.73	3.41	3.23
3.89	4.09	3.87	4.05	3.87	3.96	4.08	3.87	3.54	4.24	4.01	3.87	3.77	3.74	3.42	3.23
3.89	4.10	3.87	4.06	3.87	3.96	4.10	3.88	3.55	4.27	4.02	3.88	3.76	3.72	3.43	3.24
3.90	4.10	3.87	4.08	3.88	3.97	4.21	3.91	3.56	4.30	4.02	3.89	3.74	3.83	3.44	3.25
3.90	4.11	3.88	4.08	3.88	3.97	4.20	3.91	3.57	4.30	4.03	3.90	3.73	3.83	3.44	3.26
3.92	4.11	3.92	4.09	3.89	3.98	4.20	3.92	3.63	4.31	4.03	3.90	3.74	3.83	3.44	3.26
3.94	4.12	3.93	4.09	3.90	3.98	4.19	3.92	3.62	4.34	3.16	3.91	3.72	3.85	3.44	3.27
3.98	4.12	3.94	4.08	3.90	3.98	4.18	3.93	3.62	4.35	3.30	3.11	3.71	3.61	3.46	3.27
3.99	4.14	3.95	4.08	3.91	3.98	4.17	3.94	3.62	4.37	3.20	3.21	3.71	3.64	3.47	3.29
3.99	4.14	3.95	4.08	3.91	3.99	2.88	3.94	3.52	4.39	3.61	3.37	3.68	3.66	3.09	3.30
3.99	4.17	3.97	4.05	3.91	3.99	3.06	3.97	3.53	3.40	3.64	3.54	3.67	3.65	3.11	3.30
4.02	4.18	3.99	4.06	3.91	4.00	3.31	3.97	3.54	3.40	3.67	3.55	3.66	3.73	3.12	3.30
4.02	4.18	3.99	4.07	3.92	4.00	3.54	3.99	3.55	3.55	3.69	3.59	3.65	3.71	3.12	3.31
4.03	4.19	4.01	4.08	3.92	4.00	3.55	4.01	3.56	3.50	3.71	3.60	3.66	3.70	3.13	3.32
4.04	4.20	4.01	4.08	3.93	4.00	3.60	4.02	3.57	3.50	3.72	3.60	3.65	3.73	3.13	3.34
4.04	4.22	4.01	3.76	3.94	4.00	3.60	4.03	3.58	3.51	3.76	3.61	3.66	3.68	3.15	3.34
Avg = 4.03		Avg = 3.97		Avg = 3.93		Avg = 3.88		Avg = 3.80		Avg = 3.74		Avg = 3.71		Avg = 3.29	

Table 6-2 Bubble diameter of different types of absorbent at flow rate 1.3 ml/s

Tap water		Non-ionic 0.1 CMC		Non-ionic 0.5 CMC		Non-ionic 1 CMC		Non-ionic 3 CMC		Non-ionic 5 CMC		Emulsion 50 mg/L		Emulsion 300 mg/L	
3.81	3.71	4.09	3.79	3.79	4.47	3.82	4.37	3.74	4.07	3.98	3.87	3.80	3.98	3.82	3.53
3.82	3.79	3.82	3.92	3.92	4.47	3.83	4.41	3.77	4.11	3.99	3.88	3.81	3.99	3.82	3.53
3.83	3.92	3.83	4.16	4.16	4.47	3.84	4.41	3.79	4.12	3.50	3.88	3.82	3.50	3.85	3.53
3.84	4.16	3.84	4.17	4.17	3.60	3.85	4.46	3.83	4.12	3.60	3.89	3.82	3.60	3.87	3.54
3.85	4.17	3.85	4.21	4.21	4.50	3.86	3.55	3.85	4.12	3.71	3.89	3.85	3.71	3.87	3.55
3.86	4.21	3.86	4.22	4.22	4.52	3.87	3.55	3.87	4.12	3.80	3.90	3.87	3.80	3.88	3.57
3.87	4.22	3.87	4.22	4.22	3.60	3.88	3.59	3.92	4.14	3.90	3.91	3.87	3.90	3.88	3.59
3.88	4.22	3.88	4.22	4.22	4.20	3.92	3.60	3.97	4.14	4.01	3.91	3.88	4.01	3.89	3.59
3.89	4.22	3.89	4.36	4.36	4.40	4.16	3.60	4.00	4.16	4.02	3.91	3.88	3.94	3.89	3.60
3.90	4.36	3.90	4.37	4.37	4.30	4.17	4.40	4.01	4.22	4.00	3.93	3.89	3.94	3.90	3.60
3.83	4.37	3.83	4.41	4.41	4.00	4.21	4.30	4.01	4.22	4.00	3.93	3.89	3.94	3.91	3.63
3.72	4.41	3.82	4.41	4.41	3.87	4.22	4.00	4.01	4.22	4.00	3.94	3.90	3.95	3.91	3.64
3.73	4.41	3.83	4.46	4.46	3.88	4.22	4.02	4.02	4.23	3.76	3.94	3.91	3.95	3.91	3.65
3.73	4.46	3.86	4.46	4.46	3.89	4.22	4.05	4.03	4.29	3.87	3.94	3.91	3.96	3.93	3.67
4.57	4.46	4.20	4.47	4.02	3.90	4.36	4.06	4.06	4.30	3.80	3.95	3.91	3.97	3.76	3.67
4.57	4.47	4.40	4.47	4.05	3.83	3.71	4.08	4.06	3.67	3.80	3.95	3.93	3.97	3.77	3.68
4.59	4.47	4.30	4.47	4.06	3.82	3.79	3.89	4.23	3.65	3.81	3.96	3.93	3.97	3.78	3.69
4.60	4.47	4.00	4.49	4.08	3.83	4.50	3.90	4.24	3.64	3.82	3.97	4.02	3.97	3.79	3.69
4.62	4.49	4.02	4.52	4.09	3.86	4.52	3.83	4.28	3.60	3.82	3.97	3.52	3.98	3.80	3.73
4.60	4.52	4.05	3.71	3.82	3.84	3.60	3.82	4.28	3.60	3.85	3.97	3.51	3.50	3.80	3.74
3.81	4.54	4.06	4.54	3.83	3.85	4.20	3.83	4.29	3.61	3.80	3.97	3.80	3.76	3.80	3.75
3.80	4.57	4.08	4.40	3.71	3.86	4.09	3.86	3.53	3.62	3.87	3.98	3.80	3.87	3.81	3.52
Avg = 4.17		Avg = 4.13		Avg = 4.09		Avg = 4.01		Avg = 3.99		Avg = 3.89		Avg = 3.86		Avg = 3.73	

Table 6-3 Bubble diameter of different types of absorbent at flow rate 2.2 ml/s

Tap water		Non-ionic 0.1 CMC		Non-ionic 0.5 CMC		Non-ionic 1 CMC		Non-ionic 3 CMC		Non-ionic 5 CMC		Emulsion 50 mg/L		Emulsion 300 mg/L	
4.29	4.47	3.97	4.22	4.13	3.97	3.58	4.21	4.01	4.21	3.61	4.21	3.98	3.63	4.02	3.98
4.30	4.49	3.95	4.20	4.24	3.95	3.79	4.24	4.01	4.24	3.63	4.21	3.99	3.77	4.05	3.98
4.31	4.50	3.96	4.20	4.25	3.96	3.91	4.23	4.02	4.23	3.77	4.21	4.28	3.78	4.09	4.00
4.31	4.55	3.99	4.21	4.29	3.99	3.94	4.21	4.04	4.21	3.78	4.22	3.94	3.79	4.09	3.69
4.34	4.71	4.01	4.24	4.30	4.01	3.95	4.20	4.08	4.20	3.79	4.23	3.95	3.82	4.12	4.00
4.37	4.74	4.07	4.23	4.31	4.07	4.01	4.20	4.10	4.20	3.82	4.24	4.00	3.88	4.14	4.10
4.39	4.20	4.13	4.21	4.31	4.13	4.01	4.23	4.11	4.23	3.88	4.26	4.00	3.98	4.14	3.98
4.39	3.95	4.13	4.20	4.34	4.50	4.02	4.30	4.14	4.30	3.98	4.26	4.02	4.12	4.16	3.99
4.56	4.20	4.24	4.20	4.37	4.20	4.04	4.30	4.14	4.30	3.98	4.28	4.02	4.14	4.16	4.28
4.59	4.30	4.25	4.23	4.39	3.95	4.08	4.07	4.17	4.07	4.02	3.94	4.03	4.14	4.17	3.94
4.64	4.32	4.29	4.30	4.22	4.20	4.10	4.08	4.18	4.08	4.05	3.95	4.07	4.16	4.18	3.95
4.70	4.33	4.30	4.30	4.20	4.30	4.11	4.09	4.19	4.09	4.09	4.01	4.05	4.16	4.19	4.02
4.70	4.33	4.31	4.32	4.20	4.07	4.14	4.11	4.21	4.07	4.09	4.01	4.02	4.17	4.22	4.00
4.70	4.34	4.31	4.33	4.21	4.08	4.14	4.10	4.21	4.16	4.12	4.02	4.03	4.18	4.21	4.02
3.96	3.96	4.34	4.33	4.24	4.09	4.17	4.22	4.22	4.22	4.14	4.04	4.00	4.19	4.00	4.02
3.99	3.99	4.37	4.34	4.23	4.11	4.18	4.21	4.20	4.21	4.14	4.08	4.10	4.21	3.63	4.03
4.01	3.98	4.39	3.96	4.21	4.10	4.19	4.20	3.58	4.12	4.16	4.10	3.98	4.21	3.77	4.07
4.07	4.69	4.40	3.99	4.20	4.22	4.21	4.40	3.79	4.25	4.16	4.29	4.02	4.21	3.78	4.05
4.13	4.62	4.50	3.98	4.20	4.21	4.21	4.50	3.91	4.22	4.17	4.21	4.05	4.21	3.79	4.02
4.13	4.66	4.20	4.69	4.23	4.20	4.22	4.40	3.94	4.20	4.18	4.20	4.09	4.22	3.82	4.03
4.24	3.97	3.95	4.62	4.30	4.40	4.20	4.49	3.95	3.97	4.19	4.27	4.09	4.00	3.61	4.00
4.25	3.95	4.20	4.66	4.40	4.50	4.20	4.48	4.20	3.99	4.21	4.24	3.61	4.00	3.88	4.10
Avg = 4.33		Avg = 4.23		Avg = 4.20		Avg = 4.16		Avg = 4.12		Avg = 4.08		Avg = 4.03		Avg = 4.01	

Table 6-4 Bubble diameter of different types of absorbent at flow rate 3.0 ml/s

Tap water		Non-ionic 0.1 CMC		Non-ionic 0.5 CMC		Non-ionic 1 CMC		Non-ionic 3 CMC		Non-ionic 5 CMC		Emulsion 50 mg/L		Emulsion 300 mg/L	
5.39	5.89	5.11	5.39	5.17	5.61	4.96	5.22	4.35	5.61	4.91	5.09	5.13	5.58	4.78	5.06
5.72	5.90	5.14	5.72	5.22	5.61	5.10	4.71	4.97	5.62	5.63	5.73	5.10	5.61	4.78	5.09
5.72	5.95	5.15	5.72	5.23	5.61	4.71	5.76	4.08	5.62	5.08	5.06	5.06	4.49	4.79	5.09
5.76	5.97	5.16	5.76	5.24	5.62	5.98	5.65	4.81	5.63	4.77	4.99	4.99	4.55	4.81	5.11
5.00	5.41	5.17	5.00	5.31	5.62	4.80	5.78	4.84	5.00	4.94	5.00	4.43	4.36	4.81	5.14
5.50	5.73	5.22	5.50	5.34	5.63	5.52	4.63	5.47	5.01	4.89	5.40	5.11	4.81	4.81	5.15
5.01	5.75	5.23	5.01	5.35	5.00	5.61	5.44	4.67	5.02	4.94	5.64	5.64	4.38	4.81	5.16
5.02	5.78	5.24	5.02	5.39	5.21	5.33	5.69	5.58	5.06	4.63	5.71	5.02	5.07	4.81	5.17
5.06	5.81	5.31	5.06	5.39	5.14	5.53	5.53	5.61	5.09	4.85	5.63	5.63	5.39	4.82	5.22
5.09	5.89	5.34	5.09	5.39	5.23	5.16	4.77	4.49	5.25	4.47	5.35	5.35	4.91	4.82	5.23
5.09	5.56	5.35	5.09	5.39	5.16	4.50	5.51	4.55	5.73	5.75	5.35	5.35	5.63	4.82	5.24
5.11	5.61	5.89	5.40	5.41	5.32	4.38	5.62	4.36	5.06	4.87	5.37	5.37	5.08	4.83	5.09
5.14	5.61	5.90	5.64	5.42	5.12	5.86	4.71	4.81	4.99	5.61	5.61	5.61	4.77	4.84	5.25
5.15	5.61	5.95	5.71	5.42	5.00	5.10	5.39	4.38	4.43	4.49	5.63	5.63	4.94	4.88	5.21
5.16	5.61	5.65	5.63	5.48	4.96	4.98	5.38	5.07	5.40	4.55	5.71	5.23	4.89	4.88	5.14
5.17	5.62	5.66	5.35	5.56	4.97	5.63	4.77	5.39	5.64	4.36	5.72	5.22	4.94	5.11	5.23
5.22	5.62	5.69	5.35	5.61	4.99	5.77	5.59	4.91	5.71	4.81	4.35	4.35	4.63	4.76	5.16
5.23	5.63	4.96	5.37	5.01	5.27	5.69	4.91	5.63	5.63	4.38	4.97	4.97	4.85	4.77	4.71
5.24	5.68	4.96	5.61	5.02	5.11	5.06	4.68	5.61	5.35	5.07	4.08	4.08	4.47	4.78	4.72
5.31	5.71	4.97	5.63	5.06	5.11	4.66	5.21	5.63	5.35	5.39	4.81	4.81	5.75	5.50	4.74
5.34	5.71	4.99	5.71	5.09	5.14	5.29	4.90	5.56	5.37	4.67	4.84	4.84	5.14	5.01	4.74
5.35	5.72	5.50	5.72	5.25	5.15	5.21	5.57	5.62	5.61	5.58	5.47	5.47	4.67	5.02	5.00
Avg = 5.49		Avg = 5.39		Avg = 5.28		Avg = 5.23		Avg = 5.17		Avg = 5.09		Avg = 5.03		Avg = 4.98	

7. Method for determination of $K_L a$ coefficient (Dynamic method)

Based on the experimental results

$$\boxed{C_g(t) = f(t)}$$

Simulated by Langmuir theory

$$\boxed{C_g(t) = \frac{C^*_{g(in)} \times kt}{1 + kt}}$$

Mass balance equation

$$\boxed{Q_g C^*_{g(in)} = Q_g C_{g(out)}(t) + V_L \frac{dC_L(t)}{dt}}$$

VOCs concentration in liquid phase

$$\boxed{C_L(t) = \frac{Q_g}{V_L}[C^*_{g(in)} \times t - \int_0^t C_g(t)dt]}$$
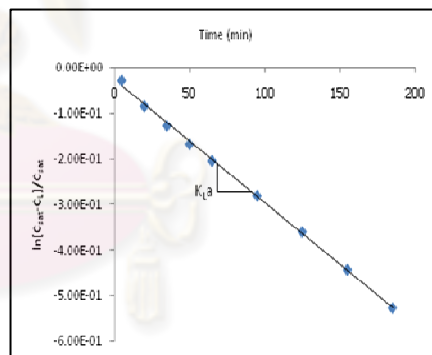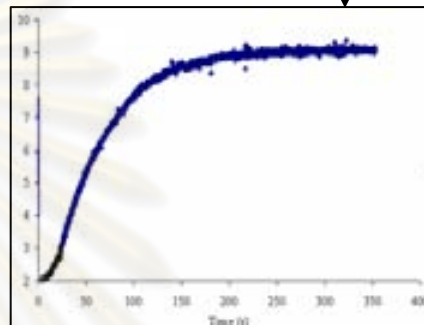
The overall mass transfer coefficient ($K_L a$)

$$\boxed{\frac{dC_L}{dt} = k_L a(C_L^s - C_L)}$$

Or, in integral form

$$\boxed{\ln[C_L^s - C_L] = \ln(C_L^S) - k_L a \times t}$$

BIOGRAPHY

Name: Miss. Sirikarn Laoraddecha

Date of Birth: January 6, 1985

Nationality: Thai

University Education: 2003-2006 Bachelor Degree of Science in

                          Environmental Science,

                          Faculty of Science, Silpakorn University,

                          Nakornpathom, Thailand

Presentation:

Sirikarn Laoraddecha and Pisut Painmanakul. *Hydrodynamic and mass transfer of benzene absorption process in bubble column.* The Proceedings of 8th National Environmental Conference, March 25 -27, 2009, at Suranaree University of Technology, Nakornrachasrima, Thailand, Organized by the Environmental Engineering Association of Thailand